

University of Technology, Sydney

Faculty of Engineering

**A SURVEY OF ELECTROCHEMICAL
SUPERCAPACITOR TECHNOLOGY**

by

Adam Marcus Namisnyk

Student Number: 98080029

Registration Number: A03-155

Major: Electrical Engineering

Supervisor: Dr. Jian Guo Zhu

A 12 Credit Point Project submitted in partial fulfillment of the
requirement for the Degree of Bachelor of Engineering

23 June 2003

Synopsis

This project was originally the brainchild of the supervisor, Dr. Jian Guo Zhu, who has a particular passion for supercapacitors as an elegant and efficient means of energy storage. The structure of the work undertaken in this thesis is largely a result of discussions between the author and Dr. Zhu about the sort of content that would be worthwhile.

This survey is essentially a literature review, synthesising the current state-of-the-art into a single, complete work accessible to readers that may not possess any prior knowledge of the technology in question. Information has been gathered from a wide variety of sources, from books and journal articles to web site content and conference proceedings.

Many electrical engineers may be aware of the existence of supercapacitors, but because the technology is relatively new it is unlikely that they will have a detailed understanding of the scientific principles and processes involved. It is therefore quite likely that more well-established, conventional technologies will be chosen for applications that may be ideally suited to the use of supercapacitors. An ignorance of their possible applications beyond their well-publicised use in hybrid electric vehicles means that supercapacitors are likely to be overlooked often as an energy storage option.

The main goal of this thesis is therefore to provide a detailed overview of supercapacitor technology as it currently stands, presented in a manner that is both informative and useful to practising engineers and engineering students. This work represents an examination into many facets of supercapacitor operation relevant to electrical engineering, and will furnish an excellent starting point for anyone wishing to become more familiar with this promising new technology.

As an additional aid to readers this thesis also includes a CD-ROM containing references used in this paper, as well as datasheets and application notes from various manufacturers.

Statement of Originality

I, Adam Marcus Namisnyk, am the sole author of this work, and all text contained herein is of my own fabrication unless otherwise indicated. Any text, figures, theories, results, or designs that are not of my own devising are appropriately referenced in order to give credit to the original author(s). All sources of assistance have been assigned due acknowledgment.

A SURVEY OF ELECTROCHEMICAL SUPERCAPACITOR TECHNOLOGY

by

Adam Marcus Namisnyk

Autumn 2003

Abstract

The electrochemical supercapacitor is an emerging technology that promises to play an important role in meeting the demands of electronic devices and systems both now and in the future. This paper traces the history of the development of the technology, and explores the principles and theory of operation. The use of supercapacitors in applications such as pulse power, backup sources, and others is discussed and their advantages over alternative technologies are considered. To provide examples with which to outline practical implementation issues, systems incorporating supercapacitors as vital components are also explored.

Acknowledgments

Sincere thanks are extended to the supervisor of this project, Dr. Jian Guo Zhu, who has been extremely helpful in not only suggesting worthwhile content, but also offering advice on authoring and styling techniques.

The author would also like to acknowledge the invaluable contribution of those that maintain the UTS library website, which contains links to a wide range of journal and conference paper collections. The availability of a large body of work online has significantly reduced the amount of time spent on research.

Table of Contents

Synopsis	i
Statement of Originality.....	iii
Abstract.....	iv
Acknowledgments	v
Table of Contents	vi
List of Figures	ix
1. Introduction.....	1
1.1 Historical background	3
1.2 Current commercial activity	6
1.3 Current research efforts	9
1.4 Future research.....	11
2. Principles of Operation	12
2.1 Basic scientific principles.....	12
2.2 The electric double-layer.....	15
2.2.1 Helmholtz's double layer.....	15
2.2.2 The Gouy-Chapman model.....	16
2.2.3 Stern and Grahame	18
2.2.4 The current model	19
2.3 Pseudocapacitance	20
2.3.1 Redox reactions	21
2.3.2 Adsorption of ions	22
2.4 Summary of scientific background	23

3. Capacitor construction	24
3.1 Electrode materials.....	24
3.1.1 Carbon.....	24
3.1.2 Conducting polymers.....	27
3.1.3 Metal-oxides.....	29
3.1.4 Hybrid and composite configurations	30
3.2 Electrolytes	32
3.3 Separator.....	33
3.4 Summary of EDLC construction	33
4. EDLC performance	34
4.1. Measurement techniques	34
4.1.1. Cyclic voltammetry	34
4.1.2. Constant-current charging and Ragone plots.....	37
4.1.3. Impedance spectroscopy.....	39
4.1.4. Constant-power cycling	40
4.2. Capacitor modelling	42
4.2.1. The classical equivalent circuit	43
4.2.2. The 3 branch model.....	45
4.2.3. Porous electrodes as transmission lines.....	48
4.3. Performance characteristics.....	51
4.4. Summary of performance considerations	56
5. Applications	57
5.1. Memory backup	57
5.2. Electric vehicles	58
5.3. Power quality	63
5.4. Battery improvement.....	65
5.5. Electromechanical actuators	68
5.6. Adjustable-speed drive ‘ride-through’	68

5.7.	Portable power supplies.....	70
5.8.	Remote power from renewable sources	72
5.9.	Summary of EDLC applications.....	73
6.	Design considerations	75
6.1.	Voltage decay	75
6.2.	EDLC bank sizing.....	76
6.3.	Voltage balancing	77
6.4.	Summary of design with EDLCs	83
7.	Example systems	84
7.1.	Household power generation	84
7.2.	Ride-through system for ASDs.....	89
7.3.	The HY.POWER electric car.....	93
8.	Future directions of the technology	95
9.	Conclusions and recommendations	97
	References.....	99
	Definitions and abbreviations	108

List of Figures

Figure 1.1 - Ragone plot of various energy storage devices.....	2
Figure 1.2 - The capacitor patented by General Electric.....	5
Figure 1.3 - An electrolytic energy storage device patented by SOHIO.....	5
Figure 1.4 - A capacitor patented by SOHIO.....	6
Figure 1.5 - A range of EDLCs sold by Ness Capacitor Co. in Korea.....	7
Figure 1.6 - TEM image of an activated carbon electrode.....	9
Figure 1.7 – FE-SEM image of carbon nanotubes.....	10
Figure 2.1 - Electrostatic capacitor topology.....	13
Figure 2.2 - EDLC charge storage mechanism.....	13
Figure 2.3 - Conceptual diagram of EDLC construction.....	15
Figure 2.4 - Helmholtz double layer model.....	17
Figure 2.5 – Gouy-Chapman diffuse model.....	17
Figure 2.6 - Stern-Grahame model.....	19
Figure 2.7 - A double layer model including layers of solvent.....	20
Figure 2.8 - Cyclic voltammogram of a ruthenium-oxide electrode in sulfuric acid electrolyte.....	21
Figure 2.9 - Voltammetry of H adsorption and desorption on a Pt surface.....	23
Figure 3.1 - Effect of pore diameter on specific capacitance.....	25
Figure 3.2 - Voltammetry plot of modified carbon electrodes.....	26
Figure 3.3 - Tangled network of carbon nanotubes.....	27
Figure 3.4 - Charging process of conducting polymer electrodes.....	28
Figure 3.5 – Cyclic voltammogram of a polymer film.....	29
Figure 3.6 - Cyclic voltammogram for MnO film with KCl electrolyte.....	30
Figure 3.7 - Ragone plot of hybrid (▲) and carbon (●) supercapacitors.....	31
Figure 3.8 - A carbon nanotube coated in polypyrrole.....	32

Figure 4.1 – Comparison of ideal and real cyclic voltammograms.....	35
Figure 4.2 – Cyclic voltammograms at increasing sweep rates.....	36
Figure 4.3 – Transition of an EDLC based on adsorption pseudocapacitance to irreversibility at higher sweep rates.....	37
Figure 4.4 - Charging at 5 A compared to ideal RC behaviour.	38
Figure 4.5 – Ragone plots of two EDLC devices.....	39
Figure 4.6 – Complex impedance plot of conventional capacitor and EDLC.....	40
Figure 4.7 – Constant-power cycling waveforms.	41
Figure 4.8 - Experimental data obtained from power-cycling tests and fitted with a line of best fit.	42
Figure 4.9 - The classical equivalent circuit of an EDLC.	43
Figure 4.10 - Test circuit for measuring ESR.	44
Figure 4.11 - Voltage and current waveforms for a 470 F capacitor charged to 3 V and discharged into a 0.2 Ω load.....	44
Figure 4.12 - Comparison of classical model to experimental data.	45
Figure 4.13 - The 3 branch model.	46
Figure 4.14 - Porous electrode representation as a five element transmission line.....	49
Figure 4.15 - Potential step response of transmission line model.....	50
Figure 4.16 - Potential response to sinusoidal input at various pore depths.....	50
Figure 4.17 - Transmission line model with complex impedance.	50
Figure 4.18 – Impedance plot of a 0.47 F, 11 V Capattery by Evans.	53
Figure 4.19 – Comparison of Ragone plots for supercapacitors using organic and aqueous electrolytes.....	54
Figure 4.20 – Charging characteristics at different currents.....	55
Figure 4.21 – Comparison of a) impedance spectroscopy and b) phase response for two EDLCs.....	55

Figure 5.1 – Scheme for memory backup of clock memory via supercapacitor.....	58
Figure 5.2 – Electric drive train using a fuel cell and supercapacitors.....	59
Figure 5.3 – Power flows in an EV test drive for the fuel cell, supercapacitors, and inverter.....	59
Figure 5.4 – The supercapacitor modules of a prototype EV.	60
Figure 5.5 – Block diagram of an HEV using supercapacitors and an induction motor.....	62
Figure 5.6 – Improved power quality on distribution side by DVR.....	64
Figure 5.7 – Pulsed current load experienced in a mobile phone.	65
Figure 5.8 – Runtime extension when using an EDLC in combination with a battery.....	66
Figure 5.9 – A battery subjected to a pulsed current with (bottom) and without (top) a supercapacitor.....	67
Figure 5.10 – Energy storage options for different ASD power ratings.....	69
Figure 5.11 – Distribution of power fluctuation duration and size.	70
Figure 5.12 – An integrated supercapacitor and DC converter.....	71
Figure 5.13 – Discharge profile of integrated EDLC & DC-converter for different loads.	71
Figure 5.14 – A ride-through system for adjustable-speed drives.	74
Figure 6.1 – Simulated energy loss while discharging an EDLC bank balanced with resistors.....	78
Figure 6.2 – Simulated energy loss while discharging a bank balanced with zener diodes	78
Figure 6.3 – A series connection of EDLCs including active voltage balancing.	79
Figure 6.4 – Philosophy of voltage balancing with equalising current sources.....	80
Figure 6.5 – Buck-boost topology for active voltage balancing.	80
Figure 6.6 – Active voltage balancing for a series of EDLCs.	81
Figure 6.7 – Reducing component count by utilising parallel strings.	82

Figure 7.1 – Block diagram for a remote power generation system.	85
Figure 7.2 – Average daily usage of household power.	85
Figure 7.3 – Power generation system prototype.	86
Figure 7.4 – Fuel cell and supercapacitor current response to a 500 W step input load.	88
Figure 7.5 – System architecture of a ride-through system for adjustable-speed drives.	90
Figure 7.6 – Effect of load on ride-through time.	91
Figure 7.7 – Effect of load on recharge time.	92
Figure 7.8 – RTS response to a 100kW load.	92
Figure 7.9 – EV system architecture.	93
Figure 7.10 – The Volkswagen Bora HY.POWER.	94

1. Introduction

Electrochemical capacitors are currently called by a number of names: supercapacitor, ultracapacitor, or electrochemical double-layer capacitor. The list of different names is almost as large as the number of manufacturers, and since the technology is only currently beginning to find itself a market a universal term does not seem to have been agreed upon as yet. The term ‘supercapacitor’ finds itself in common usage, being the tradename of the first commercial devices made by Nippon Electric Company (NEC), but ‘ultracapacitor’ is also commonly used, originating from devices made by the Pinnacle Research Institute (PRI) for the US military. Within this thesis the technology will be referred to as much as possible by the term ‘electrochemical double-layer capacitor’, (EDLC), thus reducing reliance on the use of any commercial names, but sometimes the term ‘supercapacitor’ will be used for the sole purpose of reducing the tedium of repeated usage of the term ‘EDLC’. It should be understood that the two terms are used interchangeably, and that they both refer to a capacitor that stores electrical energy in the interface that lies between a solid electrode and an electrolyte.

While electrostatic capacitors have been used as energy storage elements for nearly a century, low capacitance values have traditionally limited them to low-power applications as components in analogue circuits, or at most as short-term memory backup supplies. Recent developments in manufacturing techniques have changed this, however, and with the ability to construct materials of high surface-area and electrodes of low resistance has come the ability to store more energy in the form of electric charge. This has combined with an understanding

of the charge transfer processes that occur in the electric double-layer to make high-power electrochemical capacitors possible.

EDLCs therefore represent a new breed of technology that occupies a niche amongst other energy storage devices that was previously vacant. They have the ability to store greater amounts of energy than conventional capacitors, and are able to deliver more power than batteries. The current position of the EDLC is easily visualised by means of a Ragone plot (Fig. 1.1), which graphically represents a device's energy and power capabilities.

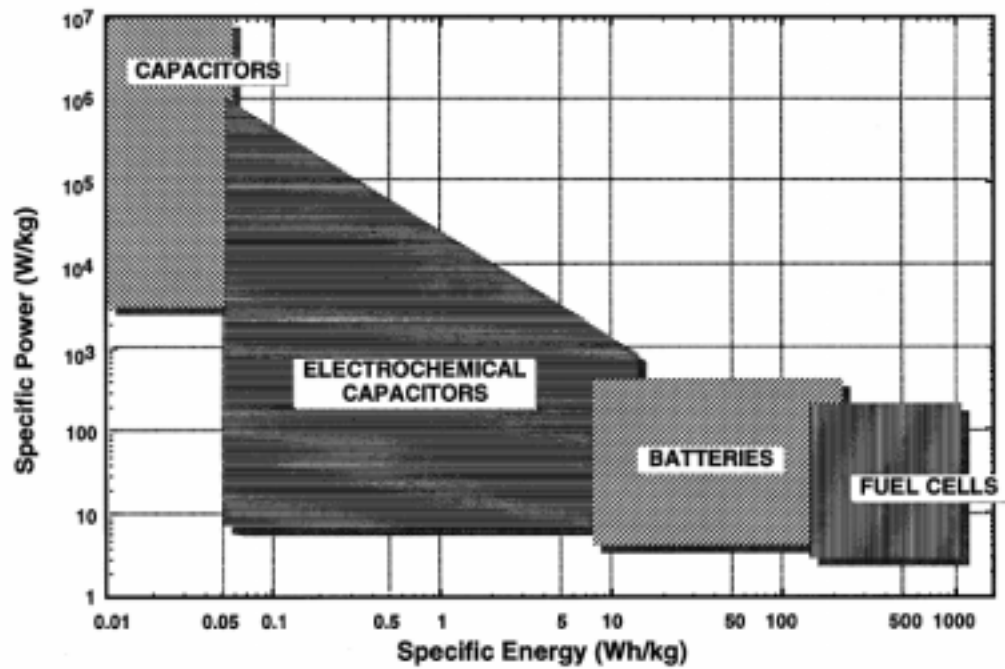


Figure 1.1 - Ragone plot of various energy storage devices [1].

Besides bridging the gap between capacitors and batteries, supercapacitors also possess a number of desirable qualities that make them an attractive energy storage option. The mechanisms by which EDLCs store and release charge are completely reversible, so they are extremely efficient and can withstand a large number of charge/discharge cycles. They can store or release energy very quickly, and can operate over a wide range of temperatures.

Supercapacitors have only very recently begun to make themselves known as a viable energy storage alternative, and while most electrical engineers may be aware of the technology it is probable that few possess an understanding of the processes involved and the applications that are possible. Ignorance of the full capabilities of EDLCs will most likely lead to more conventional alternatives being selected instead.

It is therefore the aim of this thesis to present a complete overview of electrochemical double-layer capacitor technology for the purpose of fostering a better understanding within the engineering community. This work will cover various aspects of the technology relevant to the field of electrical engineering, providing an introduction and a firm foundation from which to embark on further endeavours. The content of this thesis is intended for use by practising electrical engineers or engineering students who wish to become more informed about this new technology.

This survey will cover the historical development of supercapacitors, and draw a brief picture of the current state of the technology. The scientific principles behind the device's operation will be covered, and various theories and models will be discussed. Applications which make good use of the EDLC's best properties will be considered, and their advantages over alternative technologies will be presented. Design considerations will be outlined and illustrated with examples, and conclusions about the future direction of the technology will be drawn.

1.1 Historical background

The storage of electrical charge in the interface between a metal and an electrolytic solution has been studied by chemists since the nineteenth century, but the practical use of double-layer capacitors only began in 1957, when a patent was placed by General Electric for an electrolytic capacitor using porous

carbon electrodes (Fig. 1.2) [2]. Although the patent admits that “it is not positively known exactly what takes place when the devices... are used as energy storing devices,” it was believed that energy was being stored in the pores of the carbon, and it was noted that the capacitor exhibited an “exceptionally high capacitance.” Later, in 1966, The Standard Oil Company, Cleveland, Ohio (SOHIO) patented a device that stored energy in the double-layer interface (Fig. 1.3) [3]. At this time SOHIO acknowledged that “the ‘double-layer’ at the interface behaves like a capacitor of relatively high specific capacity.” SOHIO went on to patent a disc-shaped capacitor in 1970 utilising a carbon paste soaked in an electrolyte (Fig. 1.4) [4]. By 1971, however, a subsequent lack of sales led SOHIO to abandon further development and license the technology to NEC [5]. NEC went on to produce the first commercially successful double-layer capacitors under the name “supercapacitor.” These low voltage devices had a high internal resistance and were thus primarily designed for memory backup applications, finding their way into various consumer appliances [6].

By the 1980’s a number of companies were producing electrochemical capacitors. Matsushita Electric Industrial Co., (otherwise known as Panasonic in the Western world), had developed the “Gold capacitor” since 1978. Like those produced by NEC, these devices were also intended for use in memory backup applications [7]. By 1987 ELNA had begun producing their own double-layer capacitor under the name “Dynacap” [8]. The first high-power double-layer capacitors were developed by PRI. The “PRI Ultracapacitor,” developed from 1982, incorporated metal-oxide electrodes and was designed for military applications such as laser weaponry and missile guidance systems [9]. News of these devices triggered a study by the United States Department of Energy (DoE) in the context of hybrid electric vehicles, and by 1992 the DoE Ultracapacitor Development Program was underway at Maxwell Laboratories [10].

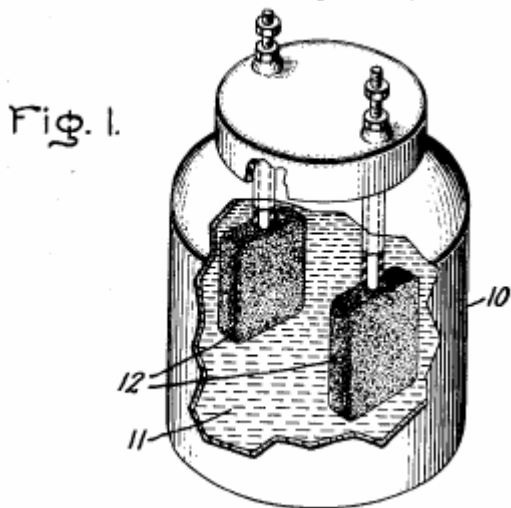


Figure 1.2 - The capacitor patented by General Electric [2].

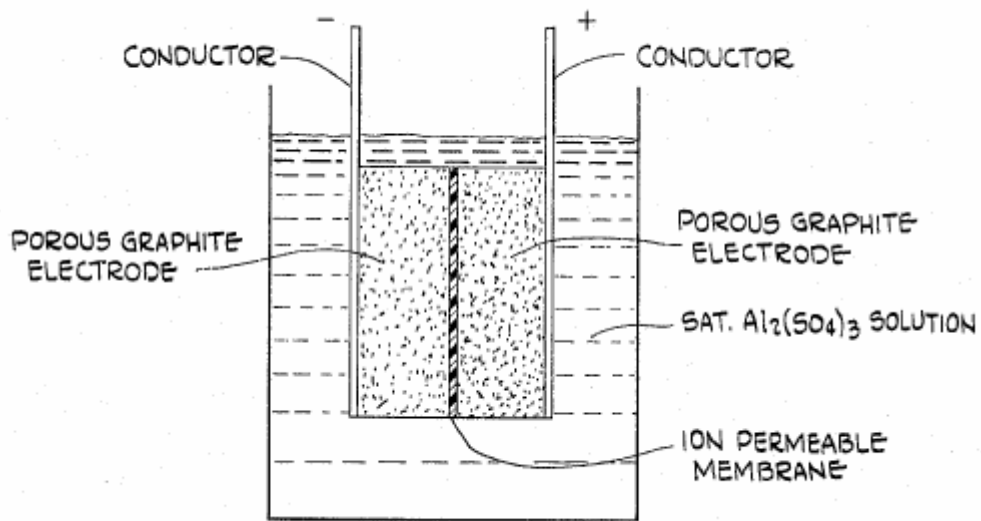


Figure 1.3 - An electrolytic energy storage device patented by SOHIO [3].

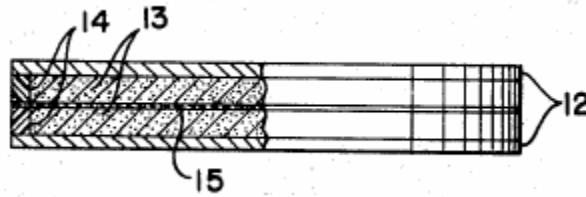


Figure 1.4 - A capacitor patented by SOHIO [4].

1.2 Current commercial activity

A number of companies around the world currently manufacture EDLCs in a commercial capacity. NEC and Panasonic in Japan have been producing EDLC components since the 1980's. In the U.S.A Epcos, ELNA, AVX, and Cooper produce components, while Evans and Maxwell produce integrated modules that include voltage balancing circuitry. Kold Ban International markets a supercapacitor module designed specifically for starting internal combustion engines in cold weather. Cap-XX in Australia offers a range of components, as does Ness Capacitor Co. in Korea. In Canada, Tavrma manufactures a range of modules. ESMA in Russia sells a wide variety of EDLC modules for applications in power quality, electric vehicles, and for starting internal combustion engines.



Figure 1.5 - A range of EDLCs sold by Ness Capacitor Co. in Korea [11].

The products currently available from present manufacturers as detailed on their websites are summarised in Table 1.

Company name	Country	Device name	Capacitance range (F)	Voltage range (V)	Web address
AVX	USA	Bestcap	0.022 - 0.56	3.5 - 12	http://www.avxcorp.com
Cap-XX	Australia	Supercapacitor	0.09 - 2.8	2.25 - 4.5	http://www.cap-xx.com
Cooper	USA	PowerStor	0.47 - 50	2.3 - 5	http://www.powerstor.com
ELNA	USA	Dynacap	0.033 - 100	2.5 - 6.3	http://www.elna-america.com/index.htm
ESMA	Russia	Capacitor modules	100 - 8000	12 - 52	http://www.esma-cap.com/?lang=English
Epcos	USA	Ultracapacitor	5 - 5000	2.3, 2.5	http://www.epcos.com
Evans	USA	Capattery	0.01 - 1.5	5.5, 11	http://www.evanscap.com
Kold Ban	USA	KAPower	1000	12	http://www.koldban.com
Maxwell	USA	Boostcap	1.8 - 2600	2.5	http://www.maxwell.com
NEC	Japan	Supercapacitor	0.01 - 6.5	3.5 - 12	http://www.nec-tokin.net
Ness	Korea	EDLC	10 - 3500	3	http://www.nesscap.com
Panasonic	Japan	Gold capacitor	0.1 - 2000	2.3 - 5.5	http://www.maco.panasonic.co.jp
Tavrma	Canada	Supercapacitor	0.13 - 160	14 - 300	http://www.tavrma.com

Table 1 - Summary of current EDLC's commercially available.

1.3 Current research efforts

Research is currently being conducted at a number of institutions in the interests of improving both the energy and power densities of EDLC technology. Activated carbons are the most commonly used electrode material in commercial supercapacitors at present, and a good deal of research is interested in determining the factors that contribute to the specific capacitance and series resistance in such materials. The Université Henri Poincaré-Nancy in France has performed research on the correlation between the porous electrode structure and series resistance [12]. Other work done by another French laboratory at the Conservatoire National de Arts et Métiers confirms the impact of pore size distribution on specific capacitance [13].

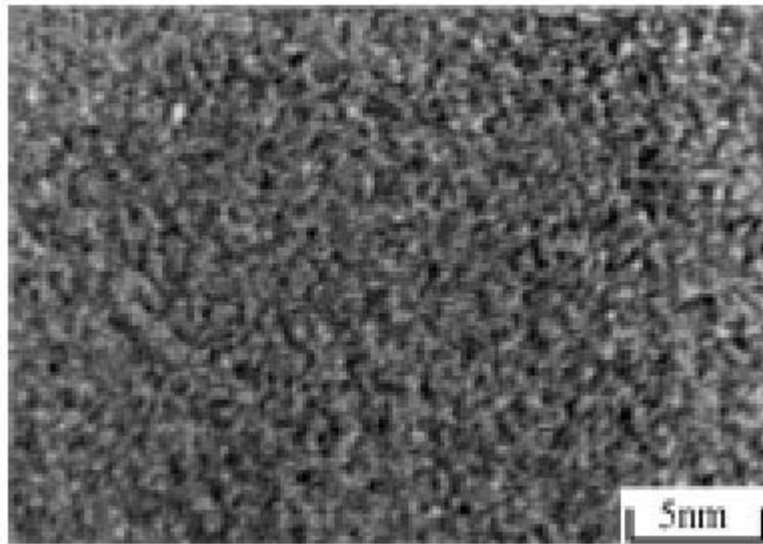


Figure 1.6 - TEM image of an activated carbon electrode [5].

Nanotubular carbons have been explored recently, and a number of academic institutions such as the Poznan University of Technology, Poland, and Sungkyunkwan University in Korea have constructed electrodes that demonstrate a higher specific capacitance than that achievable by activated carbons [14, 15]. Studies at the Chinese Academy of Science have taken this a step further and shown that activated carbon nanotubes have an even higher

specific capacitance than normal carbon nanotubes [16]. Considerable interest has also been shown in conducting polymer materials, and research suggests that high specific capacitances should be attainable [17].

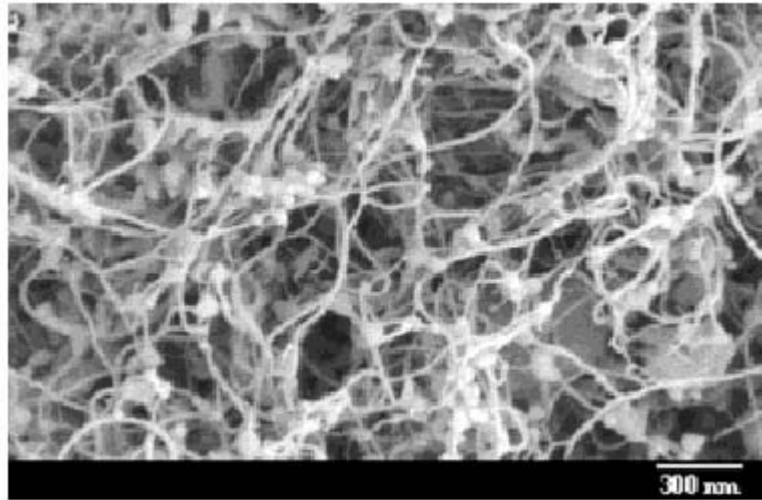


Figure 1.7 – FE-SEM image of carbon nanotubes [14].

Metal-oxides have always been an attractive electrode material due to their low resistance and high specific capacitance, but their excessive cost has generally ruled them out as a commercially viable option. Traditionally a strong sulfuric acid has been used as an electrolyte with metal-oxide electrodes in order to increase the ion mobility, and hence the rate of charge and discharge. This limits, however, the choice of electrode materials because most become unstable and corrode in a strongly acidic electrolyte. Research at the University of Texas, USA, has therefore focused on the possibility of using a milder, potassium-chloride aqueous electrolyte for use with metal-oxides. The work suggests that the replacement is indeed possible, and should widen the availability of possible electrode materials. Manganese-oxide, a cheaper alternative to ruthenium-oxide, has been confirmed as a good electrode candidate by the Imperial College, London, [18].

The most promising results seem to lie in the use of hybrid configurations, which consist of activated carbons and conducting polymers or metal-oxides. Studies at the University of Bologna, Italy have resulted in a supercapacitor that has a positive activated carbon electrode and a negative polymer electrode that outperforms configurations solely using activated carbon [19]. Work at the National Cheng Kung University in Taiwan indicates that high specific capacitance can be achieved by the deposition of conducting polymers onto activated carbon [20]. Frackowiak et al. at the Poznan University of Technology have demonstrated an increase in specific capacitance of carbon nanotubes coated with a polymer [21].

Also of interest is the study of solid-state supercapacitors being conducted at the University of Twente in The Netherlands, in which yttria-stabilised zirconia is used instead of a liquid electrolyte [22].

1.4 Future research

Activated carbons currently dominate the market as an electrode material, but progress in the development of conducting polymers and metal oxides is continuing at a steady rate. The exploitation of pseudocapacitive effects to enhance double-layer capacitance seems to be a prevalent goal amongst current researchers, and offers a good chance of developing the next generation of high-power, high-energy supercapacitors.

The scientific principles behind what occurs in an electric double-layer will now be explained, and factors regarding the physical materials used in EDLC fabrication will be discussed.

2. Principles of Operation

Supercapacitors are able to be developed as energy storage devices based on an understanding of the physical processes that take place. This chapter covers the scientific principles that lie behind the capabilities of the EDLC.

2.1 *Basic scientific principles*

Electrochemical capacitors operate on principles similar to those of conventional electrostatic capacitors. It is therefore instructive to undertake a brief review of electrostatic capacitor operation.

A conventional capacitor stores energy in the form of electrical charge, and a typical device consists of two conducting materials separated by a dielectric (Fig. 2.1). When an electric potential is applied across the conductors electrons begin to flow and charge accumulates on each conductor. When the potential is removed the conducting plates remain charged until they are brought into contact again, in which case the energy is discharged. The amount of charge that can be stored in relation to the strength of the applied potential is known as the capacitance, and is a measure of a capacitor's energy storage capability. Equations 2.1 & 2.2 apply to an electrostatic capacitor.

$$C = \frac{Q}{V} = \epsilon \frac{A}{d} \quad (2.1)$$

$$U = \frac{1}{2} CV^2 = \frac{1}{2} QV \quad (2.2)$$

C is capacitance in Farads, Q charge in Coulombs, V is electric potential in Volts, ϵ is the dielectric constant of the dielectric, A is conductor surface area, d is dielectric thickness, and U is the potential energy.

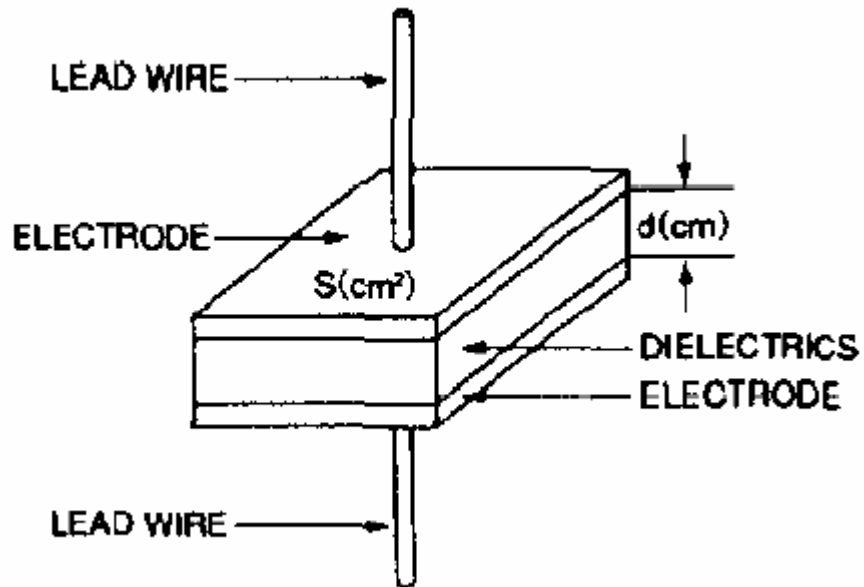


Figure 2.1 - Electrostatic capacitor topology [23].

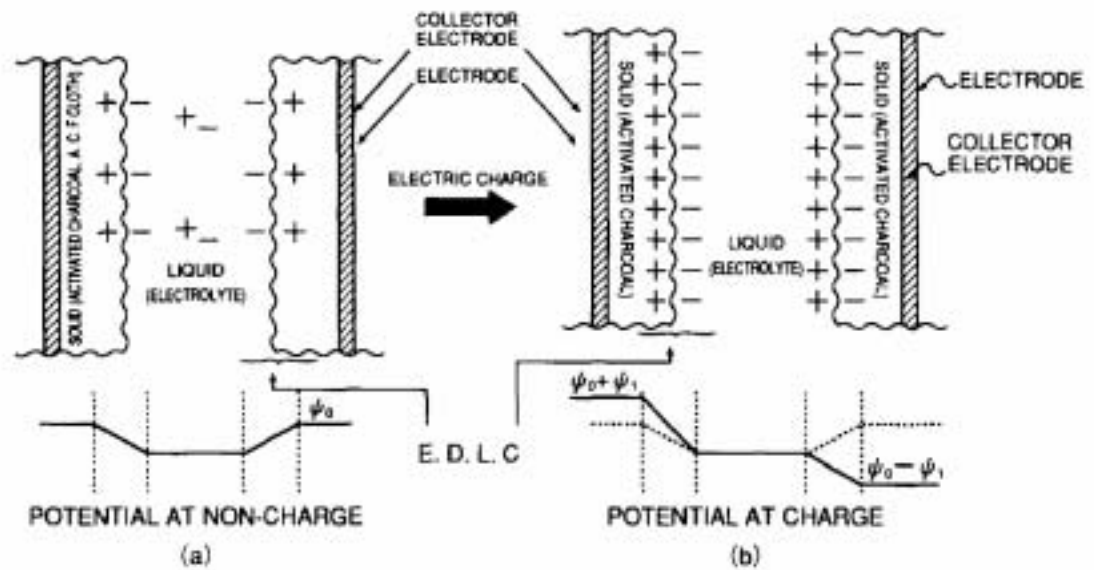


Figure 2.2 - EDLC charge storage mechanism [23]

EDLCs store electrical charge in a similar manner, but charge does not accumulate on two conductors separated by a dielectric. Instead the charge accumulates at the interface between the surface of a conductor and an

electrolytic solution (Fig. 2.2). The accumulated charge hence forms an electric double-layer, the separation of each layer being of the order of a few Angstroms. An estimate of the capacitance can be obtained from the double-layer model proposed by Helmholtz in 1853, in which the double-layer consisted of two charge monolayers. One layer forms on the charged electrode, and the other layer is comprised of ions in the electrolyte. The specific capacitance of such a double-layer given by Equation 2.3.

$$\frac{C}{A} = \frac{\epsilon}{4\pi\delta} \quad (2.3)$$

C is the capacitance, A is the surface area, ϵ is the relative dielectric constant of the medium between the two layers (the electrolyte), and δ is the distance between the two layers (the distance from the electrode surface to the centre of the ion layer) [5]. This approximation is roughly correct for concentrated electrolytic solutions.

Supercapacitor devices consist of two electrodes to allow a potential to be applied across the cell, and there are therefore two double-layers present, one at each electrode/electrolyte interface. An ion-permeable separator is placed between the electrodes in order to prevent electrical contact, but still allows ions from the electrolyte to pass through (Fig. 2.3). The electrodes are made of high effective surface-area materials such as porous carbon or carbon aerogels in order to maximise the surface-area of the double-layer. High energy densities are therefore achievable in EDLCs due to their high specific capacitance, attained because of a high electrode/electrolyte interface surface-area and a small charge layer separation of atomic dimensions.

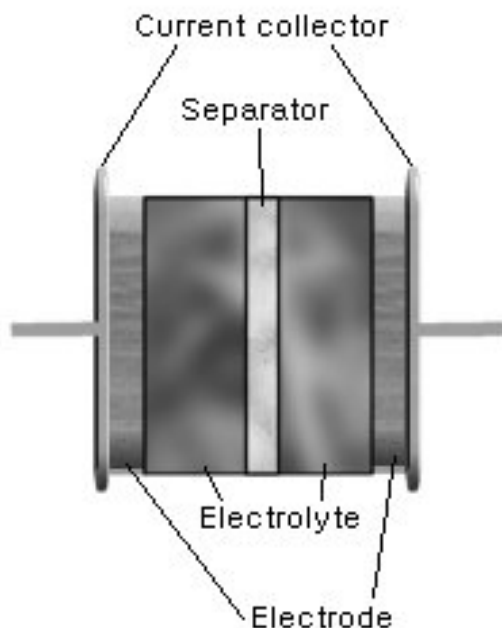


Figure 2.3 - Conceptual diagram of EDLC construction.

In addition to the capacitance that arises from the separation of charge in the double-layer, a contribution to capacitance can be made from reactions that can occur on the surface of the electrode. The charge required to facilitate these reactions is dependent on the potential, resulting in a Faradaic ‘pseudocapacitance’. Due to the fundamental differences between double-layer capacitance and pseudocapacitance the two topics shall be discussed separately.

2.2 The electric double-layer

The understanding of the electrical processes that occur at the boundary between a solid conductor and an electrolyte has developed gradually. Various models have been developed over the years to explain the phenomena observed by chemical scientists.

2.2.1 Helmholtz’s double layer

When Helmholtz first coined the phrase “double layer” in 1853, he envisioned two layers of charge at the interface between two dissimilar metals. Later, in

1879, he compared this metal/metal interface with a metal/aqueous solution interface [24]. In this model, the interface consisted of a layer of electrons at the surface of the electrode, and a monolayer of ions in the electrolyte (Fig. 2.4). In surface science it is often useful to work in terms of differential capacitance, defined by Equation 2.4.

$$C = \frac{\partial \sigma}{\partial E} \quad (2.4)$$

σ is the charge density and E is the electric potential. According to the Helmholtz model the differential capacitance is given by Equation 2.5.

$$C_1 = \frac{\epsilon}{4\pi\delta} \quad (2.5)$$

C_1 is the differential capacitance predicted by the Helmholtz model, and is a constant value dependent only on dielectric constant and charge layer separation.

2.2.2 The Gouy-Chapman model

In the early 1900's, Gouy considered observations that capacitance was not a constant and that it depended on the applied potential and the ionic concentration. To account for this behaviour Gouy proposed that thermal motion kept the ions from accumulating on the surface of the electrode, instead forming a diffuse space charge (Fig. 2.5). To formulate this model the Poisson equation was used to relate potential to charge density, and the Boltzmann equation was used to determine the distribution of ions. Ions were thus considered as point charges with no volume. Gouy's theory results in a differential capacitance described by Equation 2.6.

$$C_G = \frac{\epsilon\kappa}{4\pi} \cosh \frac{z}{2} \quad (2.6)$$

In Equation 2.6, z is the valency of the ions and κ is the reciprocal Debye-Hückel length defined by Equation 2.7.

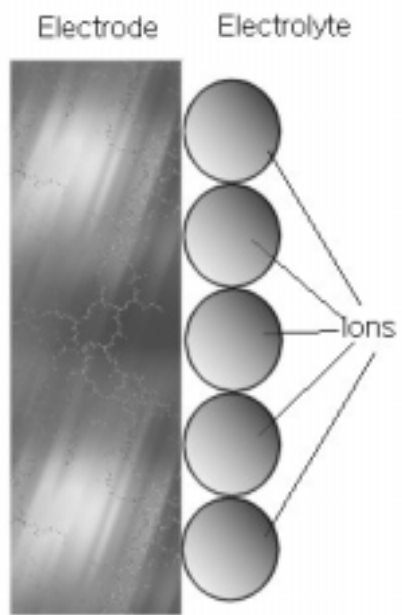


Figure 2.4 - Helmholtz double layer model.

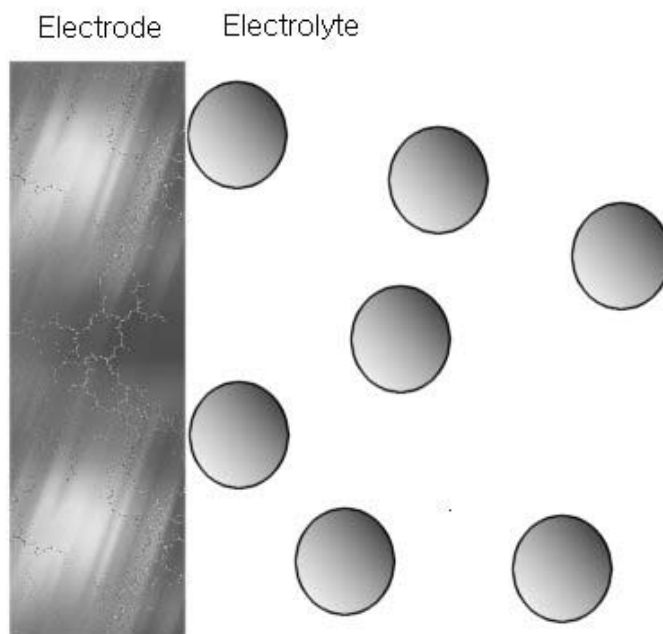


Figure 2.5 – Gouy-Chapman diffuse model.

$$\kappa = \sqrt{\frac{8\pi n e^2 z^2}{\epsilon k T}} \quad (2.7)$$

n is the number of ions per cubic centimetre, T is the absolute temperature, and k is the Boltzmann constant [24]. The capacitance, C_G , resulting from the diffuse charge distribution is therefore no longer a constant.

This model was also worked on by D.C. Chapman, and is today referred to as the Gouy-Chapman model.

2.2.3 Stern and Grahame

In 1924, Stern modified the Gouy-Chapman model by including a compact layer as well as Gouy's diffuse layer. The compact Stern layer consisted of a layer of specifically adsorbed ions [25]. Grahame divided the Stern layer into two regions. He denoted the closest approach of the diffuse ions to the electrode surface as the outer Helmholtz plane (this is sometimes referred to as the Gouy plane). The layer of adsorbed ions at the electrode surface was designated as being the inner Helmholtz plane (Fig. 2.6).

Grahame combined the capacitance resulting from the Stern layer, C_1 (Eq. 2.5), and that resulting from the diffuse layer, C_G (Eq. 2.6). The total capacitance is then described by Equation 2.8.

$$\frac{1}{C} = \frac{1}{C_1} + \frac{1}{C_G} \quad (2.8)$$

Equation 8 becomes invalid if specific adsorption of ions occurs, however, and if this is the case, the capacitance is equated by Equation 2.9.

$$\frac{1}{C} = \frac{1}{C_1} + \frac{1}{C_G} \left(1 + \frac{\partial \sigma_A}{\partial \sigma} \right) \quad (2.9)$$

σ is charge density on the electrode, and σ_A is the surface charge of the adsorbed ions [24].

This model has not been significantly improved upon since its formulation, but any capacitive effects that may result from dipoles interacting with the charged electrode surface are not considered in this model.

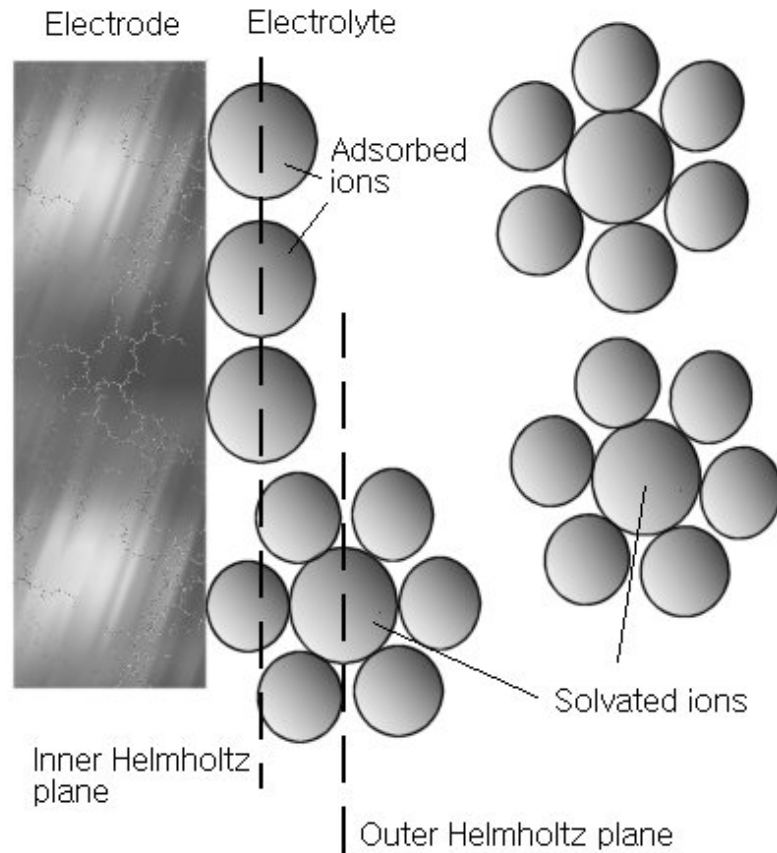


Figure 2.6 - Stern-Grahame model.

2.2.4 The current model

In 1963 Bockris, Devanathan and Muller proposed a model that included the action of the solvent [25]. They suggested that a layer of water was present within the inner Helmholtz plane at the surface of the electrode. The dipoles of these molecules would have a fixed alignment because of the charge in the electrode. Some of the water molecules would be displaced by specifically adsorbed ions. Other layers of water would follow the first, but the dipoles in these layers would not be as fixed as those in the first layer (Fig. 2.7).

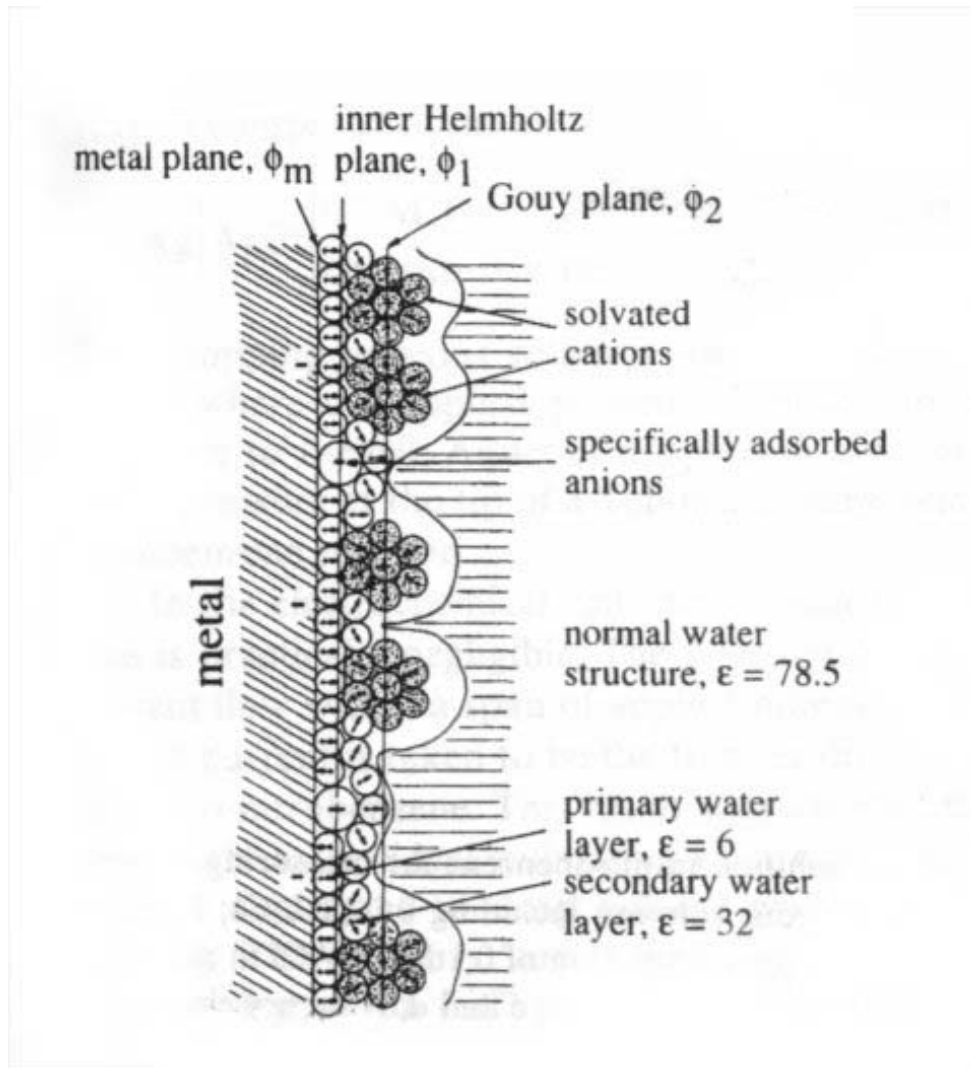


Figure 8 - A double layer model including layers of solvent [25].

2.3 Pseudocapacitance

Pseudocapacitance arises from reversible Faradaic reactions occurring at the electrode, and is denoted as ‘pseudo’-capacitance in order to differentiate it from electrostatic capacitance. The charge transfer that takes place in these reactions is voltage dependent, so a capacitive phenomenon occurs. There are two types of reactions that can involve a charge transfer that is voltage dependent.

2.3.1 Redox reactions

In a redox reaction involving an oxidant, *ox*, and reductant, *red*, of the form, $ox + ze^- \longleftrightarrow red$, the potential, E , is given by the Nernst equation as shown in Equation 2.10.

$$E = E^0 + \frac{RT}{zF} \ln \frac{\mathfrak{R}}{1 - \mathfrak{R}} \quad (2.10)$$

E^0 is the standard potential, R is the gas constant, T is the absolute temperature, F is the Faraday constant, and \mathfrak{R} is defined as $[ox] / ([ox] + [red])$, (where square brackets denote species concentrations). The amount of charge q (given by the product zF), is therefore a function of the potential E . Differentiation of Equation 2.10 thus produces a pseudocapacitive relation [26].

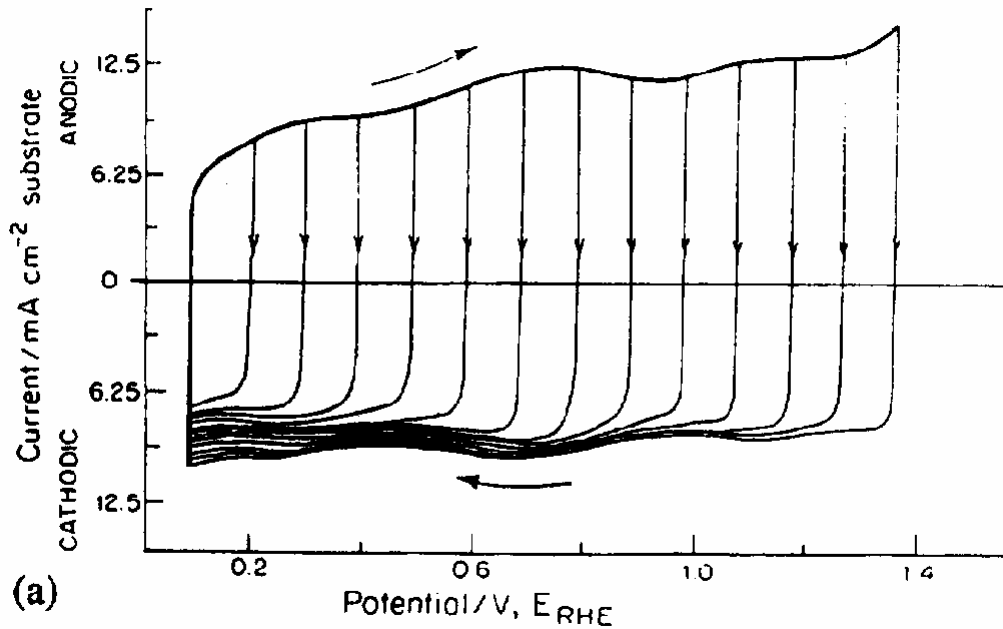


Figure 2.8 - Cyclic voltammogram of a ruthenium-oxide electrode in sulfuric acid electrolyte [26].

Redox pseudocapacitance in ruthenium-oxides was studied at the University of Ottawa, Canada. In Figure 2.8 the voltage/current characteristic demonstrates

the highly reversible nature of the Faradaic redox reactions. The charge/discharge curve is a result of overlapping redox reactions, as well as a significant double-layer capacitance due to the porous structure of the hydrous oxide [26].

2.3.2 Adsorption of ions

The deposition of ions to form a monolayer on the electrode substrate is a reversible process that results in a Faradaic charge transfer, and hence gives rise to pseudocapacitance in a similar manner to that demonstrated in redox reactions. The adsorption/desorption process can be written as Equation 2.11,



where A is the ionic species, S is the substrate, c is the concentration of depositable ions, $1-\theta_A$ is the fractional free surface area available for adsorption at a coverage, θ_A , and V is the electrode potential [27].

If it assumed that sites are occupied randomly in a fixed lattice, an equation for coverage can be determined from the Langmuir adsorption equation. This yields the relation shown in Equation 2.12.

$$\frac{\theta_A}{1-\theta_A} = Kc \exp\left(\frac{-VF}{RT}\right) \quad (2.12)$$

K being the electrochemical equilibrium constant. A change in coverage $d\theta$ is directly proportional to the charge dq , expressed by Equation 2.13.

$$dq = q_l d\theta \quad (2.13)$$

where q_l is the amount of charge required to form or disperse a complete monolayer. Since θ is a function of V , differentiation of Equation 2.12 results in a pseudocapacitive relation described by Equation 2.14 [26].

$$C_\phi = \frac{q_l F}{RT} \frac{Kc \pm \exp\left(\frac{-VF}{RT}\right)}{\left(1 + Kc \pm \exp\left(\frac{-VF}{RT}\right)\right)^2} \quad (2.14)$$

Figure 2.9 shows the charging profile resulting from hydrogen being deposited and released from a platinum surface. The process is highly reversible, and a number of current peaks are evident. The peaks arise due to the formation of various H array configurations before the final monolayer is formed [26].

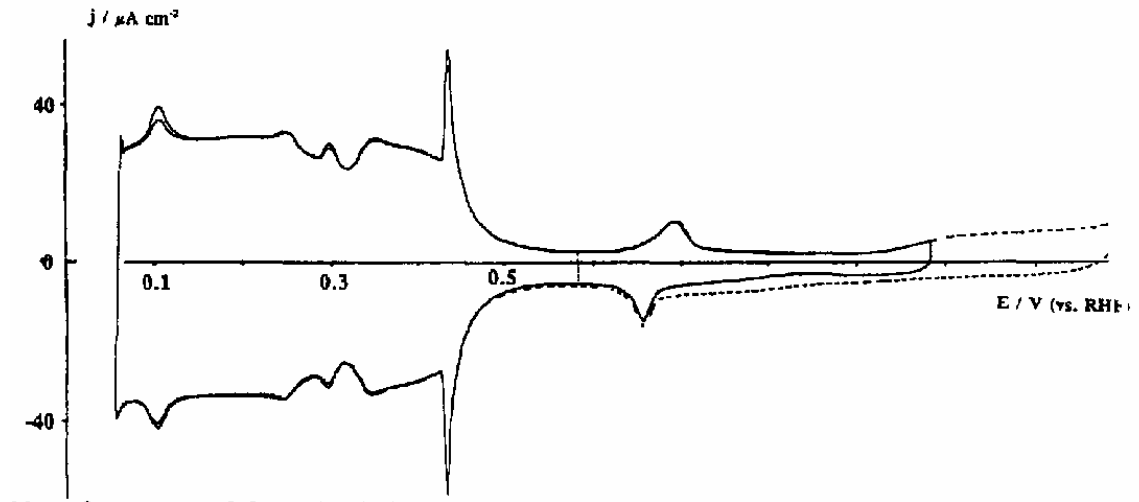


Figure 2.9 - Voltammetry of H adsorption and desorption on a Pt surface [26].

2.4 Summary of scientific background

The high values of specific capacitance attainable through EDLC technology are a result of double-layer capacitance, and often pseudocapacitance. Double-layer capacitance offers good charge storage capabilities thanks to possessing high surface-area materials as electrodes, and the fact that charge separation occurs at atomic dimensions. Pseudocapacitance that arises from redox or ion sorption reactions further improves the achievable capacitance.

3. Capacitor construction

A wide variety of EDLC materials and processes for cell construction currently exist. This chapter covers the properties of various available materials and describes the aspects of each alternative that have a significant impact on device performance.

3.1 *Electrode materials*

Selection of electrode materials plays a crucial role in determining the electrical properties of a supercapacitor. Double-layer charge storage is a surface process, and the surface characteristics of the electrode greatly influence the capacitance of the cell. Carbon is the most widely used electrode material, but considerable research is being conducted into metal-oxides and conducting polymers.

3.1.1 Carbon

Carbon has been utilised as a high surface area electrode material ever since development of the electrochemical capacitor began. Today, it is still an attractive option because of its low cost, availability, and long history of use. Carbon electrodes can take a number of manufactured forms such as foams, fibres, and nanotubes.

One might expect the specific capacitance to be directly proportional to the carbon electrode's surface area, however this is not always the case. Often, a type of carbon with a lower surface area will have a higher specific capacitance than a type with a larger surface area. This is because the actual double-layer capacitance varies depending on the process used to prepare the carbon.

Treatment of activated carbon materials influences the porous structure of the electrode surface, and it is the accessibility of the pores to the electrolyte that is important. The mobility of the ions within the pores is different to the mobility of ions in the bulk of the electrolytic solution, and is greatly influenced by pore size. If the pores are too small to allow easy access to electrolyte ions they will not contribute to double-layer capacitance. The pore size must therefore be chosen to suit the electrolyte and thereby ensure that the pore size distribution is optimal based upon the size of the ions [28]. In Figure 3.1 the effect of pore diameter on specific capacitance is clearly demonstrated, with smaller pores becoming completely inaccessible to the ions at high frequencies.

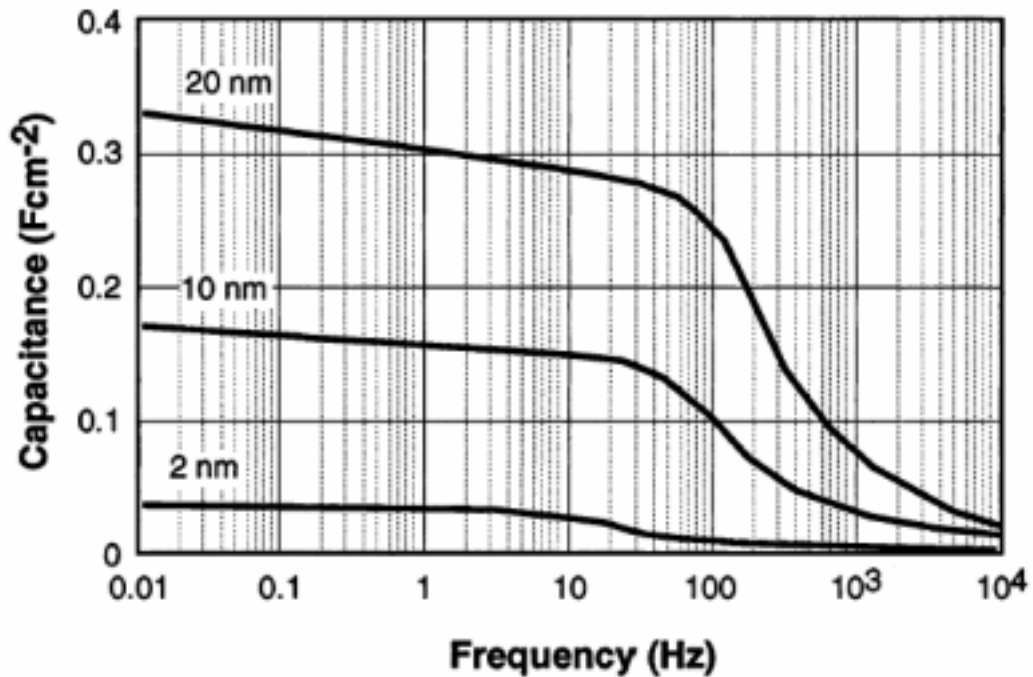


Figure 3.1 - Effect of pore diameter on specific capacitance [1].

The conductivity of the electrode is of great concern to the power density of an EDLC. Conductivity is inversely proportional to particle size, so a material of higher surface area and is therefore made of smaller particles develops an increased resistance. Power density is thus improved with the use of activated

carbons with more large pores, though this will limit energy storage due to reduced surface area. The use of binding material also affects conductivity, and power performance is improved with a decreased percentage of binder [28].

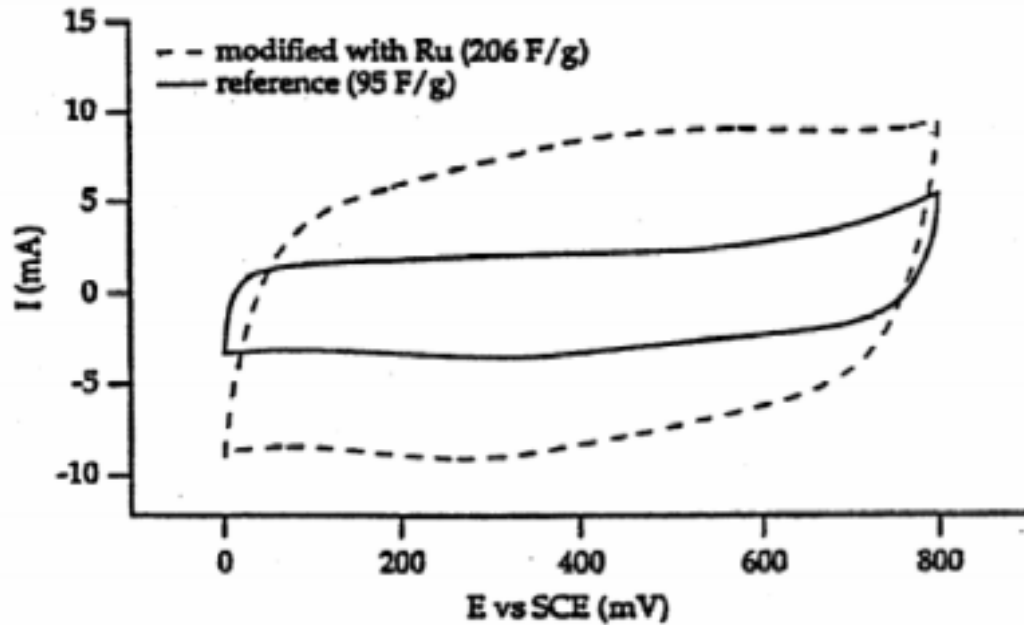


Figure 9 - Voltammetry plot of modified carbon electrodes [28].

Pseudocapacitive effects are often found to occur on the surface of activated carbons. The level of pseudocapacitance can be enhanced by treatment of the carbon to increase surface functionality. As an example, Frackowiak [28] cites the work of Miller in which the capacitance of activated carbon was enhanced by treatment with ruthenium oxides (Fig. 3.2).

Besides activated carbons, electrodes can also be formed from carbon aerogels. Aerogels are a suspension of carbon nanoparticles within a gel, and have a high surface-area, good conductivity, and may be used without binding material. Particle size is controlled by the preparation process, and smaller particles result in a larger accessible pore surface-area [28].

Nanotubes offer a new possibility for carbon electrodes, but are still being researched. Preliminary results suggest that higher capacitance is achieved by tangled networks with an open central canal (Fig. 3.3) [28].

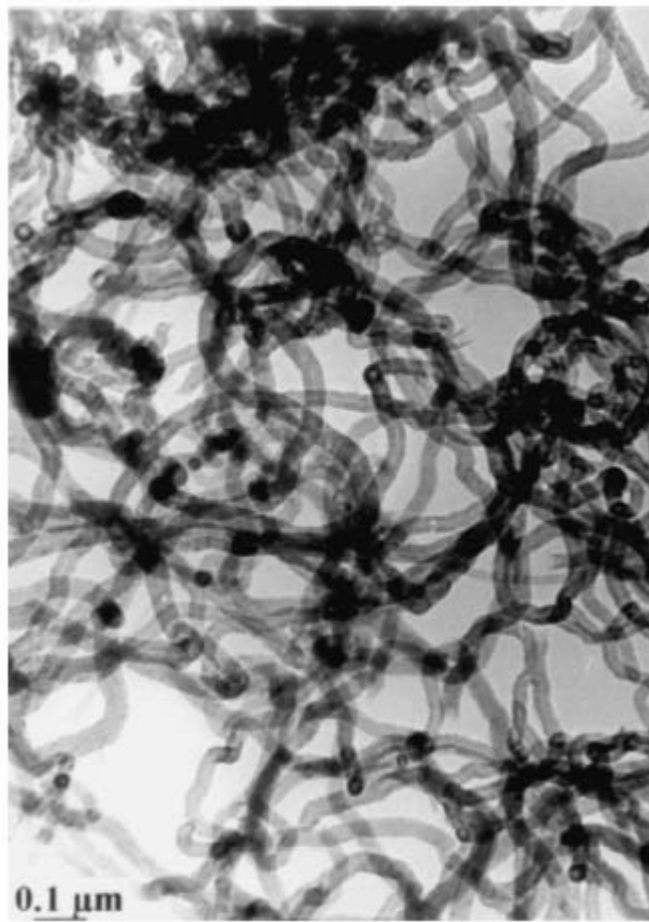


Figure 3.3 - Tangled network of carbon nanotubes [28].

3.1.2 Conducting polymers

Conducting polymers store and release charge through redox processes. When oxidation occurs, (also referred to as ‘doping’), ions are transferred to the polymer backbone. When reduction occurs (‘dedoping’) the ions are released back into the solution (Fig. 3.4). Charging in conducting polymer films therefore takes place throughout the bulk volume of the film, and not just on the surface as is the case with carbon. This offers the opportunity of achieving high levels of specific capacitance.

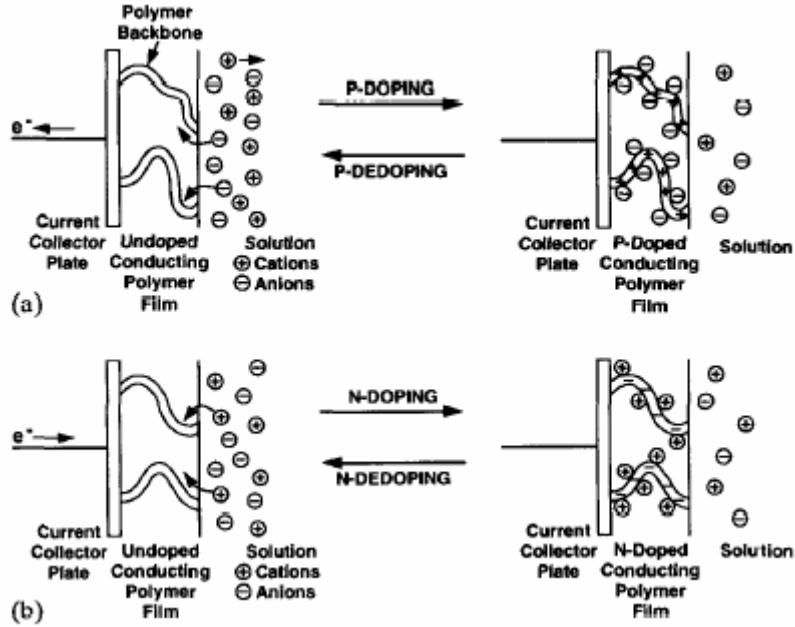


Figure 3.4 - Charging process of conducting polymer electrodes [29].

Work at the Los Alamos National Laboratory [30] has reported prototype polymer film capacitors with an energy density of 39 Wh/kg and a power density of 35 kW/kg (Fig. 3.5). The two peaks in the voltammetry plot of Figure 3.5 demonstrate that the charging process is predominately due to redox reactions, and only occurs within a narrow range of voltages in this particular case.

While long-term stability is expected to be a problem due to the phenomenon of swelling and shrinking in conducting polymers [1], some research has demonstrated stability over thousands of cycles [31].

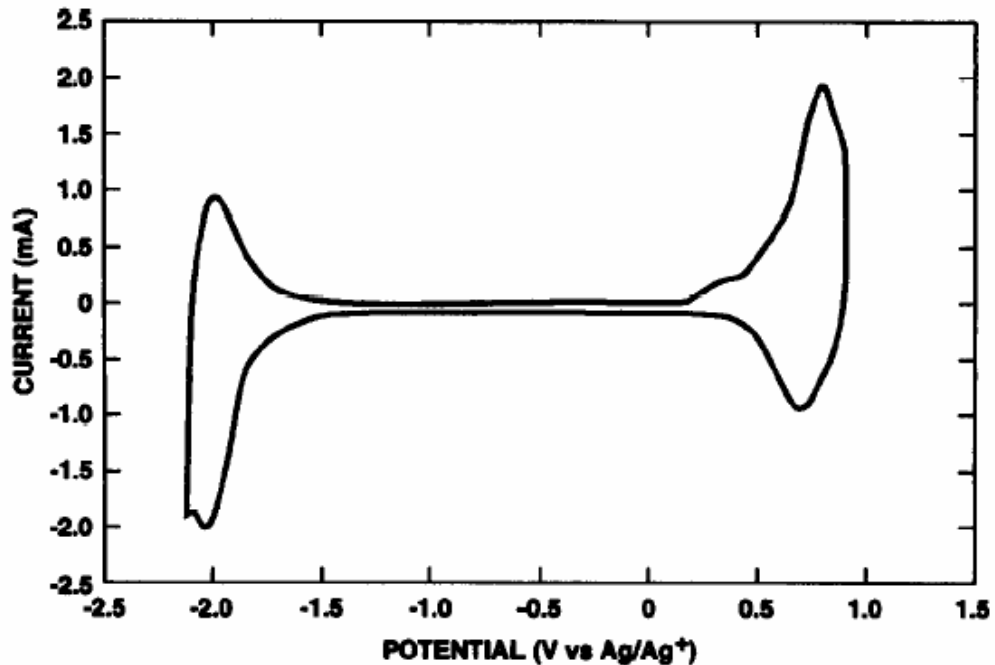


Figure 3.5 – Cyclic voltammogram of a polymer film [30].

3.1.3 Metal-oxides

Metal-oxides present an attractive alternative as an electrode material because of high specific capacitance and low resistance, possibly making it easier to construct high-energy, high-power EDLCs. Extensive research into ruthenium-oxides has been conducted for military applications, where cost is presumably less of an issue than it is for commercial ventures. The US Army Research Lab has assembled prototype cells with an energy density of 8.5 Wh/kg and a power density of 6 kW/kg [32].

Academic institutions have focused on searching for other, cheaper, materials to use instead of ruthenium-oxides, but the selection has traditionally been limited by the use of concentrated sulfuric acid as an electrolyte. It was believed high capacitance and fast charging was largely a result of H sorption, so a strong acid was therefore necessary to provide good proton conductivity. This resulted in a narrow range of possible electrode materials, however, since most metal-oxides break down quickly in acidic solutions. Milder aqueous solutions such as potassium chloride have therefore been considered for use with metal-oxides

such as manganese-oxides, and Figure 3.6 shows the charging profile of prototypes produced at the Imperial College, London. Although manganese-oxide electrodes currently appear to possess lower specific capacitances than ruthenium-oxides, the lower cost and milder electrolyte may be enough of an advantage to make them a viable alternative [33].

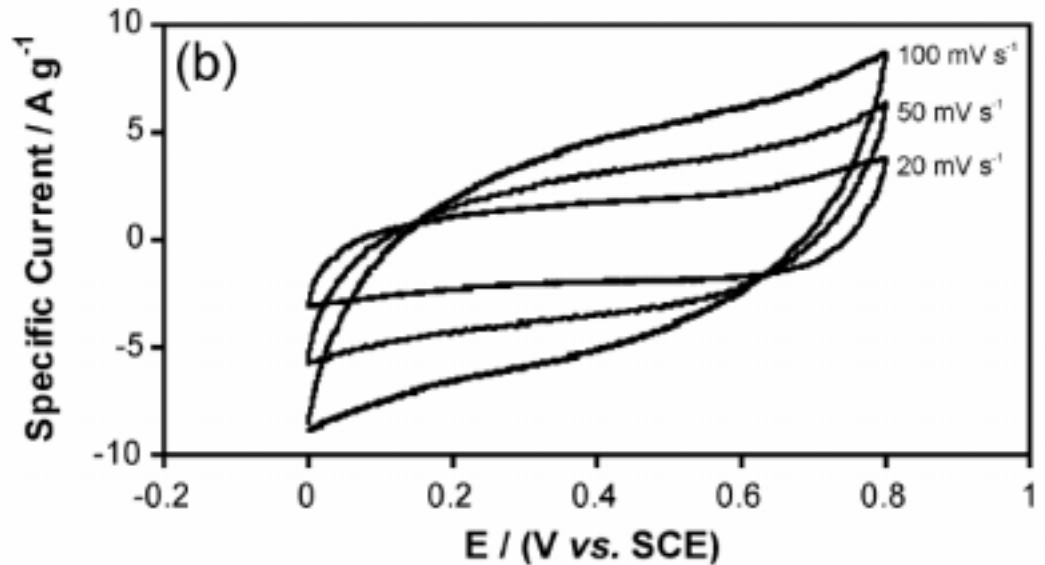


Figure 3.6 - Cyclic voltammogram for MnO film with KCl electrolyte [18].

Metal-oxide electrodes can only be used with aqueous electrolytes, thereby limiting the achievable cell voltage. Gains in power density from lower resistance are therefore often offset by losses due to the lower operating voltage.

3.1.4 Hybrid and composite configurations

Hybrid electrode configurations show considerable potential, consisting of two different electrodes made of different materials. Composite electrodes consist of one type of material incorporated into another within the same electrode.

In the course of research into polymer electrodes at the University of Bologna it was found that a sufficiently high polymer concentration could not be realised in the negative electrode. The positive polymer electrode was successfully

constructed, however, and an activated carbon was used as the negative electrode. This hybrid configuration resulted in a supercapacitor that outperformed a cell comprised of two carbon electrodes (Fig. 3.7) [34]. In Figure 3.7, \blacktriangle designates the hybrid capacitor, \bullet signifies the carbon capacitor, and the values represent current densities in mA/cm^2 .

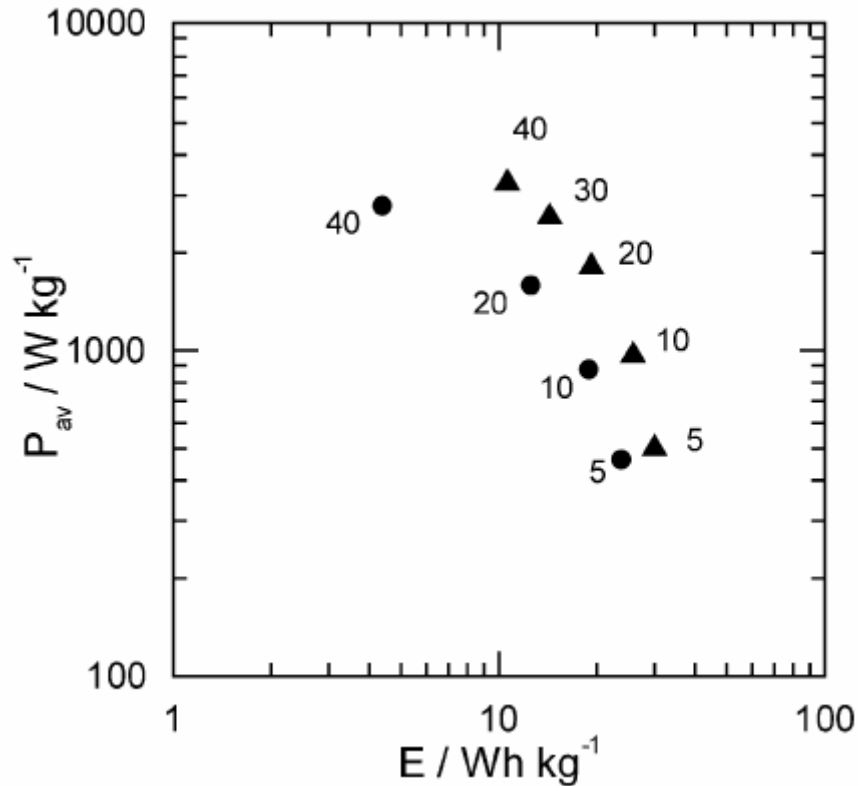


Figure 3.7 - Ragone plot of hybrid (\blacktriangle) and carbon (\bullet) supercapacitors [34].

Also of interest are the results of experiments into depositing polymers onto carbon substrates to form composite electrodes. Carbon nanotubes coated with conducting polymers have yielded particularly good results, with high specific capacitances of 180 F/g being reported [20, 21]. The improved levels of energy storage are a result of the charging taking place largely throughout the bulk of the material, along the surface of the nanotubes and along the backbone of the polymer. The pseudocapacitance arising from the redox processes in the polymer further enhances the capacitive gains.

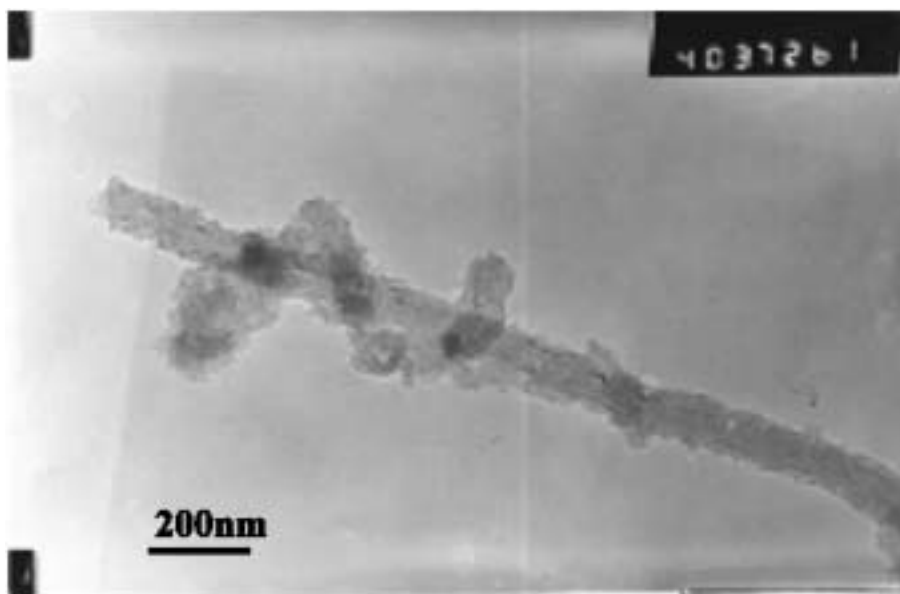


Figure 3.8 - A carbon nanotube coated in polypyrrole [35].

3.2 Electrolytes

The choice of electrolyte in an EDLC is as important as the choice of electrode material. The attainable cell voltage of a supercapacitor will depend on the breakdown voltage of the electrolyte, and hence the possible energy density (which is dependent on voltage) will be limited by the electrolyte. Power density is dependent on the cell's ESR, which is strongly dependent on electrolyte conductivity. There are currently two types of electrolyte in use in EDLCs: organic and aqueous.

Organic electrolytes are the most commonly used in commercial devices, due to their higher dissociation voltage. Cells using an organic electrolyte can usually achieve voltages in the range of 2 – 2.5 V. The resistivity of organic electrolytes is relatively high, however, limiting cell power. Aqueous electrolytes have a lower breakdown voltage, typically 1 V, but have better conductivity than organic electrolytes.

The capacitance of an EDLC is greatly influenced by the choice of electrolyte. The ability to store charge is dependent on the accessibility of the ions to the porous surface-area, so ion size and pore size must be optimal. The best pore size distribution in the electrode depends upon the size of the ions in the electrolyte, so both electrode and electrolyte must be chosen together.

3.3 Separator

The separator prevents the occurrence of electrical contact between the two electrodes, but it is ion-permeable, allowing ionic charge transfer to take place. Polymer or paper separators can be used with organic electrolytes, and ceramic or glass fibre separators are often used with aqueous electrolytes. For best EDLC performance the separator should have a high electrical resistance, a high ionic conductance, and a low thickness [36].

3.4 Summary of EDLC construction

The functional components of a supercapacitor crucial to its operation are the electrodes, electrolyte, and separator. The surface properties of the electrode material have a significant impact on specific capacitance, as do the chemical properties if pseudocapacitance is exhibited. While activated carbon is currently the most commonly used material, conducting polymers present a possible future alternative. Metal-oxides may also become viable one day. The choice of electrolyte has a significant impact on achievable power, as well as influencing specific capacitance. Aqueous electrolytes have better conductivity than organic electrolytes, but have a low breakdown voltage. The properties of the separator also have an impact on cell performance.

4. EDLC performance

The performance of an EDLC must be able to be evaluated quantitatively in order to make comparisons between different devices and technologies, and also to be able to ascertain the suitability of a particular device to a certain application. A number of methods for determining supercapacitor performance are therefore considered in this chapter. Various models of supercapacitor behaviour will then be presented.

4.1. Measurement techniques

4.1.1. Cyclic voltammetry

Cyclic voltammetry provides a measure of a supercapacitor's charge-response with regard to a changing voltage, and is therefore a means of evaluating capacitance. The procedure for obtaining a voltammogram is simple and requires no specialised equipment.

To perform cyclic voltammetry tests a series of changing voltages at a constant sweep rate (dV/dt) is applied and the response current is recorded. The capacitance can then be calculated by Equation 4.1, where I is the current and s is the sweep rate in V/s [37]. Often the voltammetry will be graphed as capacitance vs. voltage instead of current vs. voltage.

$$C = \frac{I}{s} \quad (4.1)$$

An ideal capacitor with no resistance would display a rectangular shape, but most real EDLC voltammograms take the shape of a parallelogram with

irregular peaks (Fig. 4.1). Prominent peaks that occur within narrow voltage windows are usually evidence of pseudocapacitive behaviour.

Faster sweep rates correspond to charging and discharging at higher power levels. Multiple plots obtained at increasing sweep rates are therefore often displayed on the same graph to demonstrate the impact of power levels on the charging characteristics (Fig. 4.2). From such plots it is evident that capacitance decreases at higher frequencies.

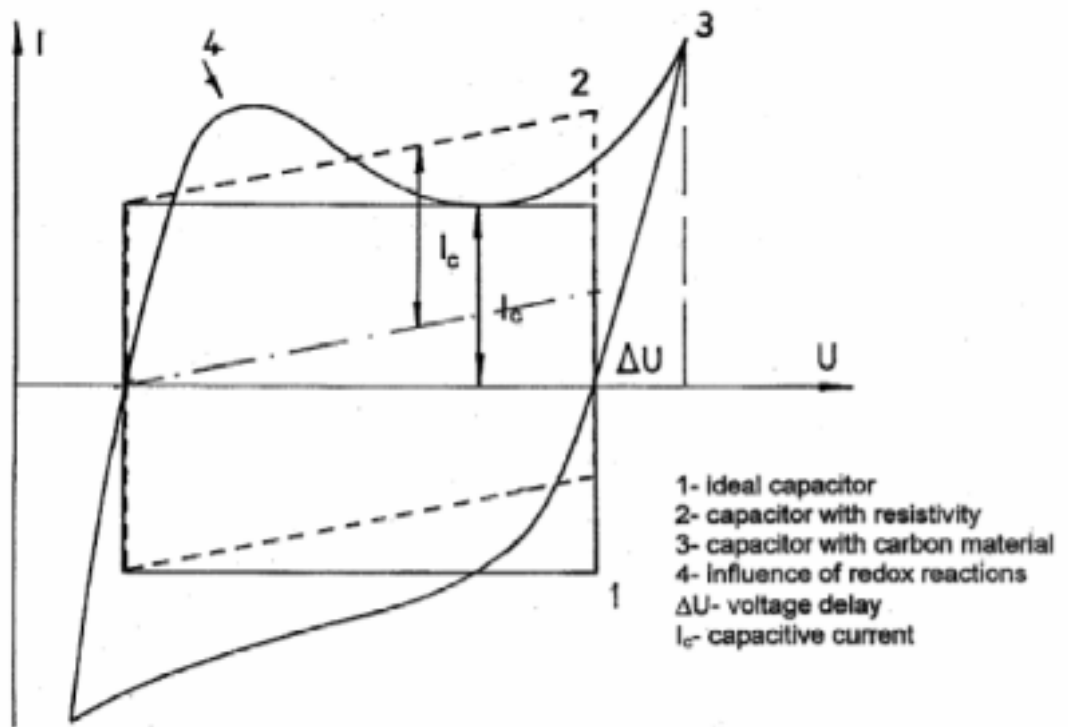


Figure 4.1 – Comparison of ideal and real cyclic voltammograms [28].

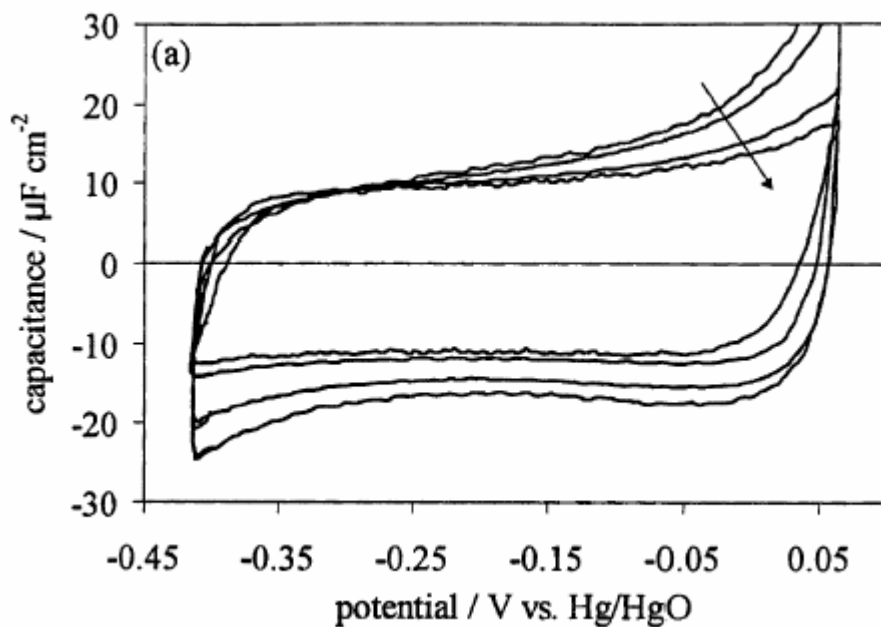


Figure 4.2 – Cyclic voltammograms at increasing sweep rates
(arrow is in direction of increasing sweep rate) [37].

Voltammetry can also provide an indication of the degree of reversibility of an electrode reaction. A voltammogram that depicts a mirror-image represents a reversible reaction, but an irreversible process will have two separate charge and discharge profiles, the ends of which do not meet up (Fig. 4.3). Reversibility is an important factor in the search for new materials.

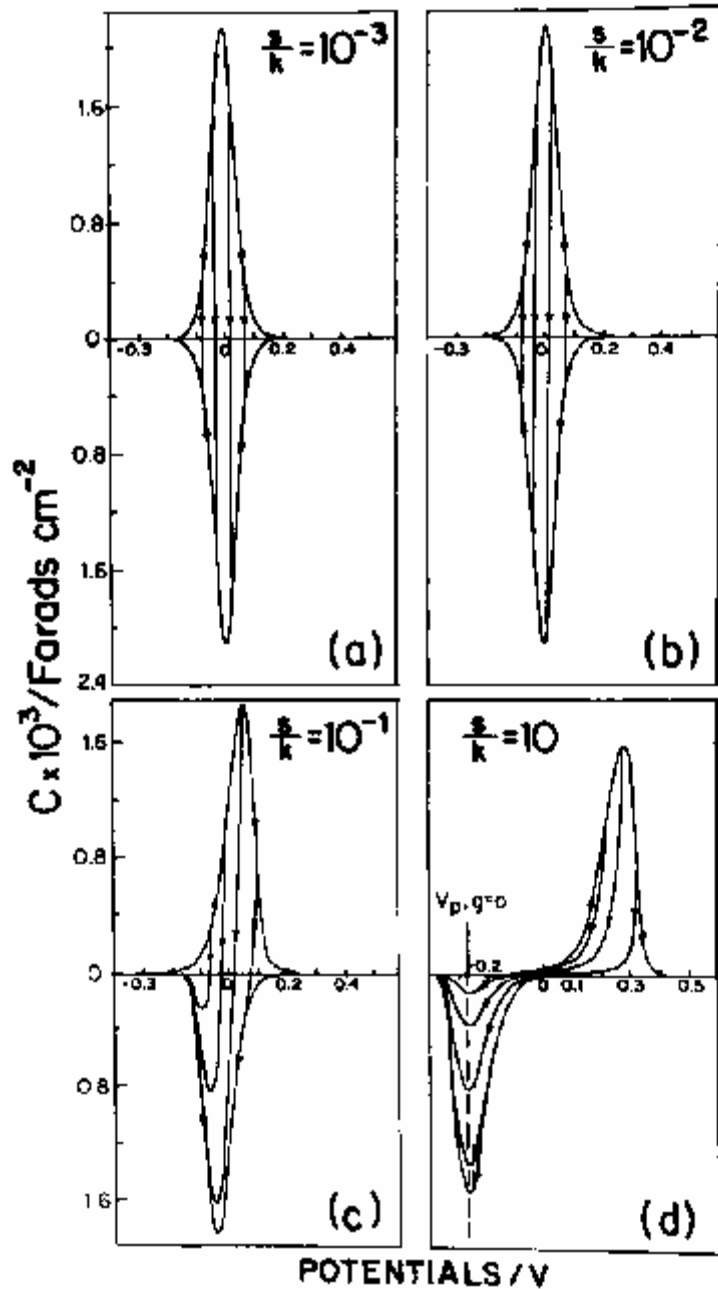


Figure 4.3 – Transition of an EDLC based on adsorption pseudocapacitance to irreversibility at higher sweep rates [38].

4.1.2. Constant-current charging and Ragone plots

A method of evaluating a supercapacitor's energy and power densities is to perform constant-current charging. Charging or discharging the cell at a

constant current results in a voltage response. The current integral, $\int i dt$, is therefore a measure of charge delivery, and power is then determined by the product $I \times V$, and energy by $\frac{1}{2} Q \times V$ [37]. If the EDLC is assumed to be a capacitance in series with an ESR, the ESR can be determined by the ratio of voltage change to current change. This procedure is only accurate at low currents, however, and there is a significant departure from predicted behaviour at higher currents [39].

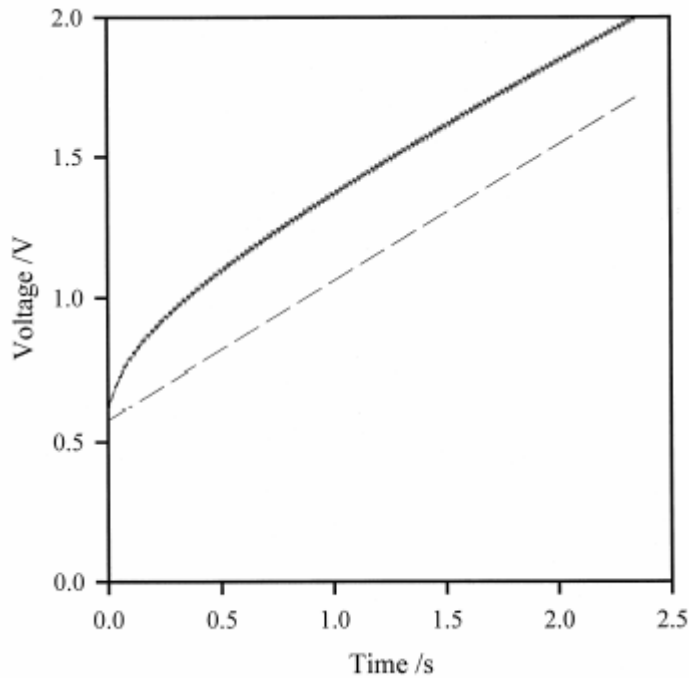


Figure 4.4 - Charging at 5A (solid line) compared to ideal RC behaviour (dashed line) [39].

The results of charging tests are often displayed in the form of Ragone plots, which graph power density against energy density and are an indication of an EDLC's energy storage capabilities at different power levels. A range of power and energy values are obtained by charging at different current values. Most devices exhibit a 'knee' shaped characteristic, with energy density rapidly decreasing at a critical power level (Fig. 4.5).

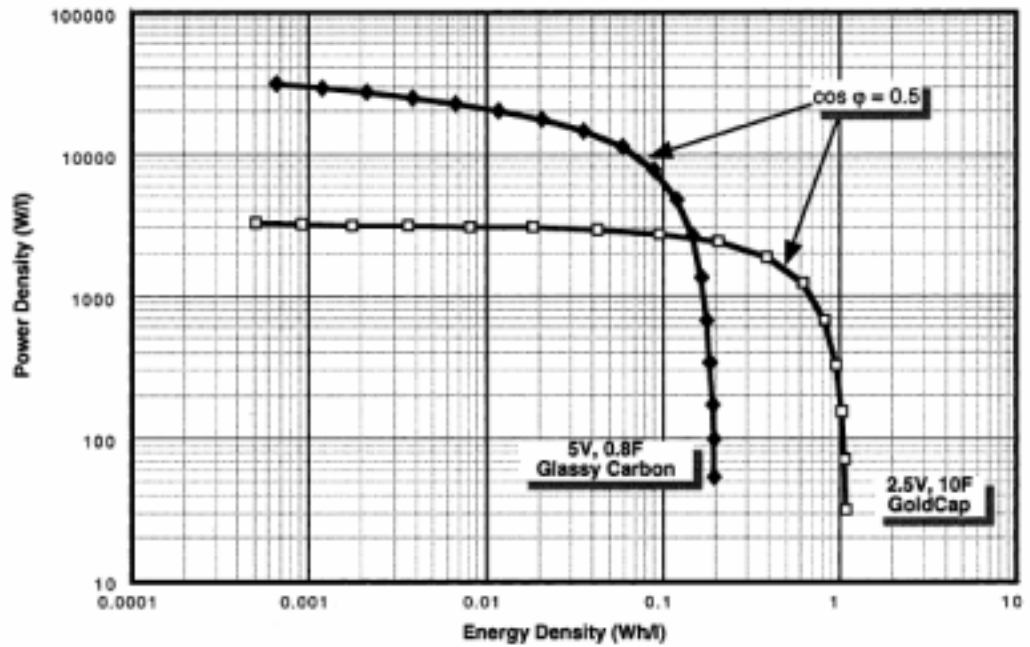


Figure 4.5 – Ragone plots of two EDLC devices [1].

4.1.3. Impedance spectroscopy

Impedance spectroscopy is a powerful method of evaluating a component's performance in the frequency domain. Special equipment is required to apply a small AC voltage and measure the changes in magnitude and phase over a range of frequencies. The impedance can then be plotted on a Nyquist diagram (Fig 4.6). An ideal capacitor is represented by a vertical straight line shifted on the real axis by its ESR. At low frequencies a supercapacitor approaches a near vertical straight line shifted on the real axis by the ESR and an additional equivalent distributed resistance (EDR).

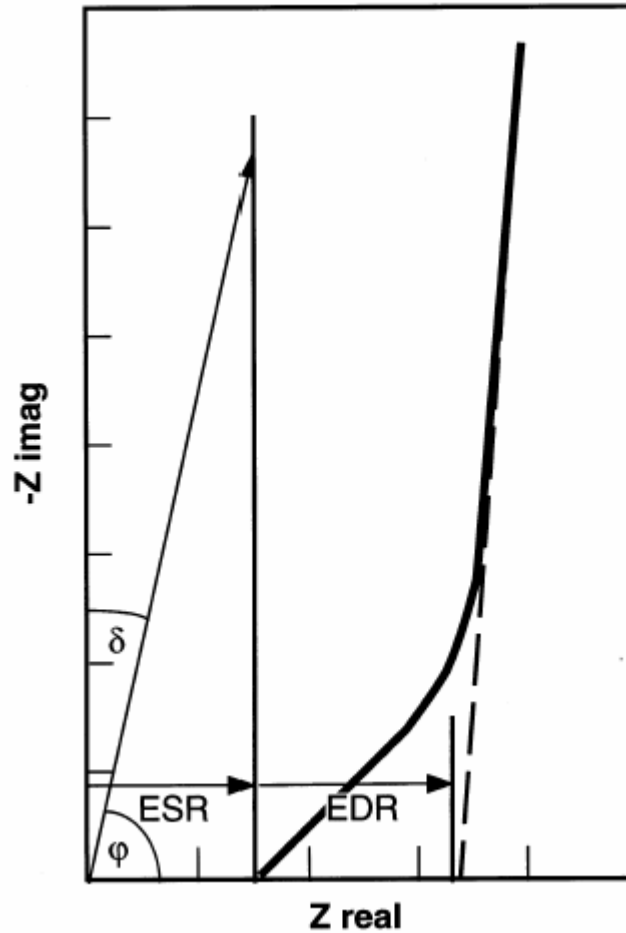


Figure 4.6 – Complex impedance plot of conventional capacitor and EDLC [1].

4.1.4. Constant-power cycling

Cyclic voltammetry, constant-current charging and impedance measurements are generally better suited to low-power measurements. During high-power operation they do not provide useful data for modelling, mainly due to the fact that most of the parameters to be determined are voltage-dependent, but changes in voltage are used to determine them. Constant-power cycling, however, can provide useful time constant information at particular power levels which can be used to evaluate different components [39]. The procedure for power cycling involves charging the EDLC at a fixed power level until a chosen voltage is reached, at which point the current is reversed and discharging takes place (Fig.

4.7). An RC time constant can then be determined from the linear equation shown as Equation 4.2, where $Q(t)$ is stored charge evaluated by the integral of the current, $V(t)$ is the terminal voltage, and V_0 is the initial voltage.

$$\frac{Q(t)}{I(t)} = C \frac{[V(t) - V_0]}{I(t)} - RC \quad (4.2)$$

By plotting $\frac{Q(t)}{I(t)}$ against $\frac{[V(t) - V_0]}{I(t)}$, the capacitance can be obtained from the slope and the RC time constant is then the y-intercept (Fig. 4.8) [39].

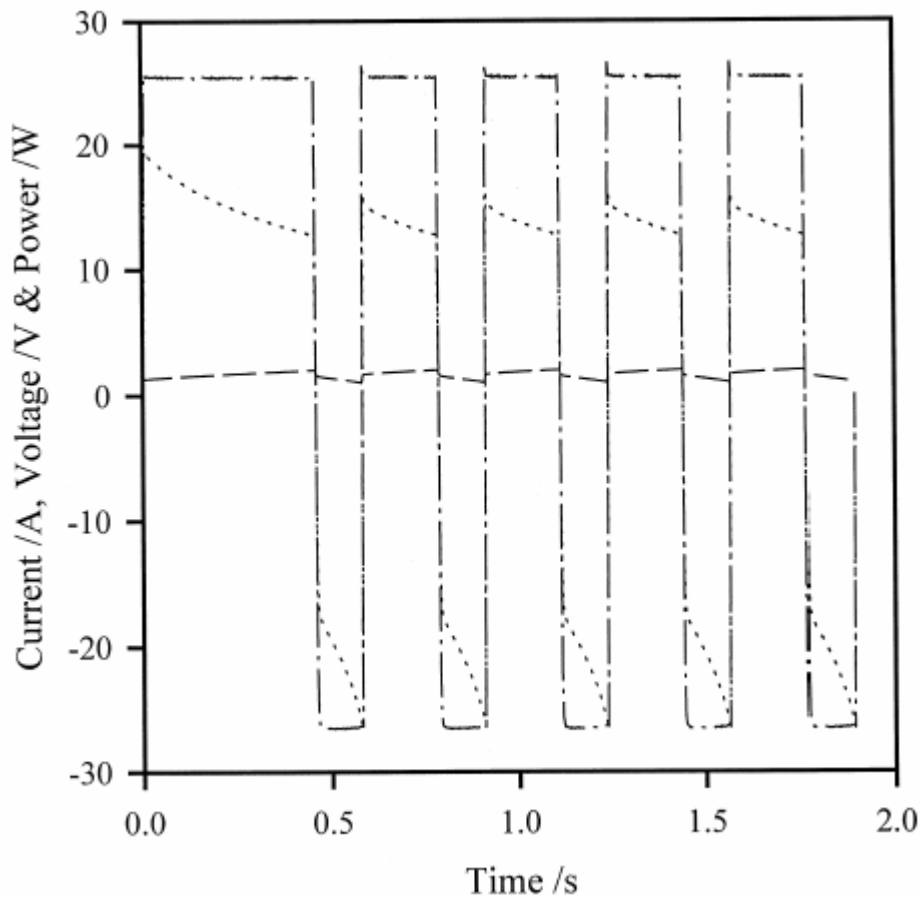


Figure 4.7 – Constant-power cycling waveforms (dashed line is voltage, dotted line is current, dash-dot line is power) [39].

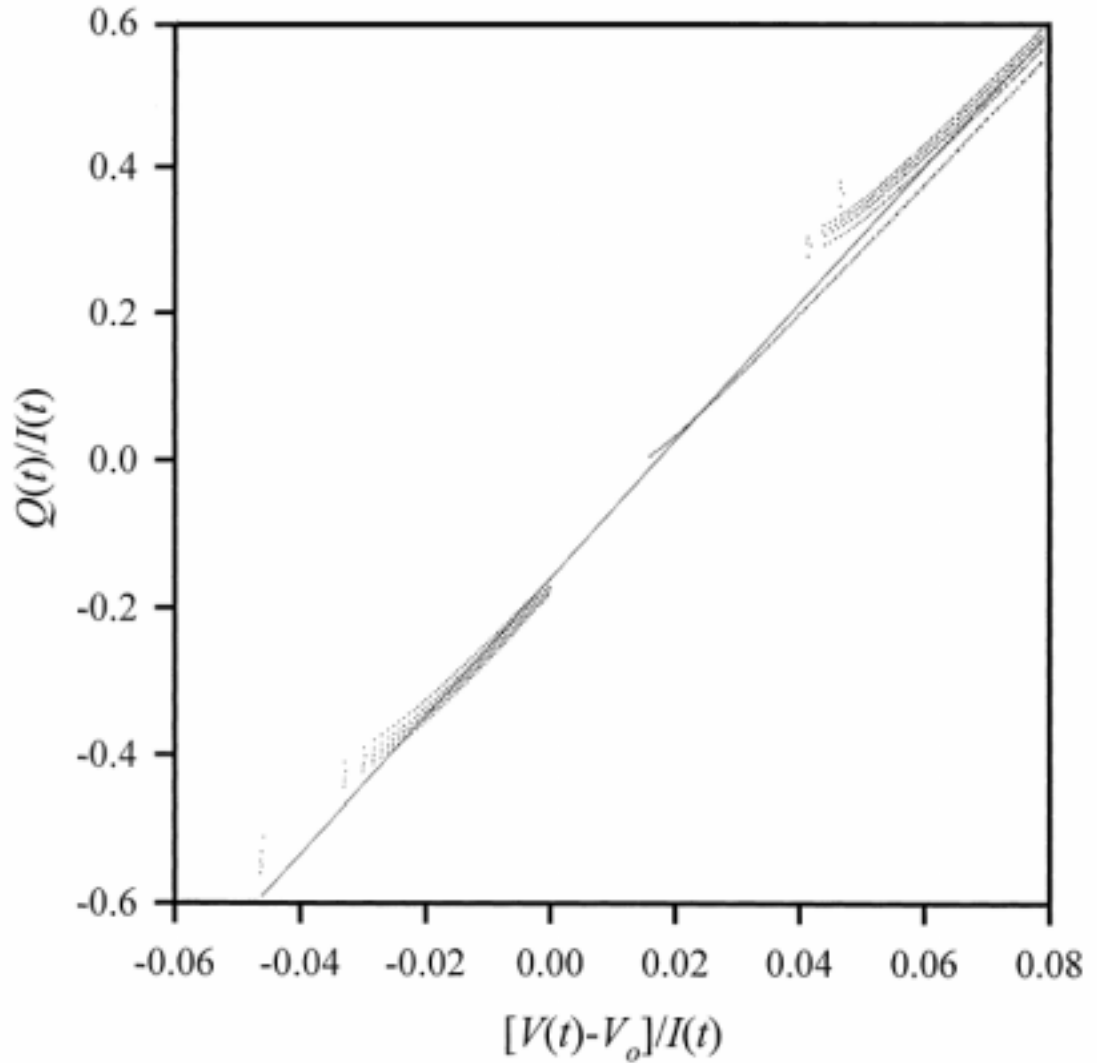


Figure 4.8 - Experimental data obtained from power-cycling tests and fitted with a line of best fit [39].

4.2. Capacitor modelling

The double-layer capacitor stores charge through processes that are very different to those that occur in conventional capacitors. It should therefore be no surprise to find that traditional models used to describe capacitor behaviour are inadequate in the case of electrochemical capacitors. A number of models currently exist that apply to the operation of double-layer capacitors.

4.2.1. The classical equivalent circuit

A simple model for a double-layer capacitor can be represented by a capacitance (C) with an equivalent series resistance (ESR) and an equivalent parallel resistance (EPR), [40]. The ESR models power losses that may result from internal heating, which will be of importance during charging and discharging. The EPR models current leakage, and influences long-term energy storage. By determining these three parameters, one is able to develop a first order approximation of EDLC behaviour.

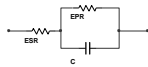


Figure 4.9 - The classical equivalent circuit of an EDLC [40].

Spyker's [40] method of determining the EPR involved slowly charging the capacitor to its rated voltage, and then allowing a significant amount of time to pass before measuring the capacitor's terminal voltage. Since the decay is exponential, the EPR can be calculated from Equation 4.3.

$$EPR = \frac{-t}{\ln\left(\frac{V_2}{V_1}\right)C} \quad (4.3)$$

where t is the time, V_1 is the initial voltage, V_2 is the final voltage, and C is assumed to be equal to the rated capacitance. The time constant of C and EPR is usually quite large, so the EPR can be ignored in the case of a short discharge up to the order of a few minutes.

To determine the ESR the EPR is ignored and the equivalent circuit is assumed to consist only of the ESR and the capacitance. The ESR can then be determined from the change in voltage, ΔV , and current, ΔI , that occurs during charging.

$$ESR = \frac{\Delta V}{\Delta I} \quad (4.4)$$

Spyker's test circuit for measuring ΔV and ΔI consisted of a MOSFET switch, a gate drive, a shunt resistor and a load resistor (Fig. 4.10). Twelve MOSFETs were combined in parallel to provide a switch with a low on-state resistance of 0.571 m Ω . When the switch was opened or closed, the change in voltage across the capacitor terminals could be measured, and the change in current could be measured via the shunt resistor.

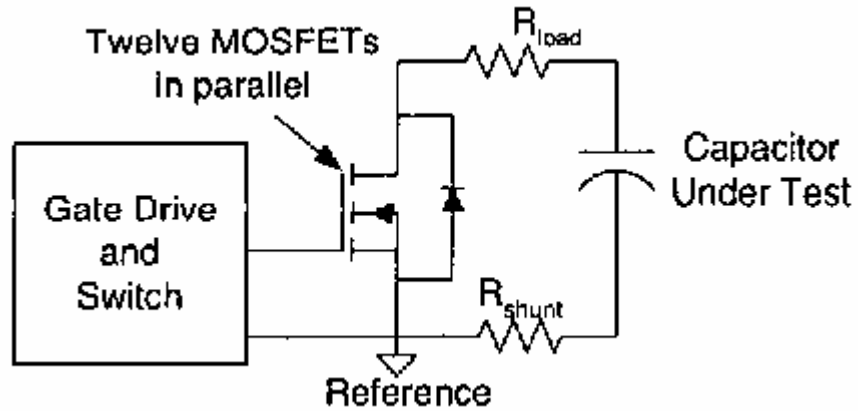


Figure 4.10 - Test circuit for measuring ESR [40].

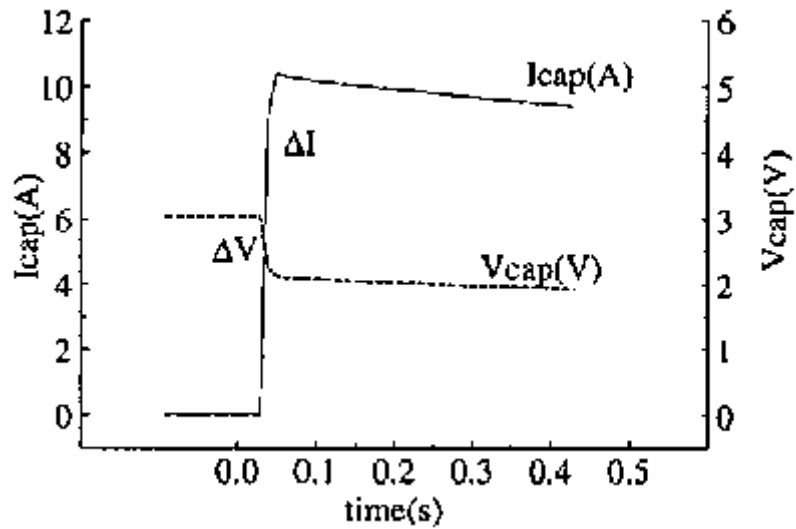


Figure 4.11 - Voltage and current waveforms for a 470 F capacitor charged to 3 V and discharged into a 0.2 Ω load [40].

The preferred method used by Spyker to measure the capacitance, C , of the equivalent circuit involves determining the change in energy, ΔE , that occurs during charging or discharging, which is given by:

$$\Delta E = \frac{1}{2} C (V_1^2 - V_2^2) \quad (4.5)$$

Since the change in energy can be determined from the integral of instantaneous power, C can be calculated from:

$$C = \frac{2 \int_{t_1}^{t_2} v(t) i(t) dt}{(V_1^2 - V_2^2)} \quad (4.6)$$

4.2.2. The 3 branch model

While the classical model provides a first approximation of a double-layer capacitor's behaviour, Zubietta [41] observed that it is insufficient when compared against experimentally observed behaviour (Fig. 4.12). He therefore proposed a model consisting of three RC branches in an attempt to achieve a better fit to the collected data.

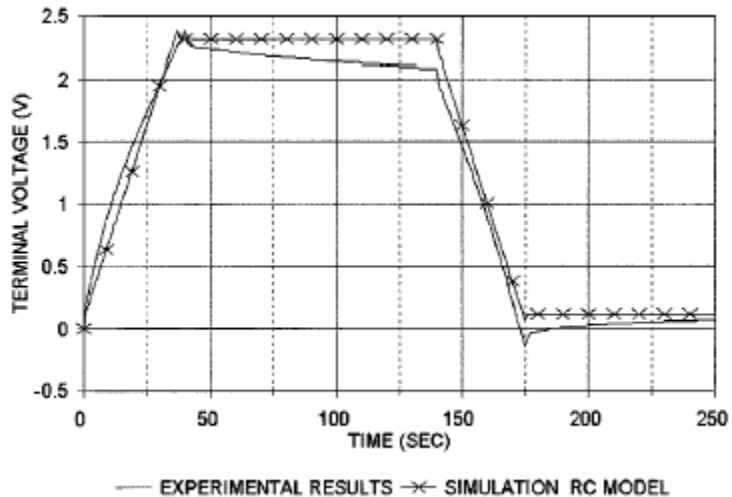


Figure 4.12 - Comparison of classical model to experimental data [41].

Each branch of the equivalent circuit possessed a significantly different time constant. The branch containing R_i , denoted the *immediate* branch, dominates behaviour in the order of a few seconds. The *delayed* branch, containing R_d , most influences behaviour in the range of minutes. The third, *long-term* branch governs the long-term response of the circuit after more than ten minutes. The immediate branch contains a voltage dependent capacitor C_{i1} that reflects the voltage dependency of the double-layer's capacitance. The resistance R_{lea} is included to model current leakage [41].

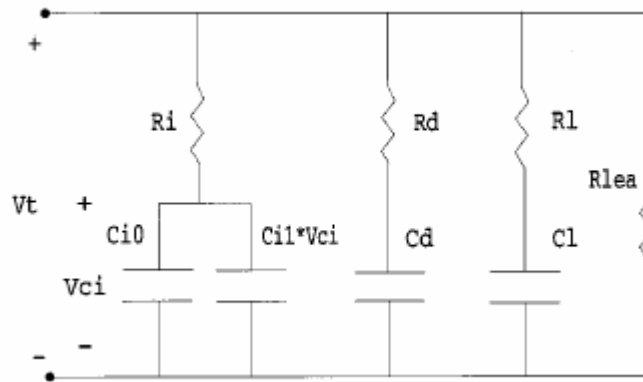


Figure 4.13 - The 3 branch model [41].

Zubieta provides a method of determining the parameters of the three branch equivalent circuit. To do this, the capacitor is subjected to a fast, controlled charge and the subsequent charge/discharge characteristic is examined. Before this can be carried out, however, all of the capacitive elements must be completely discharged so that the capacitor's initial state is known. The capacitor should therefore be short-circuited for several weeks prior to parameter measurement. A controlled current source should be used to achieve repeatable results. The charging current I_{ch} , is set at 5% of the device's short-circuit current, calculated from the rated voltage and resistance specified by the manufacturer [41].

To determine the parameters of the immediate branch the capacitor is charged, reaching I_{ch} at time t_1 . R_i is then given by measuring the voltage V_1 :

$$R_i = \frac{V_1}{I_{ch}} \quad (4.7)$$

At a later time t_2 , the change in voltage, ΔV , is measured to give C_{i0} :

$$C_{i0} = I_{ch} \frac{t_2 - t_1}{\Delta V} \quad (4.8)$$

Zubieta chose t_2 such that ΔV was 50 mV. When the voltage reaches its rated level at time t_3 , the current source is switched off, and the current will reach zero at time t_4 , and the voltage will be V_4 . The voltage dependent capacitance C_{i1} is then given by:

$$C_{i1} = \frac{2}{V_4} \left(\frac{I_{ch}(t_4 - t_1)}{V_4} - C_{i0} \right) \quad (4.9)$$

and the total charge Q_{tot} , delivered to the capacitor will be:

$$Q_{tot} = I_{ch}(t_4 - t_1) \quad (4.10)$$

To measure the delayed branch parameters the change in voltage from V_4 , ΔV , is measured at some later time t_5 . At this time current is assumed to be transferring from the immediate branch to the delayed branch, and R_d will be equal to:

$$R_d = \frac{\left(V_4 - \frac{\Delta V}{2} \right) (t_5 - t_4)}{\left(C_{i0} + C_{i1} \left(V_4 - \frac{\Delta V}{2} \right) \right) \Delta V} \quad (4.11)$$

At a time, t_6 , 3 time constants after t_5 , (where $R_d * C_d \approx 100$ s), the voltage V_6 is measured, so that the delayed branch capacitance C_d is equal to:

$$C_d = \frac{Q_{tot}}{V_6} - \left(C_{i0} + C_{i1} \frac{V_6}{2} \right) \quad (4.12)$$

The long-term branch resistance R_l is measured at some time, t_7 , by measuring the change in voltage, ΔV :

$$R_l = \frac{\left(V_6 - \frac{\Delta V}{2}\right)(t_7 - t_6)}{\left(C_{i0} + C_{i1}\left(V_6 - \frac{\Delta V}{2}\right)\right)\Delta V} \quad (4.13)$$

After 30 min it can be assumed that charge has been fully distributed to the long-term branch, at which time the voltage across each equivalent capacitor will be equal to V_8 . The long-term capacitance can then be determined by:

$$C_l = \frac{Q_{tot}}{V_8} - \left(C_{i0} + C_{i1} \frac{V_8}{2}\right) - C_d \quad (4.14)$$

Zubieta acknowledges that the model is limited by the assumption that only the immediate branch capacitance is voltage dependent. Due to this assumption the error in the model's predictions becomes greater at low voltages. Also, due to the fact that the long-term branch only accounts for thirty minutes at most, the model can not be used to predict the behaviour of a capacitor after several hours or days [41].

4.2.3. Porous electrodes as transmission lines

A treatment by de Levie [42] of the capacitance in porous electrodes resulted in each pore being modelled as a transmission line (Fig. 4.14). The transmission line models a distributed double-layer capacitance and a distributed electrolyte resistance that extends into the depth of the pore. To achieve an estimation of the double-layer capacitive effects, de Levie assumed straight, cylindrical pores of uniform diameter and a perfectly conducting electrode. The results of his derivation are shown in Figures 4.15 and 4.16. In Figure 4.15, the parameter on the x-axis, τ , depends on the depth within the pore, z , the double-layer capacitance, C , and the electrolyte resistance, R , so that:

$$\tau = \frac{1}{4} z^2 RC \quad (4.15)$$

From Figure 4.16 it is evident that while frequency is maintained throughout the pore, the amplitude decreases as the pore depth increases. To quantify the depth, λ , to which the pore is making a contribution to the charging process, de Levie gives the equations:

$$\lambda_{DC} = \sqrt{\frac{4t}{RC}} \quad (4.16)$$

$$\lambda_{AC} = \frac{1}{\sqrt{\frac{1}{2}\omega RC}} \quad (4.17)$$

where Equation 4.16. is used in DC situations, and Equation 4.17. is used for AC.

When a DC potential is applied to the opening of a pore the penetration depth therefore increases with time. For AC voltages the penetration depth increases as the frequency decreases.

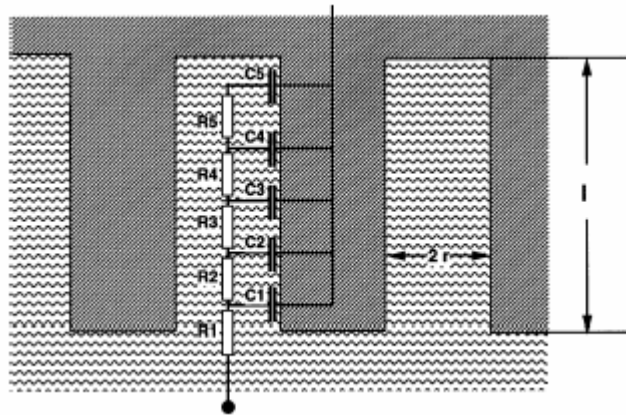


Figure 4.14 - Porous electrode representation as a five element transmission line [1].

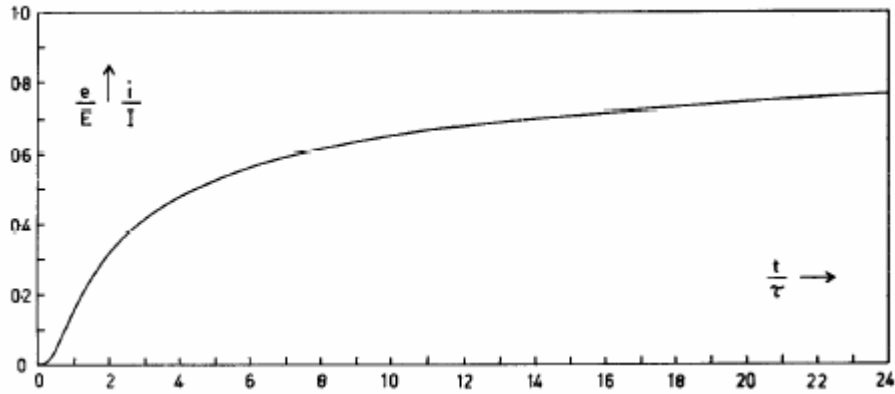


Figure 4.15 - Potential step response of transmission line model [42].

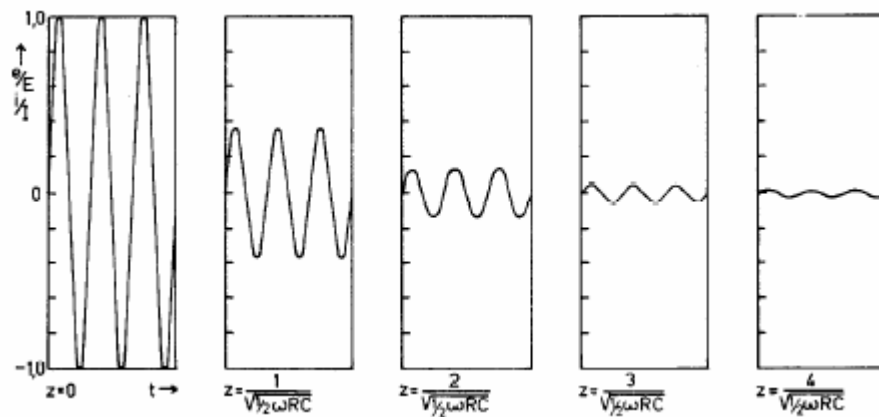


Figure 4.16 - Potential response to sinusoidal input at various pore depths [42].

To include the capacitive effects of Faradaic reactions a transmission line model possessing a distributed complex impedance can be formulated.

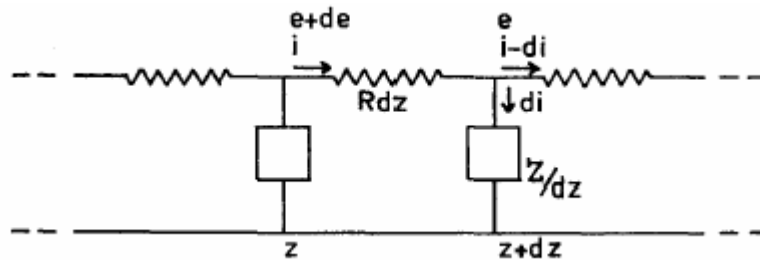


Figure 4.17 - Transmission line model with complex impedance [42].

4.3. Performance characteristics

Electrochemical capacitors behave differently to conventional capacitors, which is to be expected based upon the different charge storage mechanisms involved. The performance characteristics of EDLCs will therefore be discussed in reference to the transmission line model of porous electrodes. This model is very useful in explaining the characteristics of EDLCs, while the other basic models are better suited to the simple experimental estimation of key parameters.

The typical impedance characteristic of an EDLC has several implications for cell performance. At low frequencies the reactance, which is mainly due to capacitance, is at a maximum, and approaches the behaviour of an electrostatic capacitance (Fig. 4.6). Under such conditions ions have time to penetrate into the depth of the pores and the maximum electrode surface-area is utilised to contribute to double-layer capacitance. Distributed resistance is also at a maximum. As the frequency increases, however, the capacitance begins to decrease, and ion penetration begins to become poor with only the electrode surface being available for charging and discharging [43]. The frequency dependence of a supercapacitor's specific capacity therefore affects the relationship between power density and energy density. Since energy density is directly related to specific capacitance, and power density is related to the rate of charge delivery, it is apparent from an EDLC's impedance plot that energy density will be limited at higher rates of power delivery. This phenomenon is clearly demonstrated in Ragone plots such as that in Figure 4.5. It is also evident when charging curves at different power levels are considered. An EDLC's frequency response dictates that less charge can be stored at faster rates of charge (Fig. 4.20).

The frequency dependence of the charging characteristic is the primary reason that constant-current charging techniques are inadequate in high-power situations. It is apparent from Figure 4.20 that the measured capacitance is heavily dependent on the current used in the test.

The maximum possible power that can be supplied by a cell is dependent on voltage and resistance, given by Equation 4.18.

$$P = \frac{V^2}{4 \times ESR} \quad (4.18)$$

As described in chapter 3, cell voltage is largely dependent on the electrolyte breakdown voltage, while ESR depends on electrode and electrolyte conductivity. Choice of electrolyte is therefore influential. Organic electrolytes have a higher breakdown voltage, but have greater resistance. Advantages in having a higher cell voltage are therefore usually countered by the greater resistance. Maximum energy density is governed by Equation 2.2, and is therefore dependent on capacitance and voltage. As discussed earlier, capacitance depends on electrode and electrolyte properties. Figure 4.19 displays a comparison of maximum energy and power density of two EDLCs using organic and aqueous electrolytes with varying active film thicknesses. The capacitor using an organic electrolyte has the higher energy density because of its higher cell voltage, but the cell using an aqueous electrolyte has the greater power density as a result of its better conductance.

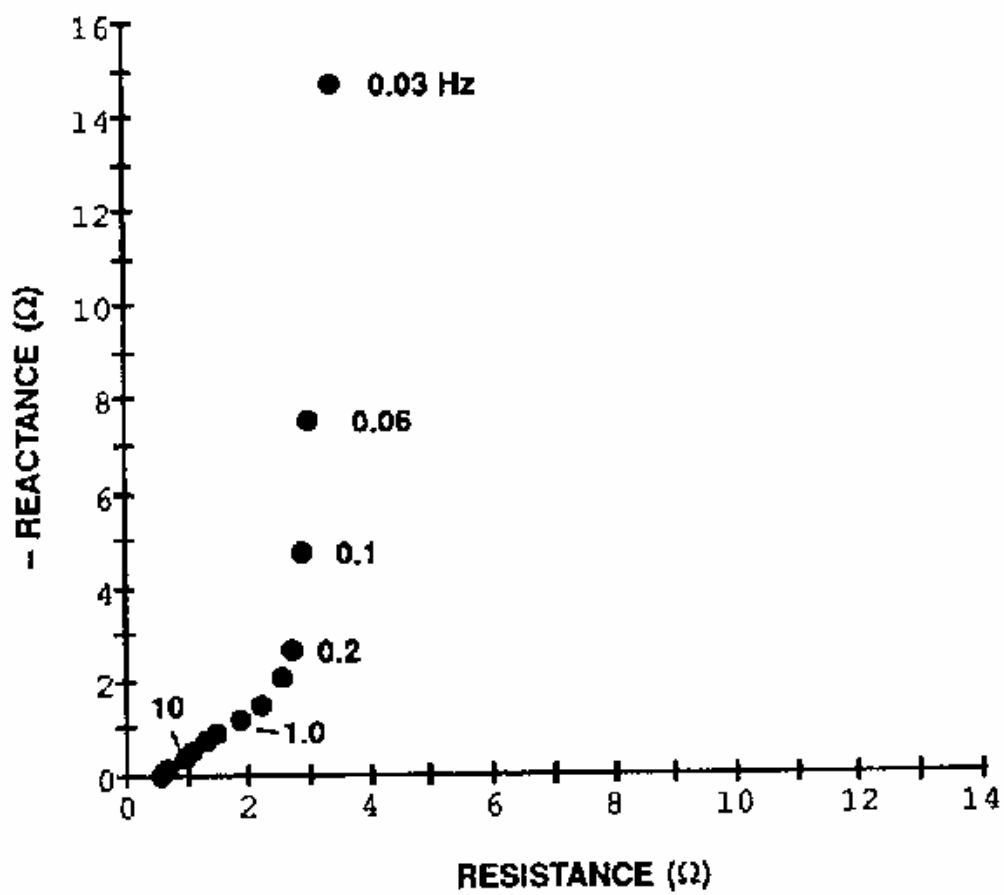


Figure 10.18 – Impedance plot of a 0.47 F, 11 V Capattery by Evans [43].

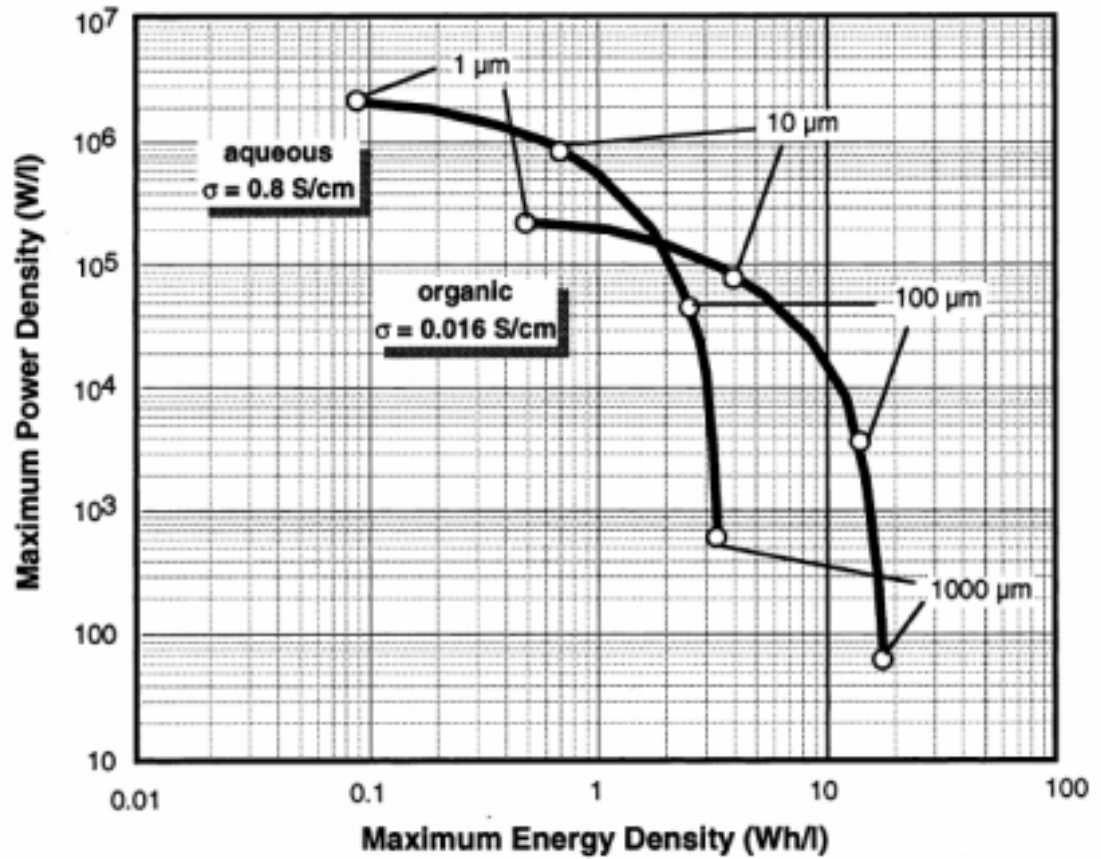


Figure 4.19 – Comparison of Ragone plots for supercapacitors using organic and aqueous electrolytes [1].

EDLC efficiency can be related to the phase angle, φ , the angle subtended at the origin of the Nyquist plot (Figs. 4.6 & 4.21 b). Power lost by heat dissipation through the internal resistance is given by $\cos(\varphi)$ [1], and the phase angle decreases from 90° to 0° with increasing frequency. It is therefore apparent that power losses increase at high frequencies.

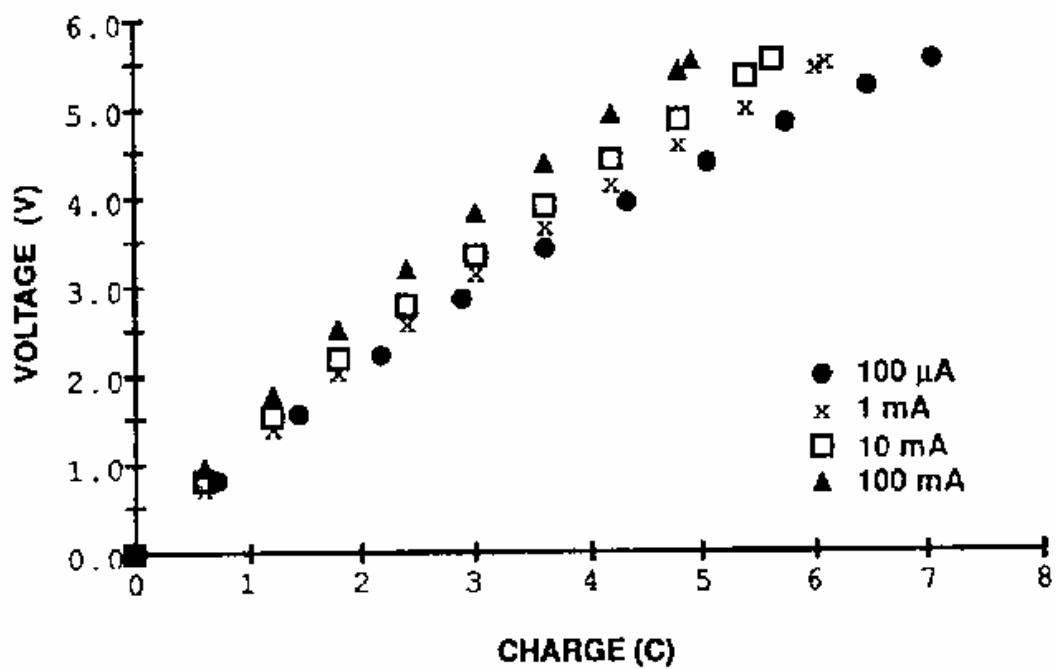


Figure 4.20 – Charging characteristics at different currents [43].

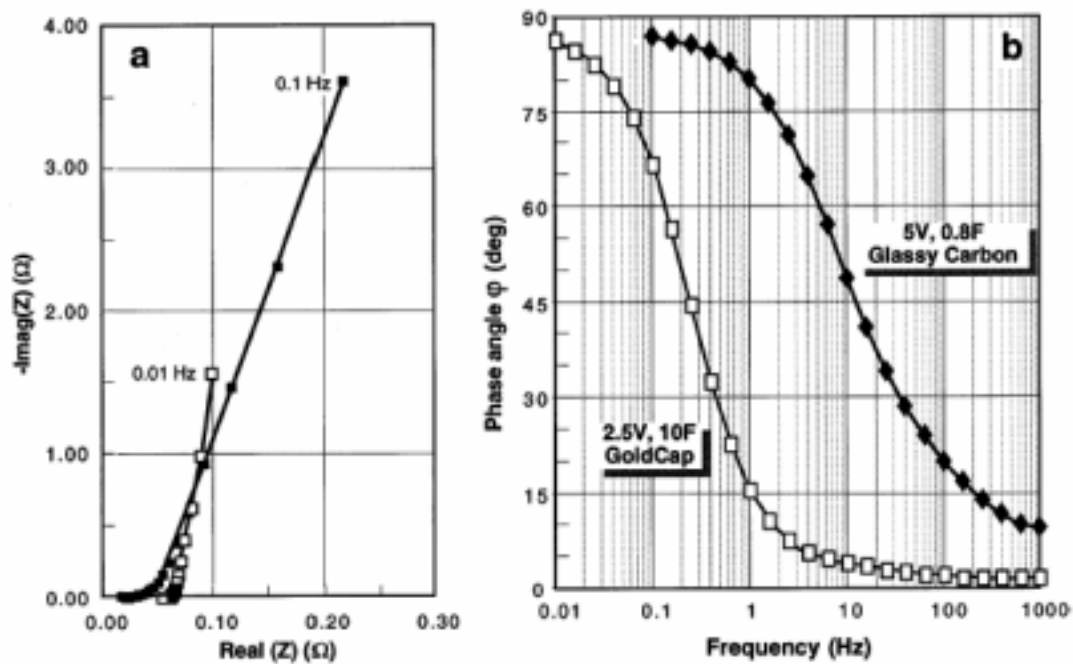


Figure 4.21 – Comparison of a) impedance spectroscopy and b) phase response for two EDLCs [1].

4.4. Summary of performance considerations

Cyclic voltammetry, constant-current charging, and impedance spectroscopy are commonly used methods of evaluating supercapacitor performance. While these tests have provided useful results in the past, they become inadequate when high-power operation is considered. Since EDLCs have traditionally been low-power devices this has not been a problem, but constant-power cycling would appear to be a better test for high-power supercapacitors.

Simple RC equivalent circuits are usually adequate for quick and easy parameter estimation in the laboratory. Such simplifications do not, however, explain the commonly observed deviations from ideal behaviour, and a transmission line model consisting of distributed RC elements within each pore provides the best method for explaining phenomena such as the frequency dependence of capacitance.

5. Applications

Electrochemical supercapacitors are still relatively new devices that have yet to experience widespread use. This has originally been due to their limited power and energy capabilities, and they therefore only saw use in low-power, low-energy applications such as for memory backup. Recently, however, significant advances have been made in improving both energy and power density, and new applications for EDLCs are being developed at an increasing rate. The following are a number of possible applications for the EDLC as an energy storage element.

5.1. *Memory backup*

Supercapacitors have long been in use as short-term backup supplies in consumer appliances. Many appliances now incorporate digital components with memory, and even a very brief interruption in the power supply would otherwise cause a loss of stored information. In such situations a supercapacitor can act as the power supply for a short period, thereby retaining data.

The common alternative to the supercapacitor in this application is the battery. Batteries do not generally have a long product lifetime, and therefore need to be replaced regularly. Today's consumer appliances are also cheap to the extent that a battery could cost up to 20% of the price of the appliance [44]. EDLCs are therefore a good choice as backup power supply due to their long lifetime.

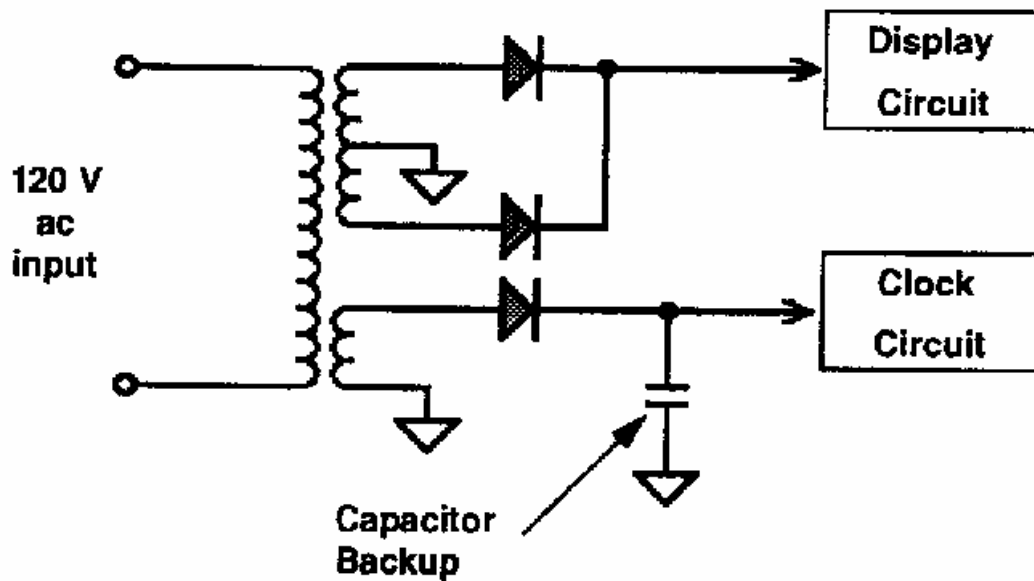


Figure 5.1 – Scheme for memory backup of clock memory via supercapacitor [44].

5.2. *Electric vehicles*

The prospect of the use of EDLCs in electric vehicles has drawn much attention to the technology, appealing to the energy-conscious because of their energy efficiency and because of the possibility of recuperating energy lost during braking. Many of the current power sources being considered for use in electric vehicles (EVs) do not meet the power requirements of vehicle acceleration. Fuel cells are promising due to their extremely high energy density, but they are currently limited in their power specifications. Both the power and energy requirements of an EV can therefore be satisfied with a combination of fuel cell and supercapacitor technology.

A combined power source configuration allows the high-energy density device such as a fuel cell to provide the average load requirements. Peak load requirements that result from accelerating or climbing up hills can be met by the high-power device such as a supercapacitor bank. The utilisation of supercapacitors also makes regenerative braking possible. Because the EDLC

bank can be recharged it is possible to store some of the energy of an already moving vehicle, and therefore increase the fuel efficiency of the EV.

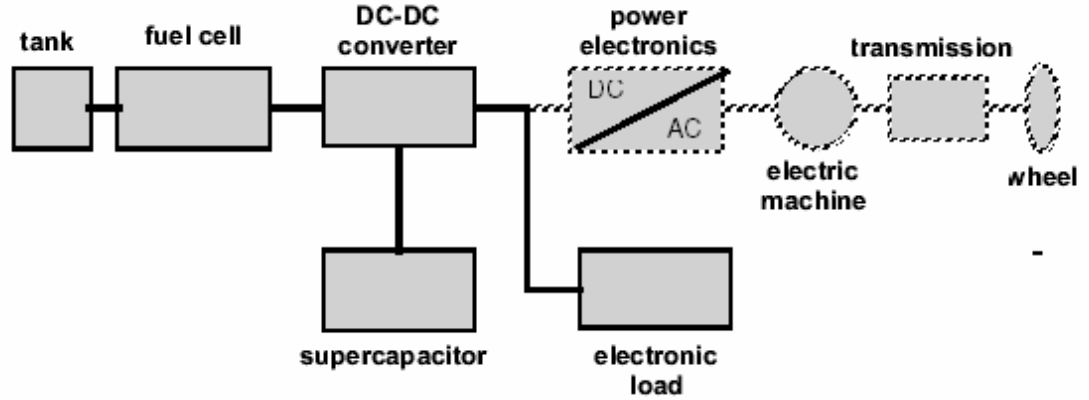


Figure 5.2 – Electric drive train using a fuel cell and supercapacitors [45].

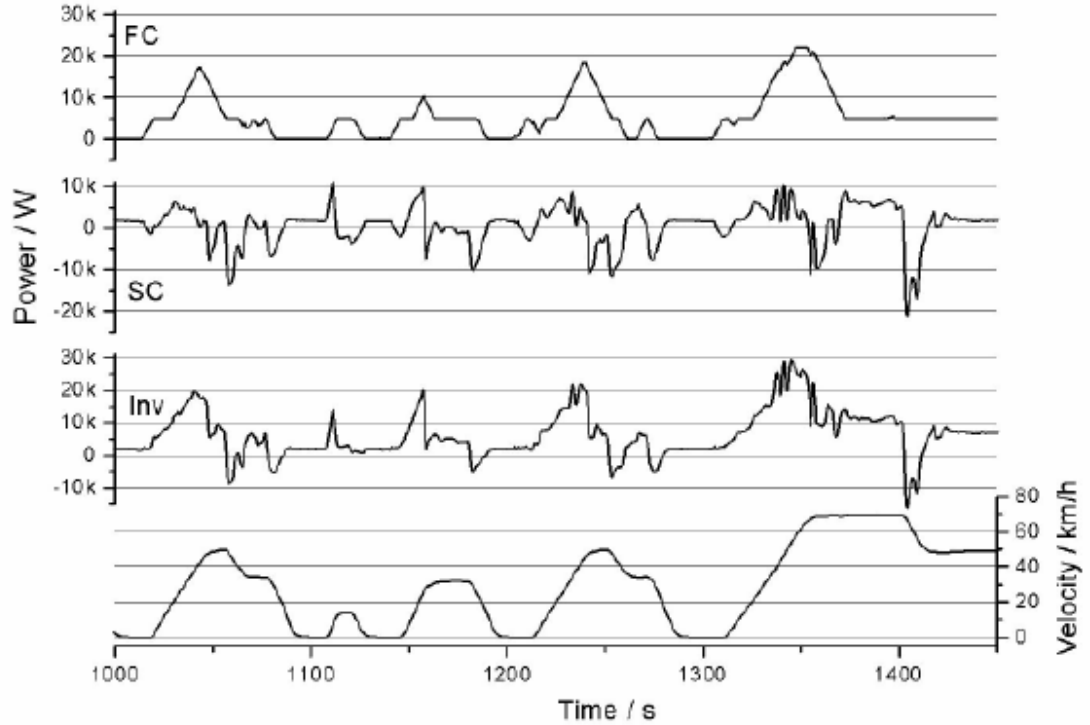


Figure 5.3 – Power flows in an EV test drive for the fuel cell, supercapacitors, and inverter [46].

The power flows during the test drive of an experimental Volkswagen Bora powered by a fuel cell and a supercapacitor bank are shown in Figure 5.3. The graph marked FC is the power supplied by the fuel cell, and SC is the power of the supercapacitor bank. The power flow of the fuel cell is a smooth function, with the fast acceleration requirements being powered by the supercapacitors. The recharging of the supercapacitors during braking periods is also shown, and in order to quantify the fuel savings made from regenerative braking fuel consumption was measured with the regenerative braking turned on and off. It was found that the fuel consumption was 6.1 L/100 km without regenerative braking, and 5.3 L/100 km with regenerative braking, amounting to a saving of 15% [46].

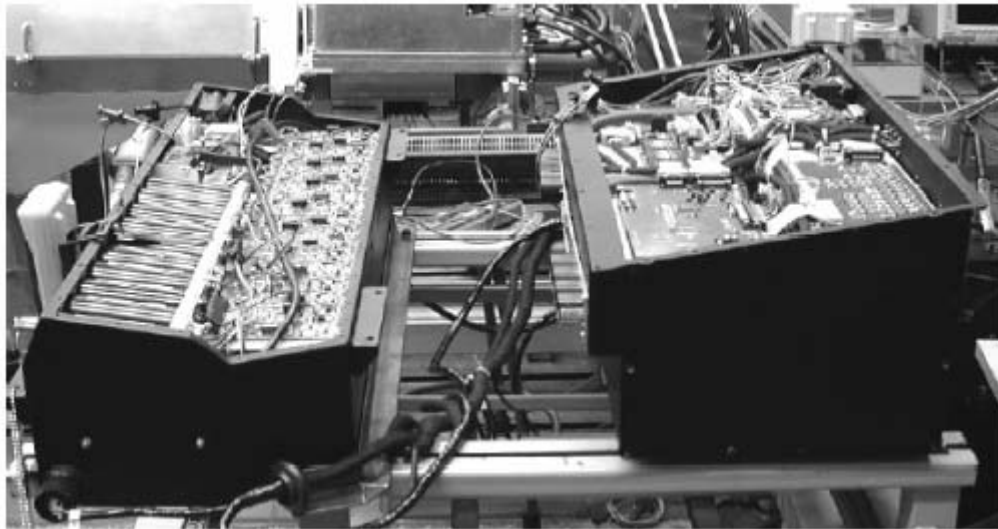


Figure 5.4 – The supercapacitor modules of a prototype EV [46].

In addition to their applications within EVs, supercapacitors could also be used to maximise the efficiency of internal combustion engines (ICEs) in hybrid vehicles (HEVs) (Fig. 5.5). 42 V electrical systems are being proposed due to the increasing power demand in luxury vehicles, and alternatives to various devices such as the starter motor will become viable [47]. Within a 42 V vehicle one such option will be the integrated starter alternator (ISA), an electrical machine that can replace both the starter motor and the alternator. The implementation of an ISA can provide greater generating ability and creates the possibility of start-stop operation of the ICE.

The ISA can start the ICE quickly and easily, so when the vehicle has stopped for an extended period of time the ICE can be turned off rather than unnecessarily burning fuel. A supercapacitor bank within this configuration provides the power for engine cranking, and is kept charged by a battery. The battery is not required to provide the power for starting the ICE and only has to charge the supercapacitors. Battery lifetime is thus lengthened.

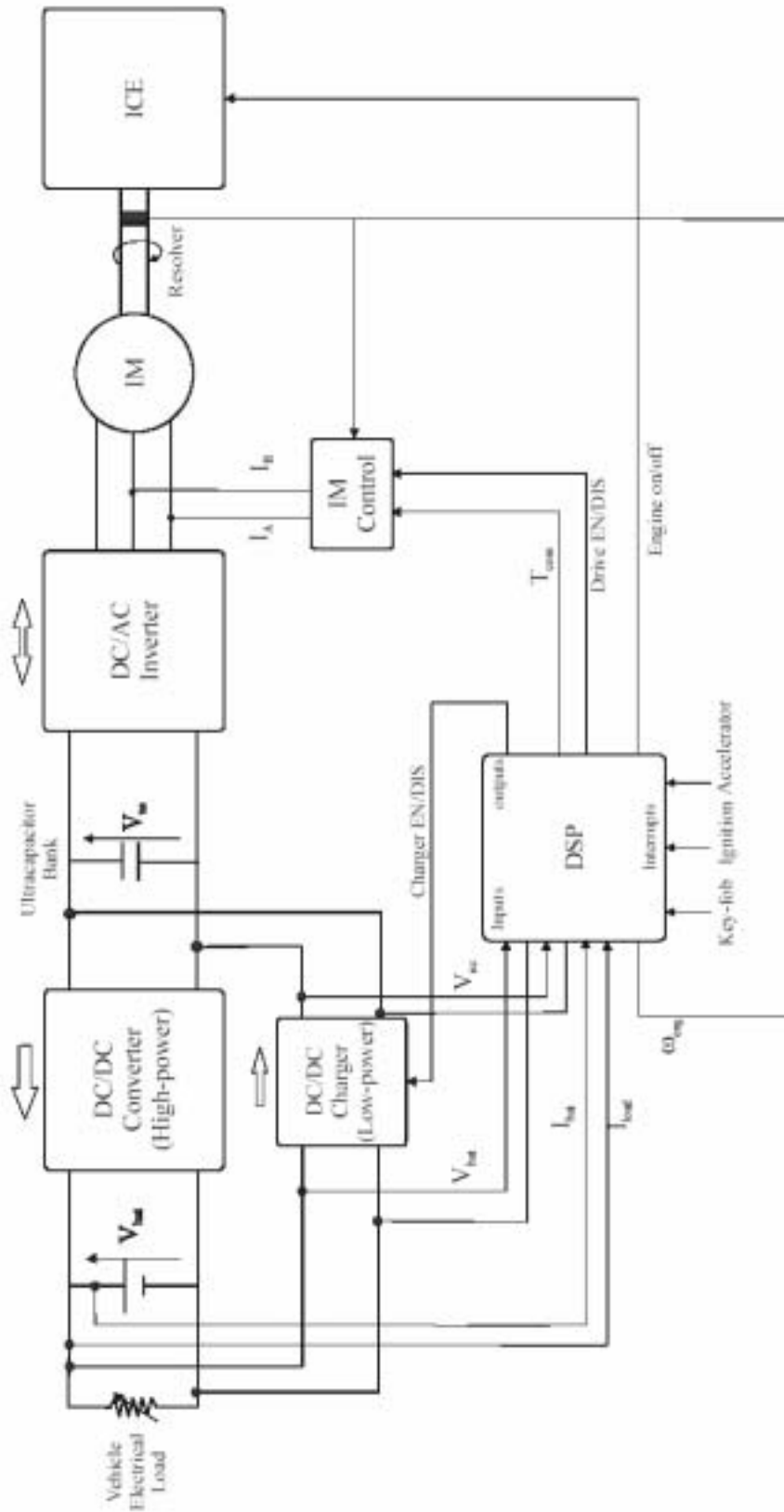


Figure 5.5 – Block diagram of an HEV using supercapacitors and an induction motor [47].

5.3. Power quality

EDLCs can be used as the energy storage device for systems designed to improve the reliability and quality of power distribution. Static condensers (Statcons) and dynamic voltage restorers (DVRs) are systems that aim to inject or absorb power from a distribution line in order to compensate for voltage fluctuations. As a result, such systems require a DC energy storage device of some sort from which energy can be drawn and in which energy can be stored.

The length of voltage disturbance that can be effectively compensated for will depend on the energy density of the DC storage device. The vast majority of voltage perturbations on the distribution bus are short-lived, most not lasting more than ten cycles [48]. The limited storage capability of the supercapacitor is therefore not a problem. The storage device must also be able to respond quickly to voltage disturbances, so the EDLC has the advantage of possessing a fast discharge time. Batteries are not generally suitable for short-duration, fast-response applications such as the Statcon or DVR, and if the battery is drained considerably, as may well occur in this situation, the device lifetime will be shortened considerably.

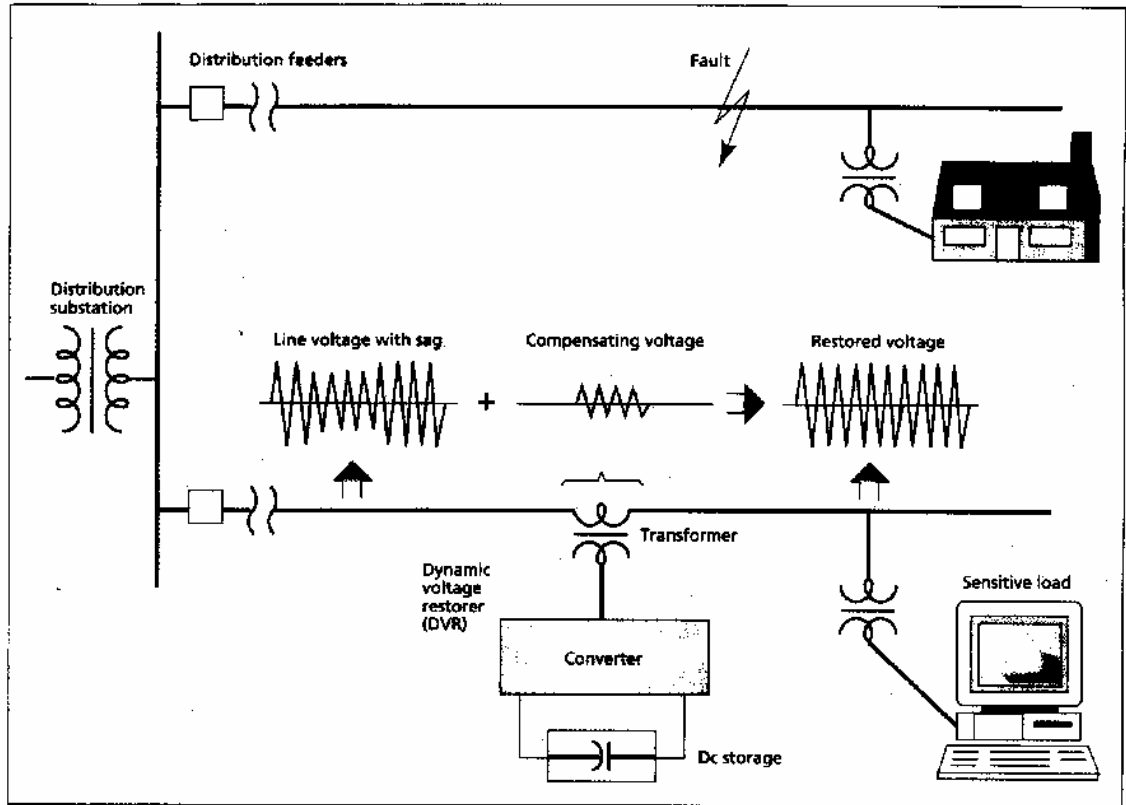


Figure 5.6 – Improved power quality on distribution side by DVR [48].

The other major technology being considered for distribution quality applications is superconducting magnetic energy storage (SMES), which also has a fast response and high efficiency. The major disadvantage of SMES systems is the operating cost incurred by maintaining the cryogenic conditions necessary for superconduction.

5.4. Battery improvement

An increasing number of portable electronic devices such as laptops and mobile phones incorporate batteries as power supplies. Many such devices draw high-power, pulsed currents (Fig. 5.7), and current profiles consisting of short, high-current bursts result in a reduction of battery performance. Using supercapacitors in combination with a battery is therefore an optimal solution.

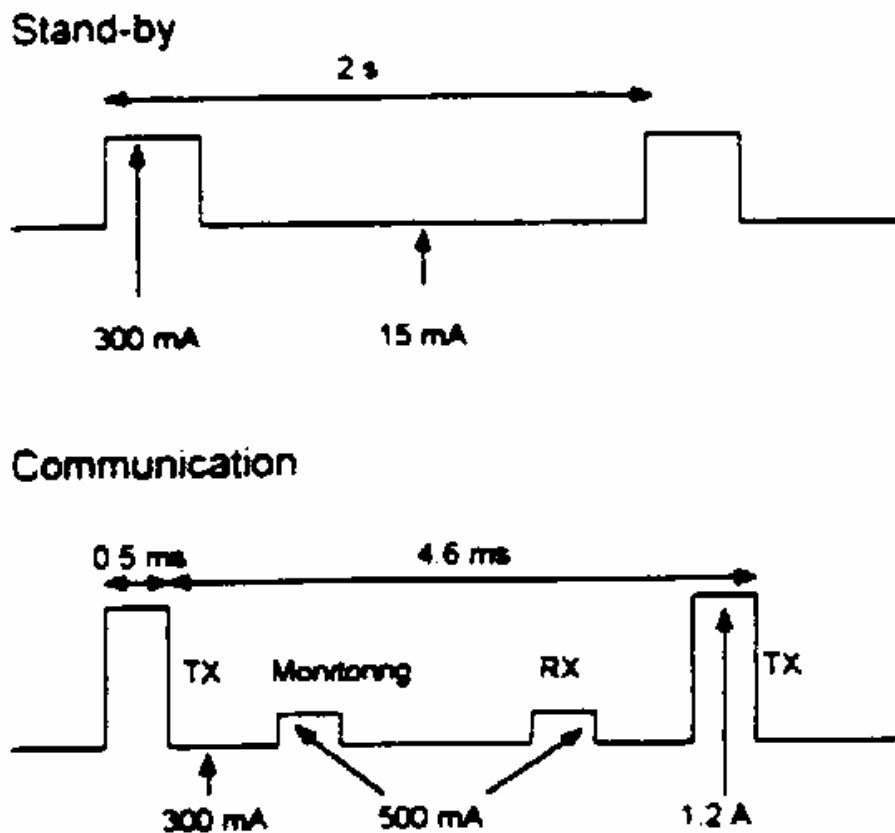


Figure 5.7 – Pulsed current load experienced in a mobile phone [49].

A supercapacitor can relieve the battery of the most severe load demands by meeting the peak power requirements, and allowing the battery to supply the average load. The reduction in pulsed current drawn from the battery results in an extended battery lifetime (Fig. 5.8).

Many electronic devices also include premature shutdown circuitry. These devices will power-down upon the detection of a low voltage, preventing loss of data. A noisy supply voltage can sometimes trigger these shutdown circuits. The supercapacitor will help prevent premature shutdowns by reducing the severity of voltage transients (Fig. 5.9) [50]. Figure 5.9 shows the effectiveness of a supercapacitor in reducing voltage transients. The top part of the diagram shows a 10.8 V lithium-ion battery pack subjected to a 2 A current pulse, while the bottom part of the diagram shows the same battery coupled with a 7 F, 5 m Ω supercapacitor subjected to the same current conditions.

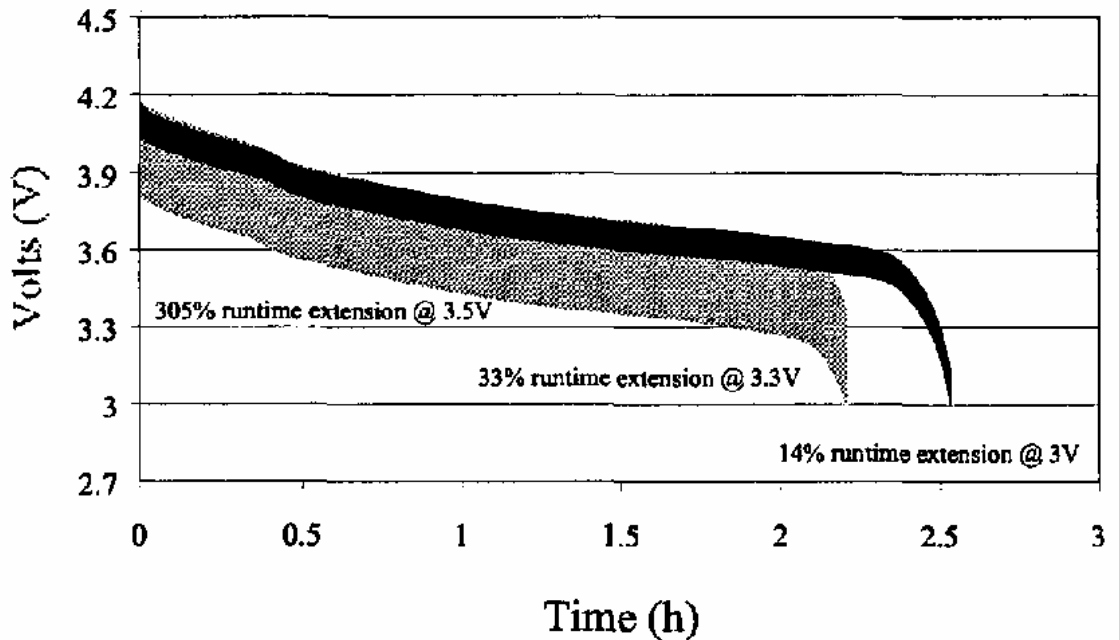


Figure 5.8 – Runtime extension when using an EDLC in combination with a battery [50].

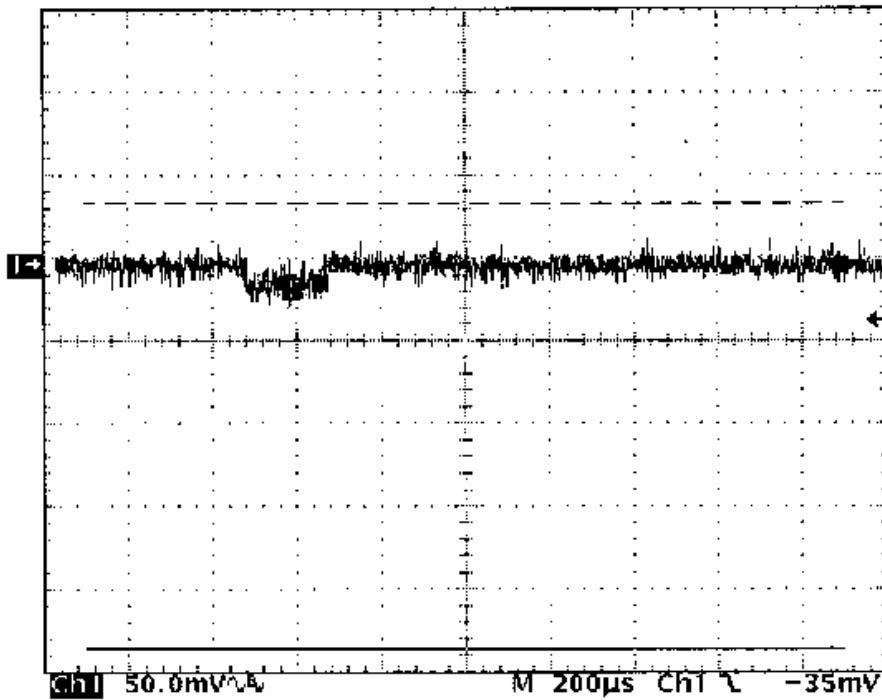
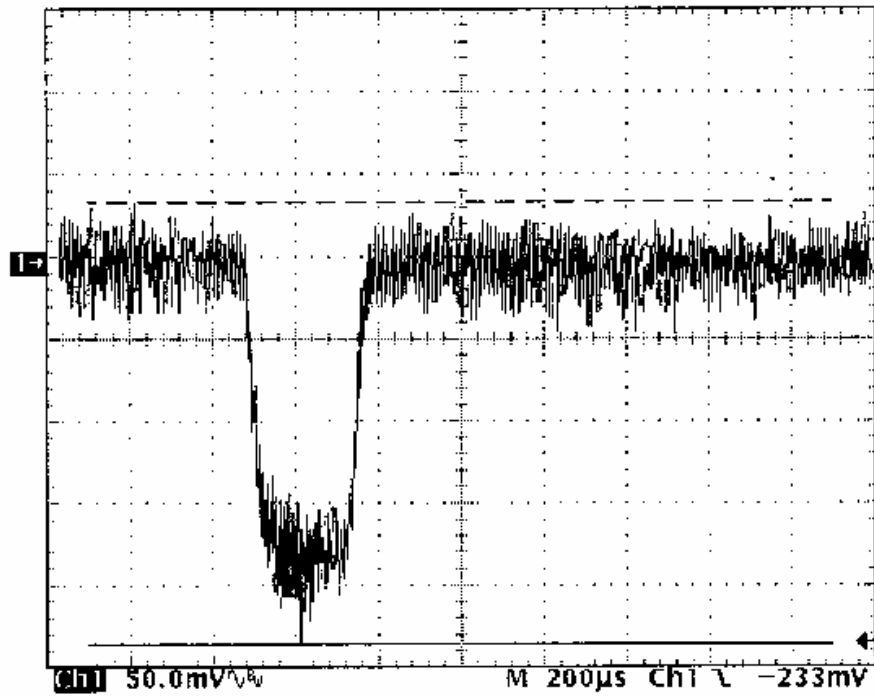


Figure 5.9 – A battery subjected to a pulsed current with (bottom) and without (top) a supercapacitor [50].

5.5. Electromechanical actuators

Electromechanical actuators can perform thrust vector control for the launch of space vehicles, or can act as flood-control actuators on submarines. Most actuation systems demand pulsed currents with high peak power requirements but fairly moderate average power requirements [51]. While a supercapacitor bank on its own is unlikely to be able to store enough energy, a battery combined with a supercapacitor can be designed to meet both average and peak load requirements. Trying to meet both requirements with a battery alone results in an oversized configuration, which is undesirable in space applications in which weight must be kept to a minimum. By designing a hybrid power source consisting of a battery and an EDLC bank weight savings of 60% can be made over using a battery alone [52].

5.6. Adjustable-speed drive ‘ride-through’

Adjustable-speed drives (ASDs) are commonly used in industrial applications because of their efficiency, but they are often susceptible to power fluctuations and interruptions. Disruptions in industrial settings are usually highly undesirable, and downtime of a machine that is part of a continuously running process can equate to significant monetary losses. The ability to design adjustable-speed drives that can ‘ride-through’ power supply disturbances is therefore a valuable one.

In order for an ASD to ride-through a disturbance at full-power, an energy storage device is needed to act as a backup power source. A number of options are available, with batteries and flywheel systems being able to provide ride-through for up to an hour. The major disadvantages of batteries and flywheel systems are their size and maintenance requirements, but batteries are currently a cheap option. Fuel cells can store a large amount of energy but can not respond quickly. SMES systems can provide reasonable ride-through capabilities, but

require sophisticated cooling systems. Supercapacitors can respond quickly to voltage fluctuations, have a long lifetime, require no maintenance, and can be easily be monitored due to the fact that their state of charge is dependent on the voltage [53]. The choice of energy storage option will largely depend upon the power requirement and the desired ride-through time (Fig. 5.10). It is obvious that supercapacitors are an advantageous choice for ride-through times of up to 5 seconds and up to a rating of 100 kVA.

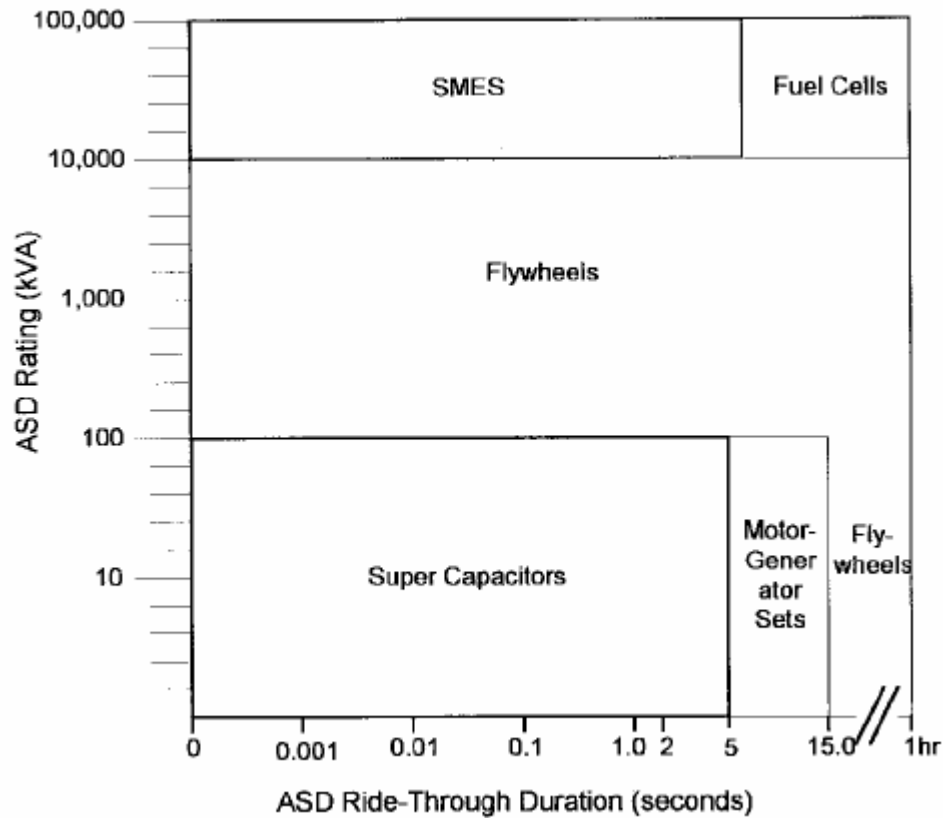


Figure 5.10 – Energy storage options for different ASD power ratings [53].

The duration of the great majority of power fluctuations will be under 0.8 seconds (Fig. 5.11), so supercapacitors are likely provide satisfactory ride-through in most applications.

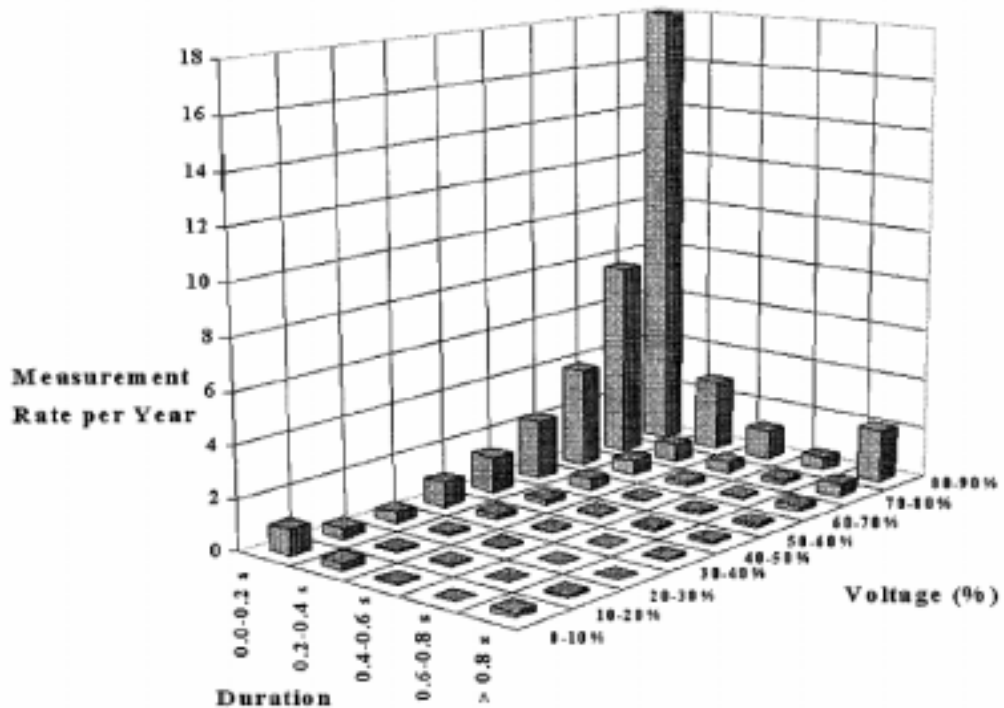


Figure 5.11 – Distribution of power fluctuation duration and size [54].

5.7. Portable power supplies

Supercapacitors are well suited to act as rechargeable stand-alone power sources for portable electronic equipment with moderate energy demands. Most devices presently using battery power supplies have long recharge times and need to be charged overnight. This has come to be accepted as a limitation of the current technology, but supercapacitors offer the opportunity to create devices that can be recharged quickly, perhaps in just a few seconds. Repeated charging and discharging can be performed without significant losses in efficiency. By using the latest light-emitting diodes (LEDs) it would therefore be possible to create a highly efficient and quickly rechargeable safety light. The need to constantly replace the batteries of handheld remote controls could be eliminated.



Figure 5.12 – An integrated supercapacitor and DC converter [55].

A complete power supply package was built recently at the University of Rio Grande [55], incorporating DC-converter circuitry on a 50 F, 2.5 V ELNA Dynacap. By using surface mount components the total package was kept to the size of a D-cell battery. The package was able to maintain a constant voltage for more than a minute with a 100 Ω load (Fig. 5.13).

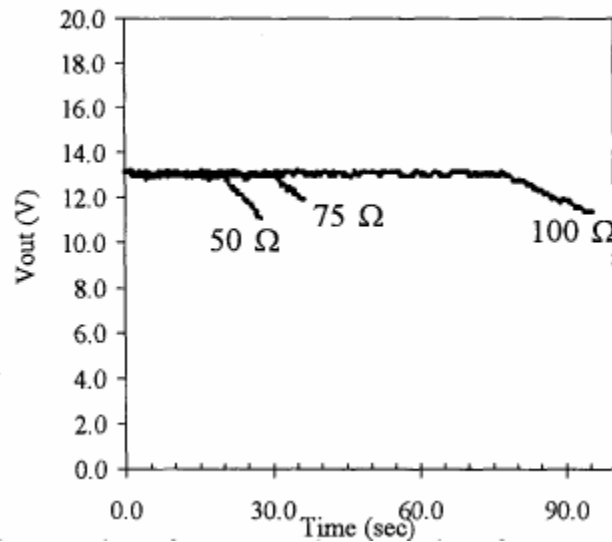


Figure 5.13 – Discharge profile of integrated EDLC & DC-converter for different loads [55].

5.8. Remote power from renewable sources

Remote power supplies that derive their energy from intermittent sources such as wind or solar radiation require energy storage to ensure that energy is available at all times. Under such circumstances EDLCs have a number of advantages over the commonly chosen battery.

Photovoltaic (PV) power supplies cycle every day, and this continuous cycling has a detrimental effect on batteries resulting in their needing to be replaced every 3-7 years [56]. Contrarily, EDLCs are able to withstand a large number of charge and discharge cycles without suffering significant losses in performance, and thus only need to be replaced every 20 years, which is the lifetime of the PV panels [56]. Lifecycle costs are therefore reduced through the elimination of frequent maintenance requirements.

Energy efficiency is always of primary concern in renewable power generation, and supercapacitors demonstrate a higher charging efficiency than batteries. A lead-acid battery, for example, can lose up to 30% of the energy during charging. EDLCs, on the other hand, may only lose 10% [56]. The ability to operate efficiently of a wider range of temperatures is also an advantage of using supercapacitors. Some remote stations may be located in cold climates and if batteries are used for energy storage the temperature will have to be maintained at close to room temperature by auxiliary systems, representing additional cost and energy consumption.

The major shortcoming of EDLC technology for application in intermittent renewable energy sources is limited energy density. This results in the capital costs of achieving energy storage equal to that of batteries in being excessive, and EDLCs are hence rarely chosen as an option. A study by Telstra Research Laboratories emphasises the reduced life-cycle costs of network termination units powered by PV panels and supercapacitors, and concludes that while

present prices exclude their use the capital costs can be expected to decrease significantly in the coming years [57].

5.9. Summary of EDLC applications

The supercapacitor is still a young technology that has yet to experience widespread implementation. It does, however, enjoy a great amount of attention with regards to its potential application in a number of areas.

A traditionally high ESR has previously limited EDLCs to memory backup applications, and they have been used in such settings for many years. Recent reductions in ESR have improved the power capabilities of supercapacitors, however, and they are now well suited to pulsed-current applications such as mobile phones and electrical actuators. They can also perform a load-levelling function when used in combination with batteries, providing peak power in devices such as laptops, reducing power demands on the battery and therefore extending battery lifetime. EDLCs can be used in a similar manner in EVs, providing power for acceleration and allowing a primary power source such as a fuel cell to supply the average power. When used in EVs supercapacitors also allow for energy to be recuperated during braking, improving the efficiency of the vehicle.

Supercapacitors can also be used on their own to provide the energy needed by power quality systems that ensure reliable and disturbance-free power distribution. EDLCs then supply the energy needed to inject power into the distribution line and thus compensate for any voltage fluctuations. They can also be used to design systems that grant adjustable-speed drives the ability to ride-through temporary power supply disturbances. Such applications are vital in industrial settings, and can prevent material and financial losses that could occur due to machine downtime.



Figure 5.14 – A ride-through system for adjustable-speed drives[58].

In portable devices like torches and remote controls EDLCs could be recharged very quickly and would probably not need to be replaced within the lifetime of the product.

As the energy storage device for a remote PV or wind turbine system the supercapacitor would offer high energy efficiency, wide operating temperature range, and greatly reduced maintenance requirements in comparison to lead-acid batteries. Their energy density is still quite limited, however, and the capital costs generally exclude them as a viable option. Reduced costs could make supercapacitors an attractive alternative in the future.

In order to use supercapacitors in any application there are a number of design hurdles that need to be overcome. The following chapter therefore considers various design considerations that must be taken into account when making use of EDLCs.

6. Design considerations

Using supercapacitors as energy storage devices in any application entails consideration of a number of factors. Firstly, an EDLC's terminal voltage decays as it is being discharged. Secondly, individual cell voltage is usually limited to a few volts, so if high voltages are required a number of cells must be connected in series. This does, however, lead to an increase in total ESR. Finally, if a series connection of cells is required, care must be taken to ensure that local over-voltages can not occur.

6.1. Voltage decay

The voltage across the terminal of a supercapacitor is directly dependent on the amount of charge remaining in it, so while it is being discharged the voltage will decay. The DC requirements of the load must therefore be considered, and two options to ensure that they are met can be taken.

If the load can function over a range of voltages then the EDLCs can be sized to allow for the voltage decay. By assuming a simple RC equivalent circuit consisting of a capacitance and ESR the voltage drop that will occur over a given time can be estimated by Equation 6.1.

$$dV = i \frac{dt}{C} + iR \quad (6.1)$$

R is the ESR and i is the average current being drawn.

If a constant DC voltage output must be supplied, a DC-DC converter should be used. Switched-mode topologies are able to maintain a constant DC output for a certain range of input voltages.

6.2. EDLC bank sizing

A large number of applications will require voltage levels much higher than that which can be achieved by a single supercapacitor. It is therefore often necessary to connect a number of supercapacitors in series in order to supply the required DC voltage. The total bank voltage is then simply the product of individual cell voltage and the number of cells in the series shown in Equation 6.2.

$$V_{total} = CN \quad (6.2)$$

C is the rated capacitance of each EDLC, and N is the number of EDLCs connected in series.

Each EDLC in a series connection will contribute its ESR to the total resistance of the bank, however, and if power requirements dictate limits on the allowed ESR then parallel connections of supercapacitors may also have to be used. For a supercapacitor bank with M parallel strings each consisting of N supercapacitors connected in series, the total equivalent resistance will be given by Equation 6.3 [59].

$$R_{total} = R \frac{N}{M} \quad (6.3)$$

R is the ESR of an individual cell. Larger numbers of parallel strings will therefore lead to reduced bank resistance.

Requirements on total bank capacitance will be determined by energy requirements, with the relation between energy and capacitance described earlier in Equation 2.2. The total capacitance of the bank is then given by Equation 6.4.

$$C_{total} = C \frac{M}{N} \quad (6.4)$$

6.3. Voltage balancing

Variations in the individual capacitance values of EDLCs connected in series result in the total voltage being unevenly distributed throughout the bank. This means that the local voltage across each supercapacitor in the array will not be equal. It is therefore possible for a local voltage greater than the EDLC's rated voltage to occur, and the cell could be deteriorated. Measures are thus required to ensure that local over-voltages can not occur.

The simplest method of limiting individual cell voltage is to connect a resistor across each supercapacitor [60]. The major disadvantage of such a solution is the power lost through the resistors. A more efficient, but still reasonably simple solution is to connect zener diodes across each capacitor. Power losses are then less because current will only flow through the diodes when an over-voltage occurs.

Simulated energy losses for voltage balancing with resistors and zener diodes are compared in Figures 6.1 and 6.2. In both cases four 1000 F EDLCs and one 800 F EDLC were connected in series and charged to 12.5 V. Energy stored at the end of the charging process amounted to 15 kJ. In the case of the voltage-balancing resistors (each 0.1 Ω), 120 kJ was required to fully charge the EDLCs, resulting in an efficiency of 12.5%. When zener diodes were used only 16.3 kJ was required, resulting in an efficiency of 92% [61]. Charging efficiency is therefore improved by using zener diodes for voltage balancing instead of resistors.

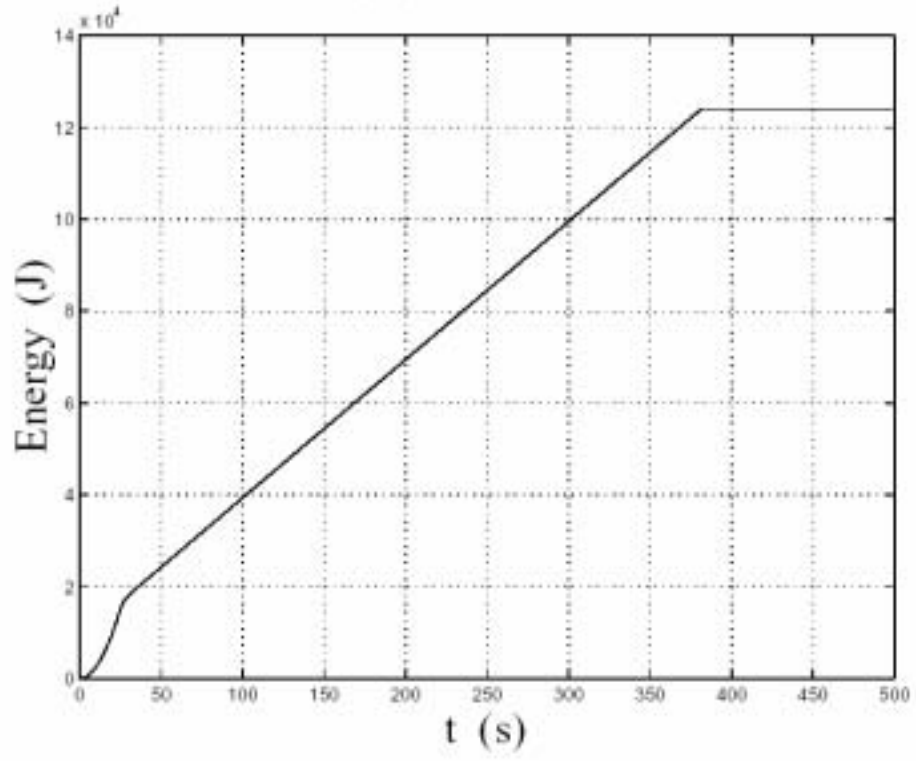


Figure 6.1 – Simulated energy loss while discharging an EDLC bank balanced with resistors [61].

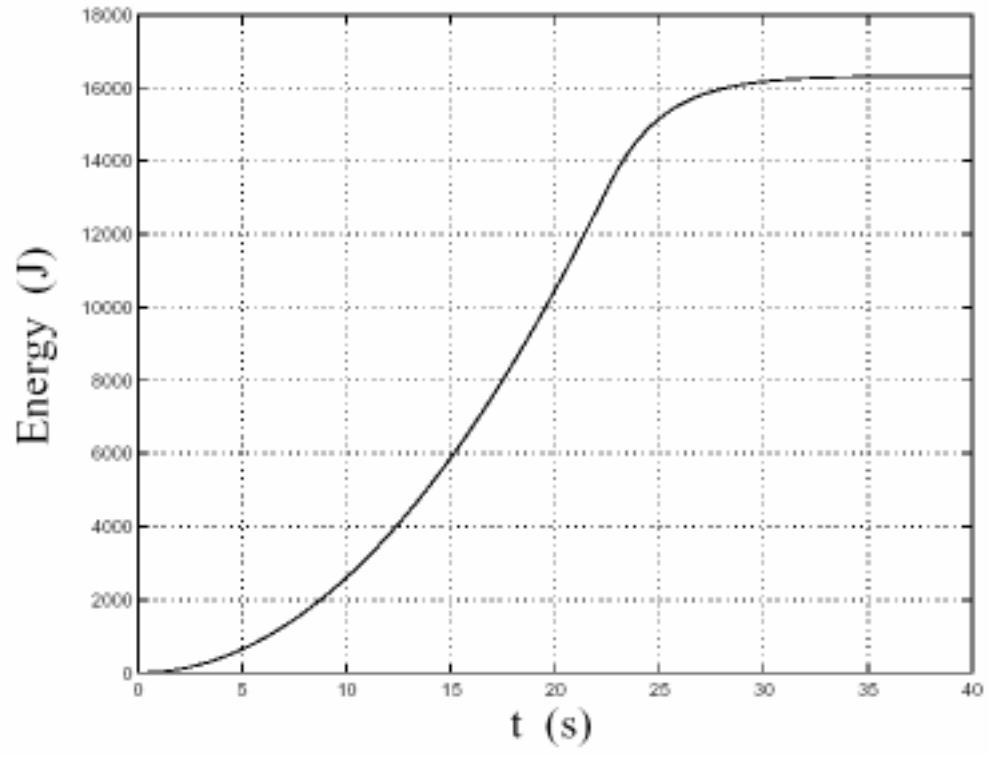


Figure 6.2 – Simulated energy loss while discharging a bank balanced with zener diodes [61].

The most efficient way of managing supercapacitor array voltage balancing is to employ active voltage sharing circuitry. In order to best understand the operation of such an active circuit, a device designed at the Swiss Federal Institute of Technology will be discussed [61].



Figure 6.3 – A series connection of EDLCs including active voltage balancing [61].

The general philosophy behind an active voltage sharing device is shown in Figure 6.4. The main charging current I is augmented by the equalising currents I_{eq} . The size and direction of the equalising currents is controlled according to the local voltages present across the corresponding supercapacitor.

The equalising current sources can be realised by the buck-boost topology shown in Figure 6.5. If the voltage U_{c1} is detected as being significantly greater than voltage U_{c2} , transistor T_1 will be switched at a certain frequency to generate a positive equalising current $2I_{eq}$. If U_{c2} is greater than U_{c1} then T_2 will be

switched to generate a negative equalising current. This process continues until the voltages are balanced.

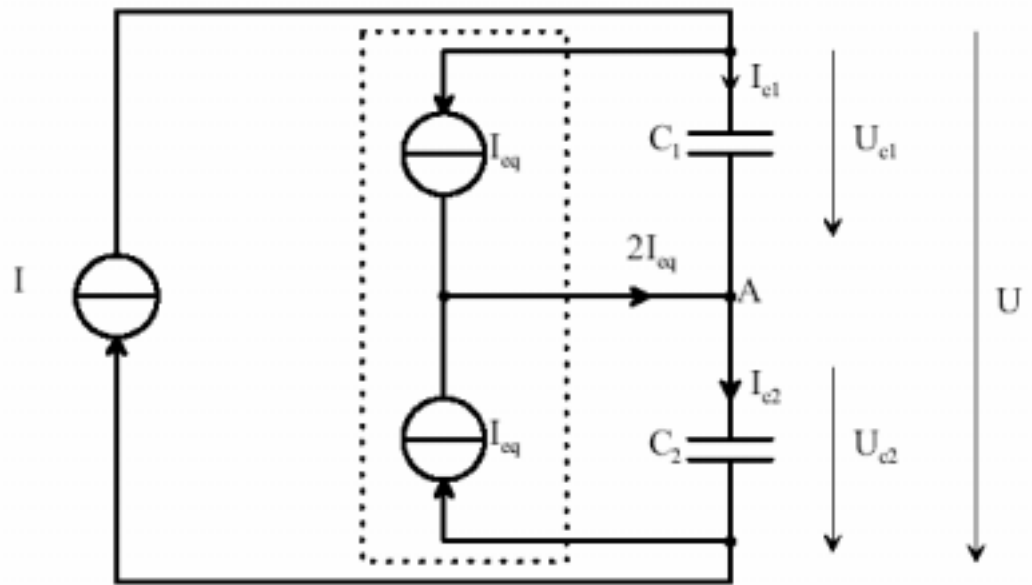


Figure 6.4 – Philosophy of voltage balancing with equalising current sources [61].

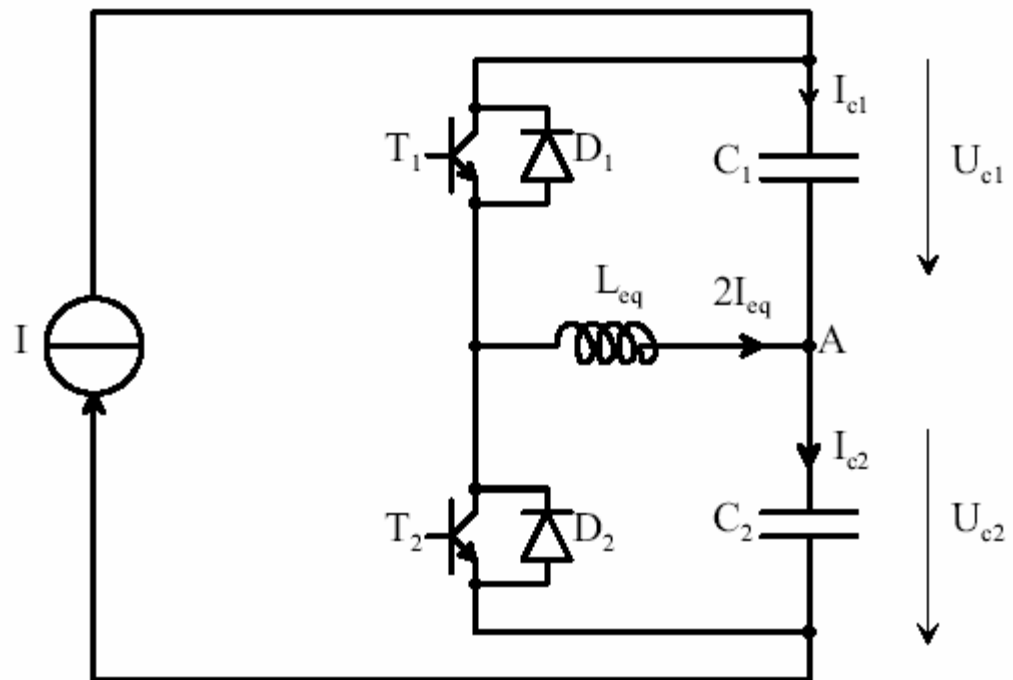


Figure 6.5 – Buck-boost topology for active voltage balancing [61].

The inductor value L_{eq} and the switching frequency f are then determined by the charging current I , the relative difference in capacitance d , as shown in Equation 6.5.

$$L_{eq}f = \frac{d + 200}{16Id} U_{c1} \left(1 + \frac{U_{c1}}{U_{c2} + U_d} \right) \quad (5.5)$$

U_d is the diode forward voltage. For details on the control structure the paper by Barrade et al. [61] should be referred to.

This design process can be extended to a longer series of supercapacitors by assigning a buck-boost converter to each pair of EDLCs (Fig. 6.6).

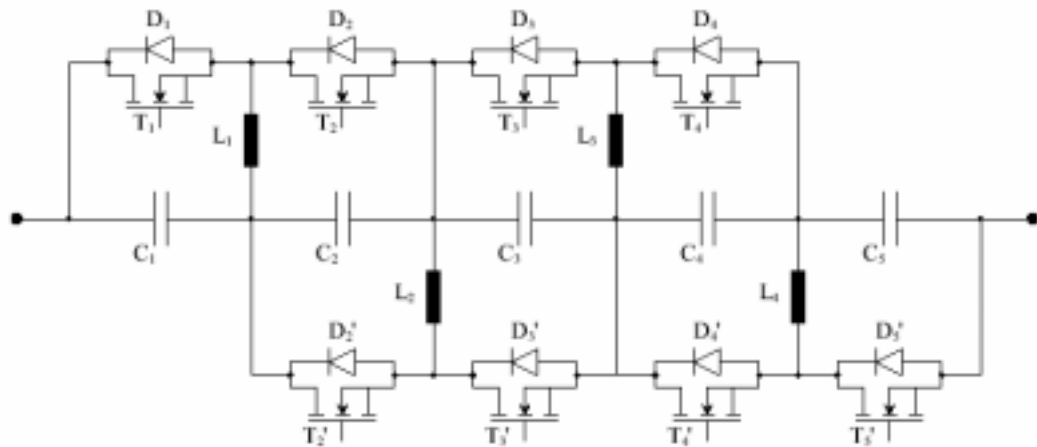


Figure 6.6 – Active voltage balancing for a series of EDLCs [61].

While this solution is the most efficient means of balancing cell voltages, a large amount of additional components are required to implement it. Nevertheless, the number of components used can be reduced by utilising parallel strings of EDLCs (Fig. 6.7). Each buck-boost converter can then control several pairs of supercapacitors [62].

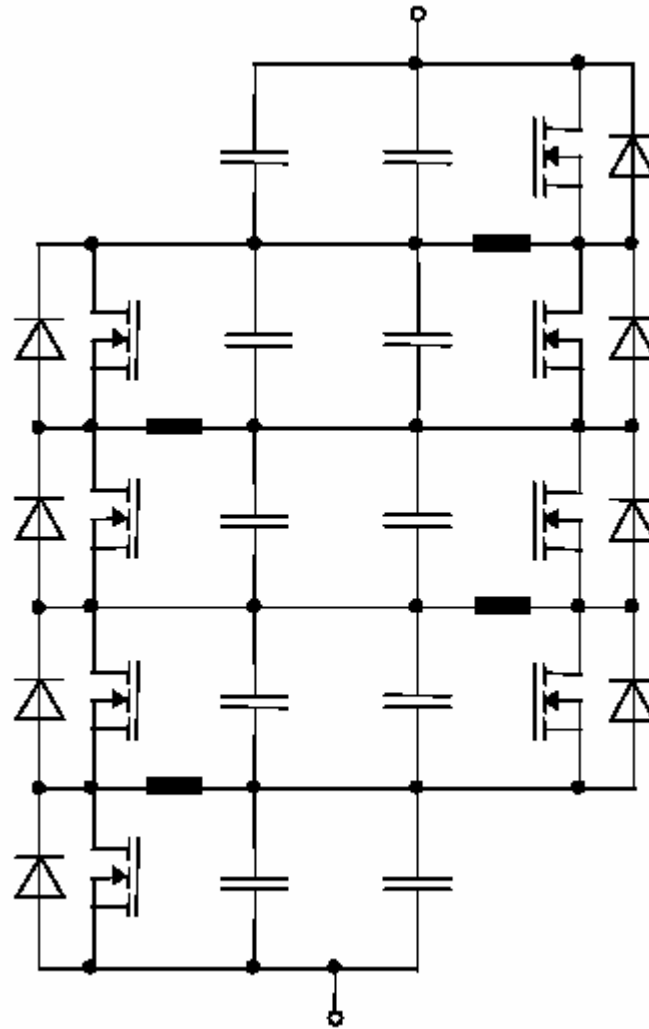


Figure 6.7 – Reducing component count by utilising parallel strings [62].

6.4. Summary of design with EDLCs

The problems of using EDLCs to provide a DC voltage are therefore overcome through a number of methods. Supercapacitor banks can be sized to ensure a maximum acceptable voltage drop over a certain period of time. Alternatively, DC-DC converters can be used to maintain a constant DC voltage. Voltage limitations of individual EDLCs can be overcome by connecting multiple EDLCs in series, while the total resistance of the array can be reduced by a greater number of parallel connections. In such an array, supercapacitors with different capacitance values will see different voltages at their terminals. In the interests of avoiding local over-voltages that could destroy the EDLCs efforts must be made to keep the voltages balanced. While resistors or zener diodes can be used to perform this function, the most efficient means is to implement active balancing circuitry that incorporates a buck-boost converter for each EDLC pair. This will require a large amount of additional components, however.

7. Example systems

This chapter will explore a range of systems that incorporate supercapacitors as an energy storage medium. By considering supercapacitors in the context of a whole system the contents of the preceding two chapters can be better understood. A range of systems will be described, from household power generation via a combination of fuel cell and supercapacitor, to a system designed to provide ride-through for an adjustable-speed drive, and a prototype electric vehicle built in Switzerland.

7.1. Household power generation

The following example is a system proposed by Nergaard et al. at the Virginia Polytechnic Institute and State University [63]. The system is designed to supply an average household with the normal 240 V AC supply that it is accustomed to, powered by a 48 V fuel cell and using supercapacitors for energy storage. The fuel cell represents a clean and renewable method of power generation, and combined with supercapacitor technology it makes environmentally sustainable remote power generation a possibility.

The general design of the system is shown in Figure 7.1, and utilises a fuel cell for main power generation, and a supercapacitor bank (referred to by Nergaard et al. as ultracapacitors) for meeting peak power requirements. The power electronics indicated by the dashed-line box consists of a DC-DC converter and an inverter, and serves to convert the DC voltage supplied by the fuel cell into the 240 V AC supply that will be used by the house.

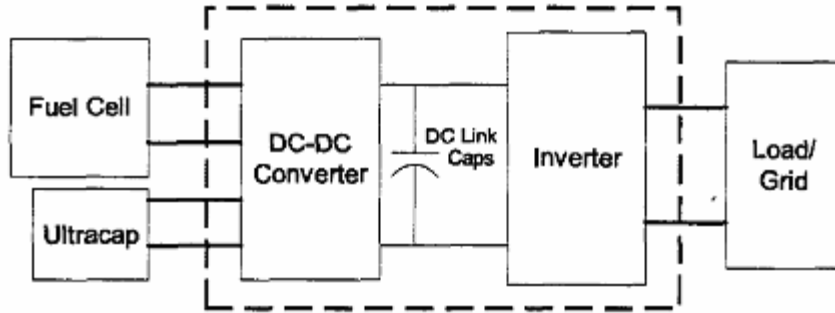


Figure 7.1 – Block diagram for a remote power generation system [63].

The average daily energy consumption of a household is shown in Figure 7.2. The maximum peak load is 6.5 kW and the average load is 2.5 kW. The inverter was therefore designed to provide a maximum of 10 kW. If the supercapacitor bank is sized to provide the peak power, the fuel cell will not need to supply 10 kW.

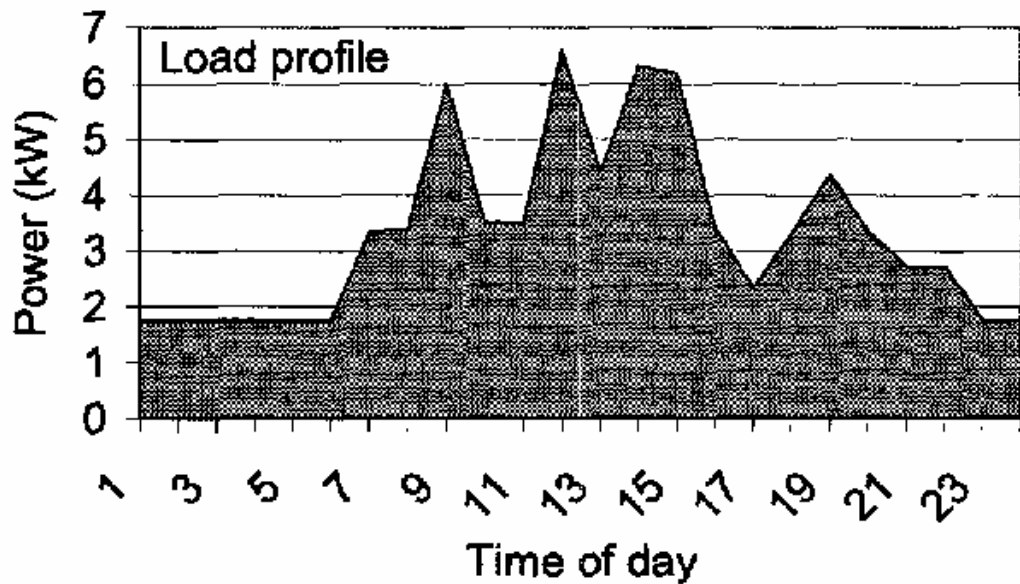


Figure 7.2 – Average daily usage of household power [63].

The prototype system is shown in Figure 7.3. A full-bridge topology was chosen for the DC-converter segment of the power electronics with an aim to reduce the voltage ratings required of the MOSFETs and hence improve efficiency. A half-bridge inverter supplies the AC power. A proton exchange membrane (PEM) fuel cell rated at 3 kW was used during testing, and two 1.65 F, 110 V supercapacitor modules were used in parallel. Each had an ESR of 140 m Ω , so the power rating of the bank was 10.8 kW.

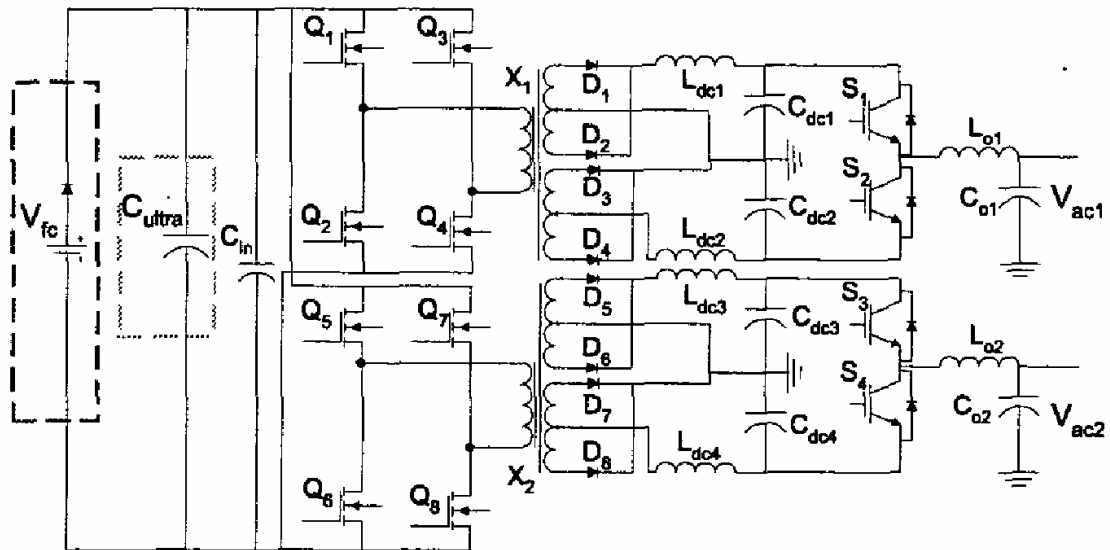


Figure 11 – Power generation system prototype [63].

Figure 7.4 shows the results of a step in load power from 1 kW to 1.5 kW. The peak in initial supercapacitor current shows the supercapacitor bank responding to the load change in a manner similar to the fuel cell. Since the load step was only small the response times of both the fuel cell and the supercapacitors was comparable. If the step had been greater than the rated power of the fuel cell, 5 kW for example, then the response of the supercapacitor would be quicker than that of the fuel cell.

Nergaard et al. observed that the fuel cell experienced significant current ripple after a load transient, and concluded that the ESR of the supercapacitor bank should be reduced as much as possible to help alleviate the problem. At a value of 70 m Ω the ESR of the supercapacitor bank can be considered to be quite high. Three 30EC303 supercapacitor modules made by ESMA could be used in series to reduce the ESR to 18m Ω , and parallel connections would reduce it even more.

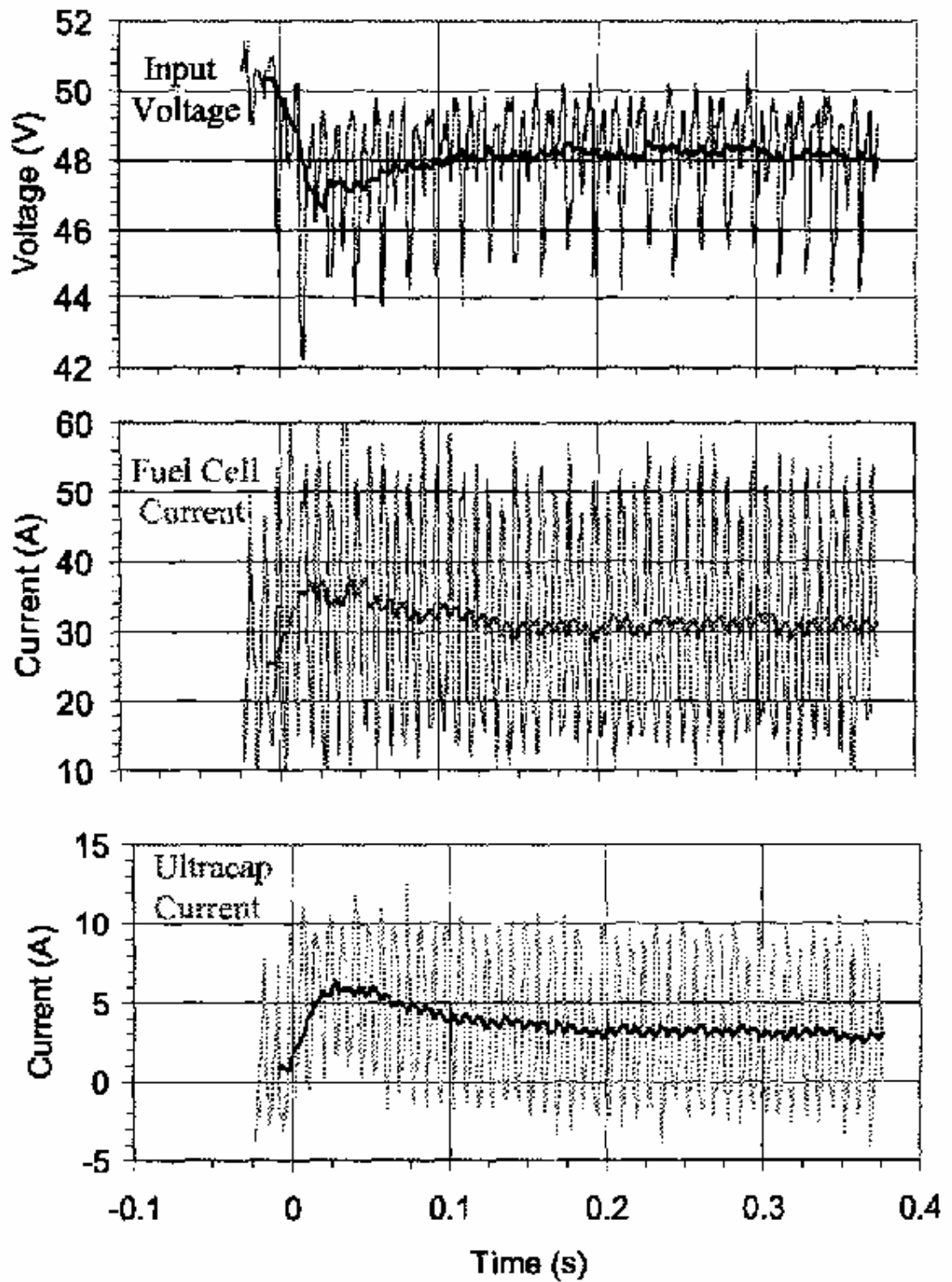


Figure 7.4 – Fuel cell and supercapacitor current response to a 500 W step input load [63].

7.2. Ride-through system for ASDs

Adjustable-speed drives and the need for ride-through were discussed previously in Section 5.6. In this example a ride-through system (RTS) designed at Maxwell Technologies is described [58].

The architecture of the RTS is shown in Figure 7.5. The boost converter regulates the DC voltage supplied by the supercapacitors, compensating for the voltage decay that occurs during discharge and ensuring a constant DC supply to the ASD. If the control circuitry monitoring the ASD supply voltage detect any sags or interruptions, it will attempt to maintain a regular supply by controlling the boost converter. While supplying constant power to the ASD the supercapacitor current will steadily increase. The control circuitry therefore monitors the EDLC bank voltage as well, and will discontinue operation if the voltage drops below a certain level. This prevents any damage that might occur to components because of excessive currents. The buck converter allows the EDLCs to be recharged slowly without drawing too much current from the ASD supply bus. The RTS is designed for a 480 V three-phase ASD and a load of up to 100 kW.

The supercapacitor bank consists of 208 Maxwell PowerCache 2500 F ultracapacitors connected in series. Each unit has a voltage of 2.3 V and an ESR of 0.85 m Ω . The EDLCs are grouped into modules of 26 cells each, and voltage balancing is managed by active circuitry in each module.

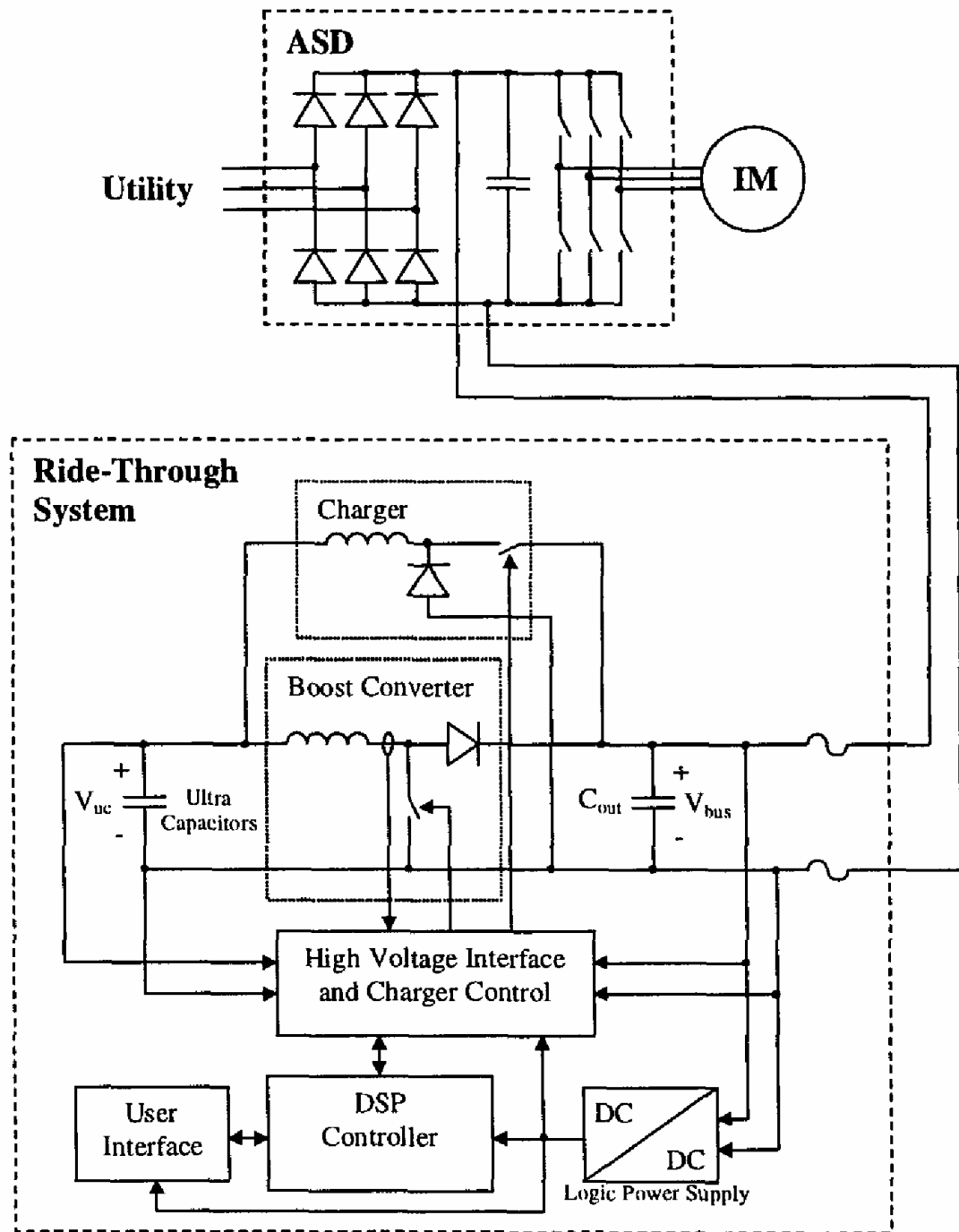


Figure 12 – System architecture of a ride-through system for adjustable-speed drives [58].

The ride-through time of the RTS depends upon the load (Fig. 7.6). At greater loads the boost converter will draw more current from the supercapacitors in order to compensate, and the voltage drop across the ESR will increase. This eventually leads to the system being shutdown much earlier, and ride-through times are thus much longer for smaller loads because more energy is released from the EDLCs. The time required to fully recharge the supercapacitor bank is therefore also dependent on the size of the load, and larger loads result in less discharged EDLCs which require less recharging (Fig. 7.7).

The RTS responds quickly to supply interruptions, and was shown to have a response time of 8 ms under a 100 kW load (Fig. 7.8).

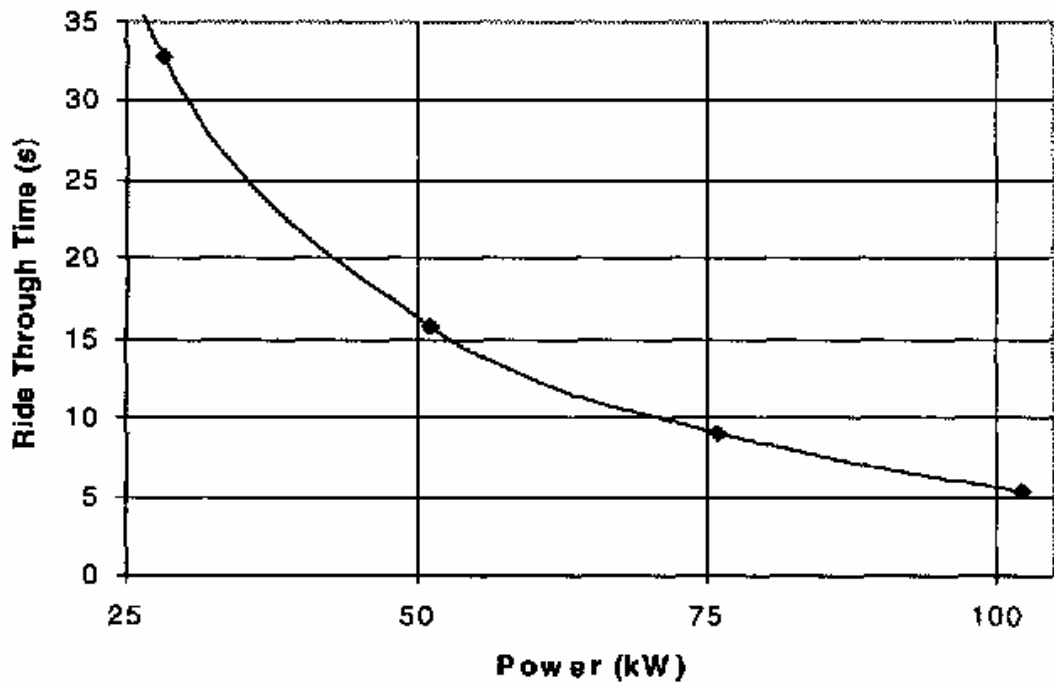


Figure 7.6 – Effect of load on ride-through time [58].

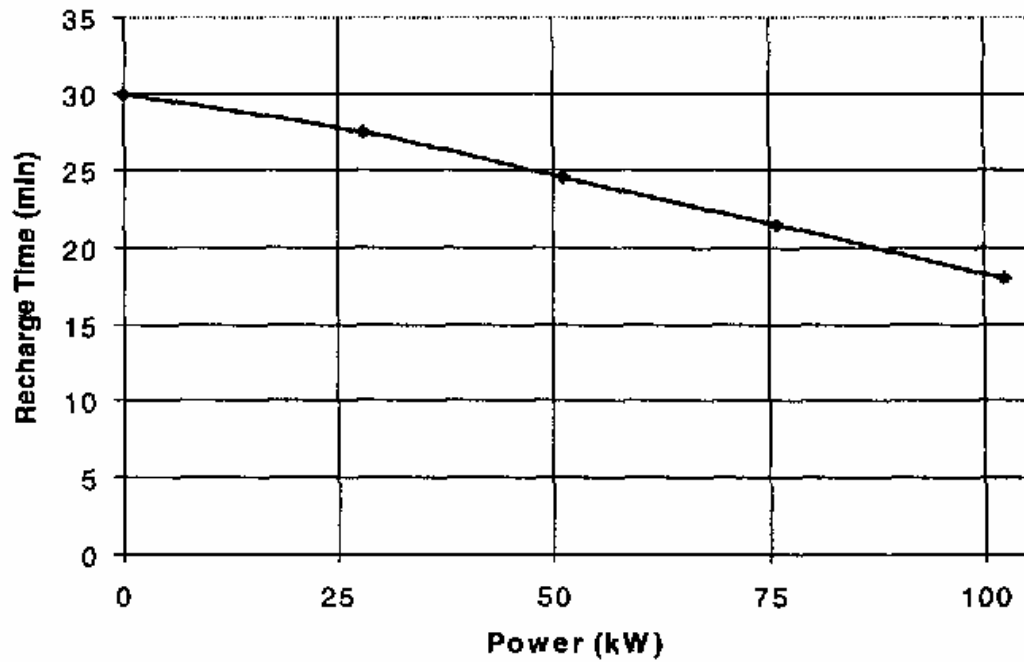


Figure 7.7 – Effect of load on recharge time [58].

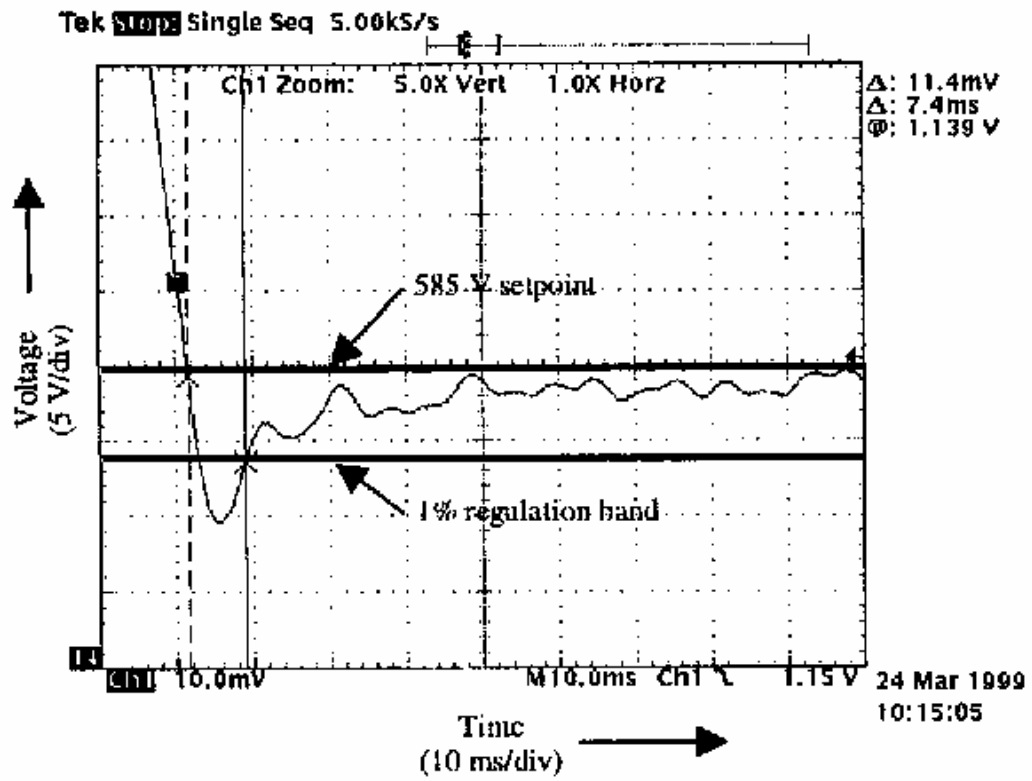


Figure 7.8 – RTS response to a 100kW load [58].

7.3. The HY.POWER electric car

Increasing concerns about vehicle emissions have spurred a great deal of research effort into the development of electric vehicles. Major problems have been encountered, however, due to the limited capabilities of battery technology. Despite this, new methods of energy storage and power generation have recently brought researchers closer to their goals, and the next example presents a prototype EV built at the Paul Scherrer Institute (PSI) in Switzerland [45].

The car is based on the Volkswagen Bora, with an electric motor driving the front wheels. The primary power source is a 48 kW fuel cell weighing 185 kg and is located in the trunk. Fuel takes the form of compressed hydrogen stored in two 25 L tanks. The supplementary power source consists of two supercapacitor modules, each consisting of 2 parallel strings of 70 supercapacitors in series. The individual EDLCs are 1500 F, 2.5 V components. The bank was designed to meet the vehicle's requirement of 360 V, and had a total ESR of 110 m Ω . The maximum energy storage of the module is 360 Wh. A number of power electronics modules are required in order to manage the various DC requirements of the energy sources and electric motor.

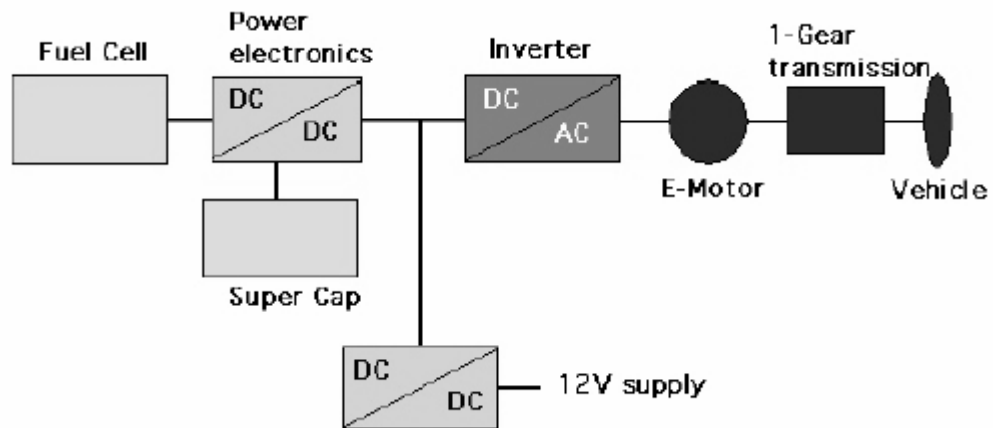


Figure 7.9 – EV system architecture [45].

The HY.POWER electric vehicle is an example of just how feasible the construction of a car powered with renewable energy has become. It can reach top speeds of up to 136 km/h, and can accelerate from 0 to 100 km/h in 12.5 seconds. Since the fuel is in the form of compressed hydrogen, the only emissions present are water. A supplementary form of energy storage such as a supercapacitor module not only allows for peak power demands to be met, but also greatly improves vehicle efficiency through regenerative braking.



Figure 7.10 – The Volkswagen Bora HY.POWER [45].

8. Future directions of the technology

Research and development efforts into EDLC technology have been steadily gathering momentum since the 1970's. This rate of progress is likely to continue as concerns about energy efficiency and sustainable development increase. The emission-free electric car has long been the dream of many of those concerned about retarding the progress of environmental degradation, and the potential use of EDLCs in EVs should continue to draw new attention to the technology.

The available energy and power of EDLC devices greatly depends upon the materials used, and significant research is directed at ways of improving the electrode and electrolyte materials. Greater understanding of the charging processes in the electric double-layer has led to a clear recognition of the crucial factors that must be addressed by electrode and electrolyte materials. New methods of carbon activation and new polymer and metal-oxide materials are continuously being developed, and improved electrolytes will result in increased cell voltages.

EDLCs will become a more competitive energy storage option as interest in the technology grows and production levels are increased. Awareness of the possible applications and advantages of EDLCs will gradually spread amongst the engineering and scientific community, and demand should increase. Manufacturers will then be able to produce cheaper devices by producing them in larger quantities and employing automated production lines.

Greater availability and more competitive prices combined with improved energy and power performance will lead to widespread adoption of supercapacitors as energy storage devices. While the technology is still in its infancy and is invisible to the public consciousness it is likely that supercapacitors will one day be as ubiquitous as the battery is today.

Established companies such as NEC and Panasonic have the advantages of existing manufacturing capabilities and other commercial product lines which can support the development of new EDLCs. New companies that do not possess manufacturing capabilities from the outset may find difficulty in obtaining the large amount of capital required, given that the market is still relatively undeveloped. It is therefore likely that most new companies will form joint ventures with larger companies that already possess manufacturing capabilities, which was the direction taken by PRI in its joint venture with Westinghouse [64].

9. Conclusions and recommendations

This survey has aimed to provide a brief overview of electrochemical double-layer capacitor technology as it stands today. Previous development efforts have been described to place the current state of the technology within an historical context. Scientific background has also been covered in order to better understand EDLC performance characteristics. Armed with a basic understanding of EDLC performance and design issues, it is hoped that the reader will be better equipped to undertake design tasks utilising supercapacitors for energy storage. Possible applications of EDLC technology have also been described to illustrate to the reader the wide range of possibilities that exist, and may perhaps even encourage the formation of ideas about new ways that supercapacitors could be used effectively.

It is apparent that the state of the EDLC as an energy storage solution is still very much in the early stages of development. The physical processes that occur during charge transfer and the implications that they have for EDLC performance are only just being fully understood and quantified. It is for this reason that current cost evaluations usually rule out supercapacitors as a viable alternative to batteries, a mature technology that has been widely available for many decades.

The handful of applications described in this survey therefore represents only a small selection of the possible uses of EDLC energy storage as the technology stands today. Because of the advantages of charging efficiency, long lifetime, fast response, and wide operating temperature range, it is tempting to try and apply EDLCs to any application that requires energy storage. The limitations of

the current technology must be fully appreciated, however, and it is important to realise that supercapacitors are only useful within a finite range of energy and power requirements. Outside of these boundaries other alternatives are likely to be the better solution.

Nevertheless, commercial EDLC devices have been available for many years now, and their quantity and performance has been steadily increasing. Both improvements in performance and the demand for better devices support each other in a mutually sustaining cycle. As devices of greater energy density and higher power become available, more new applications are formulated and demand will become greater. Increased levels of interest in the technology then lead to increased research and development efforts, which in turn will result in better devices being manufactured, and so the cycle continues. An established market will make it easier for new companies to enter the arena, and costs will drop as manufacturing quantities and demand both increase.

The most important thing to remember about supercapacitor technology is that it is a new and different technology in its own right. There may exist some similarities between EDLC operation and the operation of electrostatic capacitors, but there are fundamental differences that result from the different physical processes involved and these must be appreciated. Problems may be encountered if systems are designed based on the assumption that EDLCs behave like normal capacitors. Equivalent circuit models are therefore a useful tool to design engineers, and simulations based on these can provide good estimates on how a supercapacitor bank will behave in certain applications.

Supercapacitors are, at any rate, a part of the new wave of advanced energy storage devices that will further the push towards greater energy efficiency and more sustainable alternatives. They will be a useful tool with which to engineer highly efficient electrical and electronic systems, and as the state of the technology advances they will become progressively more commonplace.

References

- [1] Kotz, R., & Carlen, M., "Principles and applications of electrochemical capacitors", *Electrochimica Acta*, vol. 45, no. 15-16, pp. 2483-2498, 1999.
- [2] Becker, H.I., "*Low voltage electrolytic capacitor*", U.S. Patent 2800616, 23 July 1957.
- [3] Rightmire, R.A., "*Electrical energy storage apparatus*", U.S. Patent 3288641, 29 Nov 1966.
- [4] Boos, D.L., "*Electrolytic capacitor having carbon paste electrodes*", U.S. Patent 3536963, 27 Oct 1970.
- [5] Endo, M., Takeda, T., Kim, Y.J., Koshiba, K. & Ishii, K., "High power electric double layer capacitor (EDLC's); from operating principle to pore size control in advanced activated carbons," *Carbon science*, vol. 1, pp. 117-128, 2001.
- [6] NEC, 2003, *NEC-Tokin web site* [Online], Available: <http://www.nec-tokin.net/now/english/product/hypercapacitor/outline02.html> [Accessed 7 May 2003].
- [7] Yoshida, A., Imoto, K., Nishino, A. & Yoneda, H., "An electric double-layer capacitor with high capacitance and low resistance," 41st Electronic Components and Technology Conference, Atlanta, GA, USA, 1991.
- [8] ELNA, 2003, *The company information of ELNA Co.* [Online], Available: <http://www.elna-america.com/company.htm> [Accessed 13 May 2003].

- [9] Bullard, G.L., Sierra-Alcazar, H.B., Lee, H.L., & Morris, J.L., "Operating principles of the ultracapacitor," *IEEE Transactions on Magnetics*, vol. 25, pp. 102-106, 1988.
- [10] IEA, "Report on the first phase of the IEA implementing agreement for hybrid electric vehicle technology and programmes - 1993-1999," International Energy Agency, Paris, 1999.
- [11] Ness Capacitor Co., Ltd., 2000, *NessCap product line as of year 2002*, [Online], Available: <http://www.nesscap.com/prod/ba3.htm> [Accessed 3 May 2003].
- [12] Celzard, A., Collas, F., Mareche, J.F., Furdin, G., & Rey, I., "Porous electrodes-based double-layer supercapacitors: pore structure versus series resistance," *Journal of power sources*, vol. 108, pp. 153-162, 2002.
- [13] Gamby, J., Taberna, P.L., Simon, P., Fauvarque, J.F., & Chesneau, M., "Studies and characterisations of various activated carbons used for carbon/carbon supercapacitors," *Journal of power sources*, vol. 101, pp. 109-116, 2001.
- [14] An, K.H., Kim, W.S., Park, Y.S., et al., "Electrochemical properties of high-power supercapacitors using single-walled carbon nanotube electrodes", *Advanced functional materials*, vol. 11, no. 5, pp. 387-392, 2001.
- [15] Frackowiak, E., Metenier, K., Bertagna, V., & Beguin, F., "Supercapacitor electrodes from multiwalled carbon nanotubes," *Applied Physics Letters*, vol. 77, pp. 2421-2423, 2000.

- [16] Jiang, Q., Qu, M.Z., Zhou, G.M., Zhang, B.L., & Yu, Z.L., "A study of activated carbon nanotubes as electrochemical super capacitors electrode materials," *Materials Letters*, vol. 57, pp. 988-991, 2002.
- [17] Laforgue, A., Simon, P., Sarrazin, C., & Fauvarque, J., "Polythiophene-based supercapacitors," *Journal of power sources*, vol. 80, pp. 142-148, 1999.
- [18] Jiang, J., & Kucernak, A., "Electrochemical supercapacitor material based on manganese oxide: preparation and characterization," *Electrochimica Acta*, vol. 47, pp. 2381-2386, 2002.
- [19] Arbizzani, C., Mastragostino, M., & Soavi, F., "New trends in electrochemical supercapacitors," *Journal of power sources*, vol. 100, pp. 164-170, 2001.
- [20] Chen, W., Wen, T., & Teng, H., "Polyaniline-deposited porous carbon electrode for supercapacitor," *Electrochimica Acta*, vol. 48, pp. 641-649, 2003.
- [21] Frackowiak, E., Jurewicz, K., Szostak, K., Delpeux, S., & Beguin, F., "Nanotubular materials as electrodes for supercapacitors," *Fuel processing technology*, vol. 77-78, pp. 213-219, 2002.
- [22] Hendriks, M.G.H.M., Heijman, M.J.G.W., Van Zyl, W.E., Ten Elshof, J.E., & Verweij, H., "Solid state supercapacitor materials: Layered structures of yttria-stabilized zirconia sandwiched between platinum/yttria-stabilized zirconia composites," *Journal of Applied Physics*, vol. 90, pp. 5305-5307, 2001.

- [23] Nishino, A., "Capacitors: operating principles, current market and technical trends," *Journal of power sources*, vol. 60, pp. 137-147, 1996.
- [24] Sparnaay, M.J., *The electric double layer*, vol. 4, 1st ed., Pergamon Press (Aust.) Pty. Ltd., Sydney, 1972.
- [25] Matsumoto, M., "Electrocapillarity and double layer structure," in *Electrical phenomena at interfaces: fundamentals, measurements, and applications*, vol. 76, *Surfactant science series*, H. Ohshima, & Furusawa, K., Ed., 2nd ed. New York: Marcel Dekker, Inc., 1998, pp. 87-99.
- [26] Conway, B.E., Birss, V., & Wojtowicz, J., "The role and utilization of pseudocapacitance for energy storage by supercapacitors," *Journal of power sources*, vol. 66, pp. 1-14, 1997.
- [27] Conway, B.E., "Electrochemical surface science: The study of monolayers of ad-atoms and solvent molecules at charged metal interfaces," *Progress in surface science*, vol. 16, pp. 1-137, 1984.
- [28] Frackowiak, E., & Beguin, F., "Carbon materials for the electrochemical storage of energy in capacitors," *Carbon*, vol. 39, pp. 937-950, 2001.
- [29] Rudge, A., Davey, J., Raistrick, I., & Gottesfeld, S., "Conducting polymers as active materials in electrochemical capacitors," *Journal of power sources*, vol. 47, pp. 89-107, 1994.
- [30] Rudge, A., Raistrick, I., Gottesfeld, S., & Ferraris, J.P., "A study of the electrochemical properties of conducting polymers for application in electrochemical capacitors," *Electrochimica Acta*, vol. 39, pp. 273-287, 1994.

- [31] Mastragostino, M., Arbizzani, C., & Soavi, F., "Polymer-based supercapacitors," *Journal of power sources*, vol. 97-98, pp. 812-815, 2001.
- [32] Burke, A., "Ultracapacitors: why, how, and where is the technology," *Journal of power sources*, vol. 91, pp. 37-50, 2000.
- [33] Lee, H.Y., Manivannan, V., & Goodenough, J.B., "Electrochemical capacitors with KCl electrolyte," *Comptes rendus de l'Academie des sciences - Series IIC - Chemistry*, vol. 2, pp. 565-577, 1999.
- [34] Mastragostino, M., Arbizzani, C., & Soavi, F., "Conducting polymers as electrode materials in supercapacitors," *Solid state ionics*, vol. 148, pp. 493-498, 2002.
- [35] Xiao, Q., & Zhou, X., "The study of multiwalled carbon nanotube deposited with conducting polymer for supercapacitor," *Electrochimica Acta*, vol. 48, pp. 575-580, 2003.
- [36] Schneuwly, A., & Gallay, R., "Properties and applications of supercapacitors: From state-of-the-art to future trends," presented at PCIM 2000, 2000.
- [37] Conway, B.E., & Pell, W.G., "Power limitations of supercapacitor operation associated with resistance and capacitance distribution in porous electrode devices," *Journal of power sources*, vol. 105, pp. 196-181, 2002.
- [38] Conway, B.E., "Transition from 'supercapacitor' to 'battery' behavior in electrochemical energy storage," presented at Power Sources Symposium, 1990, Cherry Hill, NJ, USA, 1990.

- [39] Mahon, P.J., Paul, G.L., Keshishian, S.M., & Vassallo, A.M., "Measurement and modelling of the high-power performance of carbon-based supercapacitors," *Journal of power sources*, vol. 91, pp. 68-76, 2000.
- [40] Spyker, R.L., & Nelms, R.M., "Classical equivalent circuit parameters for a double-layer capacitor," *IEEE Transactions on Aerospace and Electronic Systems*, vol. 36, pp. 829-836, 2000.
- [41] Zubieta, L., & Bonert, R., "Characterization of double-layer capacitors for power electronics applications," *IEEE transactions on industry applications*, vol. 36, pp. 199-205, 2000.
- [42] De Levie, R., "On porous electrodes in electrolyte solutions," *Electrochimica Acta*, vol. 8, pp. 751-780, 1963.
- [43] Miller, J.R., & Evans, D.A., "Design and performance of high-reliability double-layer capacitors," presented at 40th Electronic Components and Technology Conference, 1990., Las Vegas, NV, USA, 1990.
- [44] Lai, J, Levy, S., & Rose, M.F., "High energy density double-layer capacitors for energy storage applications," *IEEE aerospace and electronics systems magazine*, vol. 7, pp. 14-19, 1992.
- [45] Kotz, R., Bartschi, M., Schnyder, B., Dietrich, P., Buchi, F.N., Tsukada, A., Scherer, G.G., Rodatz, P., Garcia, O., Barrade, P., Hermann, V., & Gallay, R., "Supercapacitors for peak-power demand in fuel-cell-driven cars," *Proceedings of the Electrochemical Society*, vol. PV 2001-21, 2001.

- [46] Kotz, R., Bartschi, M., Buchi, F., Gallay, R., & Dietrich, P., "HY.POWER - A fuel cell car boosted with supercapacitors," Proceedings of the 12th International Seminar on Double Layer Capacitors and Similar Energy Storage Devices, Deerfield Beach, Florida, US, 2002.
- [47] Spillane, D., O'sullivan, D., Egan, M.G., & Hayes, J.G., "Supervisory control of a HV integrated starter-alternator with ultracapacitor support within the 42V automotive electrical system," 18th Annual IEEE Applied Power Electronics Conference and Exposition APEC '03, 2003.
- [48] Hingorani, N.G., "Introducing custom power," *IEEE Spectrum*, vol. 32, pp. 41-48, 1995.
- [49] Andrieu, X., & Fauvarque, J.F., "Supercapacitors for telecommunication applications," Telecommunications Energy Conference 1993, Paris, France, 1993.
- [50] Smith, T.A., Mars, J.P., & Turner, G.A., "Using supercapacitors to improve battery performance," presented at Power Electronics Specialists Conference, 2002, 2002.
- [51] Merryman, S.A., "Chemical double-layer capacitor power sources for electrical actuation applications," 31st Intersociety Energy Conversion Engineering Conference, IECEC 96., 1996.
- [52] Merryman, S.A., & Hall, D.K., "Characterization of CDL capacitor power sources for electrical actuation applications," 32nd Intersociety Energy Conversion Conference, IECEC-97., 1997.

- [53] von Jouanne, A., Enjeti, P.N., & Banerjee, B., "Assessment of ride-through alternatives for adjustable-speed drives," *IEEE transactions on Industry Applications*, vol. 35, pp. 908-916, 1999.
- [54] Duran-Gomez, J.L., Enjeti, P.N., & Von Jouanne, A., "An approach to achieve ride-through of an adjustable-speed drive with flyback converter modules powered by super capacitors," *IEEE transactions on industrial electronics*, vol. 38, pp. 514-522, 2002.
- [55] Jordan, B.A., & Spyker, R.L., "Integrated capacitor and converter package," 15th Annual IEEE Applied Power Electronics Conference and Exposition APEC 2000, New Orleans, LA, USA, 2000.
- [56] Barker, P.P., "Ultracapacitors for use in power quality and distributed resource applications," IEEE Power Engineering Society Summer Meeting 2002, Knoxville, TN, USA, 2002.
- [57] Robbins, T., & Hawkins, J.M., "Powering telecommunications network interfaces using photovoltaic cells and supercapacitors," Telecommunications Energy Conference 1997, Melbourne, Vic, Australia, 1997.
- [58] Corley, M., Locker, J., Dutton, S., & Spee, R., "Ultracapacitor-based ride-through system for adjustable speed drives," 30th Annual IEEE Power Electronics Specialists Conference PESC 99, Charleston, SC, USA, 1999.
- [59] Halpin, S.M., & Ashcraft, S.R., "Design considerations for single-phase uninterruptible power supplies using double-layer capacitors as the energy storage element," 31st IAS Annual Meeting, IAS '96, San Diego, CA, USA, 1996.

- [60] Schneuwly, A., Bartchsch, M., Hermann, V., Sartorelli, G., Gallay, R., & Kotz, R., "BOOSTCAP Double-layer capacitors for peak power automotive applications," Proceedings of the 2nd International Advanced Automotive Battery Conference (AABC), Las Vegas, Nevada, USA, 2002.
- [61] Barrade, P., Pittet, S., & Rufer, A., "Energy storage system using a series connection of supercapacitors, with an active device for equalizing the voltages," International Power Electronics Conference, Tokyo, Japan, 2000.
- [62] Rufer, A., & Barrade, P., "A supercapacitor-based energy storage system for elevators with soft commutated interface," Industry Applications Conference, 2001, Chicago, IL, USA, 2001.
- [63] Nergaard, T.A., Ferrell, J.F., Leslie, L.G., & Lai, J-S., "Design considerations for a 48V fuel cell to split single phase inverter system with ultracapacitor energy storage," IEEE 23rd Annual Power Electronics Specialists Conference, Cairns, QLD, Australia, 2002.
- [64] Burke, A.F., "Prospects for ultracapacitors in electric and hybrid vehicles," 11th Annual Battery Conference on Applications and Advances, Long Beach, CA, USA, 1996.

Appendix

Definitions and abbreviations

AC	Alternating current
ASD	Adjustable-speed drive
DC	Direct current
DoE	Department of Energy (US)
DSP	Digital signal processor
DVR	Dynamic voltage restorer
EDLC	Electrochemical double-layer capacitor
EDR	Equivalent distributed resistance
EPR	Equivalent parallel resistance
ESR	Equivalent series resistance
EV	Electric vehicle
FE-SEM	Field emission scanning electron microscope
HEV	Hybrid electric vehicle
ICE	Internal combustion engine
IM	Induction machine
ISA	Integrated starter alternator
LED	Light emitting diode
MOSFET	Metal oxide semiconductor field effect transistor
NEC	Nippon Electric Company
PRI	Pinnacle Research Institute

PSI	Paul Scherrer Institute
PV	Photovoltaic
RTS	Ride through system
SMES	Superconducting magnetic energy storage
SOHIO	Standard Oil Company, Cleveland, Ohio
Statcon	Static condenser
TEM	Transmission electron microscope